PHYSICAL REVIEW
LETTERS

VOLUME 1 DECEMBER 15, 1958 NUMBER 12

INTERPRETATION OF THE TRANSVERSE MAGNETORESISTANCE IN p-TYPE INDIUM ANTIMONIDE AT LIQUID NITROGEN TEMPERATURE

C. H. Champness
Nothern Electric Laboratories,
Montreal, Quebec, Canada
(Received November 6, 1958)

The variation of the transverse magnetoresistance ratio $\Delta\rho/\rho_0$ with magnetic field in p-type indium antimonide cannot be accounted for using a single carrier model.[1,2] The results can be explained, however, assuming the presence of heavy holes and less numerous light holes, as in p-type germanium. In order to calculate the mobilities and concentrations of the holes in a simple way from the experimental data, the following assumptions are made: (1) negligible intrinsic electron concentration at 77°K; (2) spherical energy surfaces in $\vec{k}$ space for both holes; (3) energy-independent relaxation times to avoid scattering coefficients.

Assumption (1) is well satisfied. Assumption (2) and (3) however are probably not true; they are only made for convenience. Suppose we have two sets of holes with mobilities μ_1 and μ_2 and concentrations p_1 and p_2, respectively. With the above assumptions the following expressions hold for the Hall coefficient (R_H), the conductivity (σ_0), the transverse magnetoresistance ($\Delta\rho/\rho_0$), and the fractional change of the Hall coefficient ($\Delta R_H/R_{H_0}$) in a magnetic field (H):

$$R_{H_0} = \frac{p_1\mu_1^2 - p_2\mu_2^2}{e(p_1\mu_1 + p_2\mu_2)^2} \tag{1}$$

where e is the electron charge;

$$\sigma_0 = e(p_1\mu_1 + p_2\mu_2); \tag{2}$$

$$\frac{\Delta\rho}{\rho_0} = \frac{bH^2}{1+cH^2}, \tag{3A}$$

where

$$b = \frac{p_1p_2\mu_1\mu_2(\mu_1-\mu_2)^2}{(p_1\mu_1+p_2\mu_2)^2}, \tag{3B}$$

$$c = \frac{\mu_1^2\mu_2^2(p_1+p_2)^2}{(p_1\mu_1+p_2\mu_2)^2}; \tag{3C}$$

$$-\frac{\Delta R_H}{R_H} = \frac{\Delta\rho}{\rho_0}\,\frac{c^{1/2}}{(R_H\sigma)_0} \tag{4}$$

If μ_2 corresponds to the light hole, let us suppose that $\mu_2 \gg \mu_1$ and $p_2 \ll p_1$. Then Eqs. (1), (2), (3A), (3B), and (3C) may be easily solved to give μ_1, μ_2, p_1, and p_2 in terms of the quantities $(R_H\sigma)_0$, σ_0, b, and c:

$$\mu_2 = \frac{c+b}{c^{1/2}} \tag{5}$$

$$p_2 = \frac{bc^{1/2}\sigma_0}{e(c+b)^2}, \tag{6}$$

$$\mu_1 = \frac{c+b}{c}\left[(R_H\sigma)_0 - b/c^{1/2}\right], \tag{7}$$

$$p_1 = \left(\frac{c}{c+b}\right)^2 \frac{\sigma_0}{e\left[(R_H\sigma)_0 - b/c^{1/2}\right]}. \tag{8}$$

From the observed results at 77°K on a p-type sample of indium antimonide (sample A of reference 2), it was found that the magnetoresistance variation could be fitted approximately by a formula of the form of Eq. (3A) with $b = 4\times10^7$ cm^4/volt^2 sec^2 and $c = 7\times10^8$ cm^4/volt^2 sec^2. Using the value $(R_H\sigma)_0 = 5000$ cm^2/volt sec and $\sigma_0 = 4$ ohm^{-1} cm^{-1} at 77°K, Eqs. (5), (6), (7), and (8) give

$$\mu_2 = 2.8\times10^4 \text{ cm}^2/\text{volt sec},$$
$$p_2 = 4.8\times10^{13}/\text{cm}^3,$$

for a light hole, and

$$\mu_1 = 3.68 \times 10^3 \text{ cm}^2/\text{volt sec},$$
$$p_1 = 6.4 \times 10^{15}/\text{cm}^3,$$

for a heavy hole.

Thus the calculation would indicate that the light holes are 7.6 times as mobile as the heavy holes and have a density of only 0.75% of the total hole concentration.

A similar calculation for samples R and U of reference 1 gives the following results:

Sample R: $\mu_2 = 3.76 \times 10^4$ cm^2/volt sec,
$p_2 = 2.15 \times 10^{13}$/cm^3,
$\mu_1 = 7.03 \times 10^3$ cm^2/volt sec,
$p_1 = 1.93 \times 10^{15}$/cm^3,

so that

$$\mu_2/\mu_1 = 5.3 \text{ and } p_2/p_1 = 1.1\%.$$

Sample U: $\mu_2 = 6.2 \times 10^4$ cm^2/volt sec,
$p_2 = 4.6 \times 10^{12}$/cm^3,
$\mu_1 = 8.4 \times 10^3$ cm^2/volt sec,
$p_1 = 3.6 \times 10^{14}$/cm^3,

so that

$$\mu_2/\mu_1 = 7.4 \text{ and } p_2/p_1 = 1.3\%.$$

The variation of the Hall coefficient with magnetic field can be calculated from Eq. (4). For $H = 5000$ gauss it is found that $-\Delta R_H/R_{H_0} = 18\%$ for sample R and 36% for sample U. The observed values (from Fig. 5 of reference 1) were, respectively, 33% and 38%, giving good agreement for sample U but indicating that possibly a larger value of c should apply to sample R than was found from the magnetoresistance calculations alone.

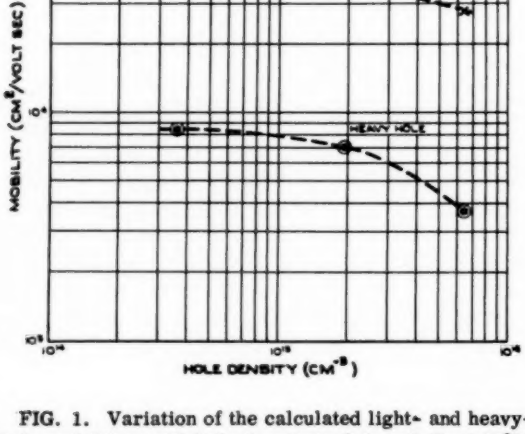

FIG. 1. Variation of the calculated light- and heavy-hole mobilities with hole density in p-type InSb at 77°K.

The variation of μ_1 and μ_2 with hole density ($p = p_1 + p_2$) shown in Fig. 1 shows that the mobilities decrease with increasing concentration of ionized acceptors as expected for impurity scattering. Because of the many approximations made in the calculation and the fact that there are only three points, a quantitative analysis to find lattice mobilities is probably not worth while. However, Fig. 1 suggests that at $p = 3.6 \times 10^{14}$ the lighter hole is still affected by impurity scattering whereas the other hole is not because of its greater mass.

The author wishes to thank Dr. A. C. Beer of the Battelle Memorial Institute for discussion and the Director of the Northern Electric Laboratories, Mr. A. B. Hunt, for permission to publish.

[1]H. P. R. Frederikse and W. R. Hosler, Phys. Rev. 108, 1146 (1957).

[2]C. H. Champness, J. Electron. and Control 4, 201 (1958).

NEW OSCILLATORY ABSORPTION OF ULTRASONIC WAVES IN BISMUTH IN A MAGNETIC FIELD*

D. H. Reneker†
Department of Physics and
Institute for the Study of Metals,
University of Chicago,
Chicago, Illinois

(Received October 27, 1958)

In the course of an attempt to study the Fermi surface in bismuth by magnetoacoustic resonance a new oscillatory absorption phenomenon has been observed. In bismuth, because of the low momentum of the carriers, the magnetoacoustic resonance of the type observed by Bömmel[1] in tin and Morse et al.[2] in copper occurs in fields of the order of 100 oersteds. However, at fields of the order of 1000 oersteds a different kind of oscillatory absorption, periodic in reciprocal magnetic field, has been seen (see Fig. 1). The period of this component is independent of the sound wavelength. Measurements of the period in $1/H$ as a function of direction of the magnetic field for some 20 directions in a plane normal to the 3-fold axis agree to within 10% or better with the period of the de Haas-van Alphen oscillations in the susceptibility as observed by Shoenberg[3]

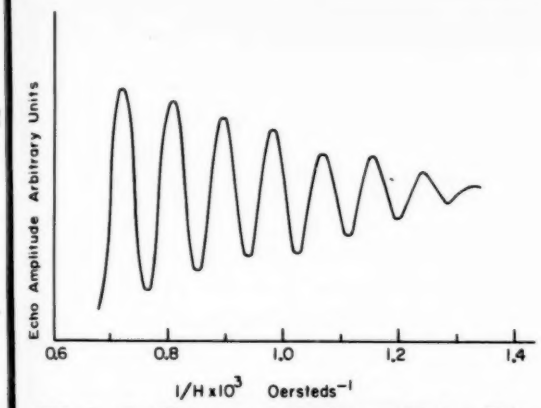

FIG. 1. Oscillatory part of pulse amplitude. This is about 5% of the total pulse amplitude, which was measured to about ½% on a recorder. Field 22.5° from 2-fold axis and normal to 3-fold axis.

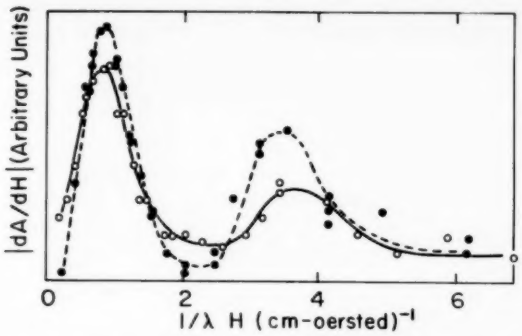

FIG. 2. Results of continuous-wave measurement showing the magnetoacoustic resonance effect. Open circles, 12 Mc/sec; filled circles, 36 Mc/sec.

or as calculated from the cyclotron-resonance effective masses given by Aubrey and Chambers.[4] The magnetoacoustic resonance absorption is observed only with the magnetic field transverse to the direction of sound propagation and it increases with field, saturating at high fields. The new oscillatory absorption appears superimposed on the magnetoacoustic resonance for this orientation or superimposed on what is essentially the zero-field absorption for other directions of H. The new phenomenon is clearly distinguished from other oscillatory absorptions described below.

The pulse echo technique[5] used in the above work was not sensitive enough to resolve clearly the second maximum of the magnetoacoustic resonance although it did offer some positive evidence for it. The phenomenological theory of Harrison[6] of magnetoacoustic resonance encouraged us to try a more sensitive modulated field continuous wave technique suggested by Reif.[7] The technique is similar to that used in nuclear resonance absorption and it measures the absolute value of the slope of the transmitted amplitude dA/dH. The amplitude A is related to the attenuation $\alpha(H)$ by the expression $A(H) = A_0 \exp[-\eta\alpha(H)l]$ where l is the length of the sample and η converts db/cm to nepers/cm. The results of this measurement are shown in Fig. 2. The effect scales with the sound wavelength as shown by plotting the slope versus $1/(\lambda H)$ for frequencies of 12 and 36 megacycles per second. For the orientation measured (longitudinal mode along 2-fold axis, field along 3-fold axis, sound velocity 2.55×10^5 cm/sec), the period observed in $1/(\lambda H)$ is approximately 2.6 (cm oersted)$^{-1}$. Using this value in Pippard's[8] formula results in a Fermi momentum for electrons within 15% of the value obtained from Shoenberg's[3] 3-ellipsoid model for the pertinent direction. Qualitative measurements of dependence on field direction are also in agreement with the 3-ellipsoid model.

At intermediate fields and for various orientations there is a third oscillatory component of the absorption whose period does not fit the three-ellipsoid model. Interpretation along the lines of the de Haas-van Alphen effect would indicate that the periods result from even smaller regions of the Fermi surface. There is some evidence to suggest that these periods scale as $1/(\lambda H)$ in which case Pippard's formula indicates that they are due to carriers with momenta higher than the presently accepted values for either electrons or holes in bismuth.

The bismuth crystal measured was grown in a graphite boat during the process of zone refining. Spectroscopic analysis shows only a trace of Cu and Ag, less than one part per million, and all other elements are present in concentrations too small to detect spectroscopically. The fact that a magnetoacoustic resonance was observed at a frequency of 12 megacycles per second indicates that the mean free path of the carriers involved is of the order $\pi\lambda$ or about 0.6 mm which is of the same order as given by residual resistance measurements on similar samples.

Further work including more orientations and modes and using both the pulse echo and continuous wave methods is in progress.

We wish to acknowledge the advice and encour-

agement which Professor A. W. Lawson has given throughout this work.

*This work was supported by a grant from the National Science Foundation.

†National Science Foundation Pre-doctoral Fellow.

[1]H. E. Bömmel, Phys. Rev. 100, 758 (1955).

[2]Morse, Bohm, and Gavenda, Phys. Rev. 109, 1394 (1958).

[3]D. Shoenberg, Trans, Roy. Soc. (London) A248, 1 (1955).

[4]J. E. Aubrey and R. G. Chambers, J. Phys. Chem. Solids 3, 128 (1957).

[5]R. L. Roderick and R. Truell, J. Appl. Phys. 23, 267 (1952).

[6]M. J. Harrison, International Conference on the Electronic Properties of Metals at Low Temperatures, Geneva, New York, 1958 (unpublished); and following Letter [Phys. Rev. Lett. 1, 442 (1958)].

[7]F. Reif (private communication).

[8]A. B. Pippard, Phil. Mag. 21, 1147 (1957).

MAGNETIC FIELD DEPENDENCE OF ULTRASONIC ATTENUATION

Michael J. Harrison*
Department of Physics and
Institute for the Study of Metals,
University of Chicago,
Chicago, Illinois
(Received October 27, 1958)

Recent experiments[1] on acoustic attenuation in metals at low temperatures indicate that when the electronic mean free path is large compared to the wavelength of sound, an impressed magnetic field can cause periodic effects in the absorption of acoustic energy. These are presumably due to coincidences between electron orbit size and sound wavelength.[2] However the behavior of the attenuation in bismuth[3] as the field is indefinitely increased is radically different from that in copper.[4] In bismuth, high fields perpendicular to the direction of sound propagation enhance sound attenuation, whereas in copper they suppress it. It is the purpose of this note to offer a simple heuristic model which has been found useful in guiding experimental work on bismuth, and which exhibits the general character of the field-dependent attenuation observed in these metals.

Because the sound wave travels several hundred times slower than an electron at the Fermi surface, the electron sees a wave which has essentially fixed nodes and antinodes. This deformation wave results in a force exerted on the electron which has the spatial periodicity of the sound wave. Suppose now that a plane wave is propagating in the x direction and gives rise to a force on the electron of the form $F=F_0\cos(kx)$, where k is the wave number of the sound wave. If a transverse magnetic field is present, an electron in a spherical band with effective mass m and momentum component p perpendicular to the magnetic field will traverse an orbit of radius pc/eH with an angular frequency $\omega_c=eH/mc$. In the course of its journey it may pass over several crests and troughs of the sound wave. The space-periodic force will weakly perturb the motion of the electron and do work on it. We assume that, on the average, the rate at which work is being done on such an orbiting electron when passing near a point $\bar{x}$ of the unperturbed orbit is proportional to the square of the local force field. The net rate of energy transfer to the conduction electron will then be given by integrating the instantaneous energy transfer per unit time along the path the particle would follow if unperturbed and dividing by the period $2\pi/\omega_c$. Thus the sound absorption will be proportional to a quantity α given by

$$\alpha=(\omega_c/2\pi)\int_0^{2\pi/\omega_c}\cos^2[kx(t)]\,dt\,, \qquad (1)$$

where $x(t)$, the x component of the unperturbed trajectory of a typical electron on the Fermi surface, is given by

$$x(t)=(pc/eH)\sin(\omega_c t)+x_0\,, \qquad (2)$$

where x_0 is the center of an electron orbit.

From Eq. (2) and Eq. (1) we obtain

$$\alpha=(2\pi)^{-1}\int_0^{2\pi}\cos^2[(kpc/eH)\sin y+kx_0]\,dy. \qquad (3)$$

There are two extreme cases for the phase kx_0. If the relevant electrons have their central positions at the minima or maxima of the deformation force $F=F_0\cos(kx)$, then we take $kx_0=n\pi$. If the relevant electrons' central positions are at the nodes of the above force field then we take $kx_0=(2n+1)\pi/2$. By elementary trigonometric identities, Eq. (3) transforms for these two cases into

$$\alpha=(4\pi)^{-1}\int_0^{2\pi}\{1\pm\cos[(2kpc/eH)\sin y]\}\,dy, \qquad (4)$$

where the (+) corresponds to $kx_0=n\pi$, and the (-) corresponds to $kx_0=(2n+1)\pi/2$.

By use of an integral representation of the

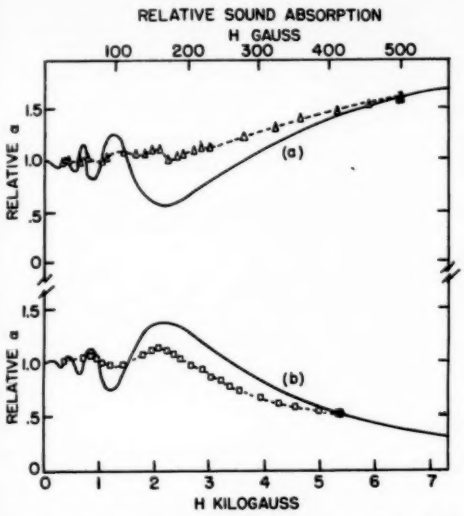

FIG. 1. Curve (a) is a plot of $2\alpha = 1 + J_0(4\pi pc/e\lambda H)$ for $p = 35 \times 10^{-22}$ g cm/sec, and $\lambda = 4.2 \times 10^{-3}$ cm. The experimental points denoted by triangles represent attenuation of a 60-Mc/sec longitudinal mode propagating along an x axis of a single crystal of bismuth; $H \| z$. Curve (b) is a plot of $2\alpha = 1 - J_0(4\pi pc/e\lambda H)$ for $p = 1.18 \times 10^{-19}$ g cm/sec, and $\lambda = 1.12 \times 10^{-2}$ cm. The experimental points denoted by boxes represent attenuation data of Morse, Bohm, and Gavenda on polycrystalline copper. The measurements were made for a 26-Mc/sec shear wave with H parallel to the direction of polarization.

Bessel function,[5] Eq. (4) may be transformed to

$$\alpha = \tfrac{1}{2}[1 \pm J_0(2kpc/eH)]. \qquad (5)$$

The upper sign gives enhanced attenuation at high magnetic field strength followed by saturation at sufficiently high fields. This is the behavior observed in bismuth. The lower sign gives suppressed attenuation at high fields, and this is the behavior observed in copper.

In both cases, however, Eq. (5) shows that at low fields α will be periodic in $1/H$ with a period given by

$$\Delta(1/H) = e\lambda/2pc, \qquad (6)$$

where $\lambda = 2\pi/k$ is the sound wavelength. This is the relation given by Pippard[2] if one notes the difference in the definition of p.

Comparison with experimental data on bismuth[6] and copper[4] is shown in Fig. 1, where the two cases given by Eq. (5) are plotted for crystal momentum values appropriate to bismuth and copper, and for those wavelengths used in the experimental work quoted. The data were normalized at the blackened high-field points with respect to attenuation at zero field, and the other points plotted accordingly.

The general character of the experimental data is indeed obtained from the above model as far as the existence of low-field oscillations, and high-field behavior in both bismuth and copper. Agreement at high fields can be improved somewhat by introducing a factor of $[1 - \pi r(H)/l]$ into our expression for α to account for effects of finite mean free path, l, where $r(H)$ is the orbit radius for field strength H. This would generally lower the solid curves in the region of secular rise and fall, bringing the slope of curve (a) above 200 gauss into better correspondence with that of the experimental points, and bringing solid curve (b) into closer agreement with the copper data above 2 kilogauss. Complications arising from a nonspherical Fermi surface and contributions from electrons with different transverse momentum tend to smear out the low field oscillations.

The author wishes to thank Professor A. W. Lawson for calling his attention to this problem.

*National Science Foundation Pre-doctoral Fellow.

[1]H. E. Bömmel, Phys. Rev. 100, 758 (1955); W. P. Mason and H. E. Bömmel, J. Acoust. Soc. Amer. 28, 930 (1956); Morse, Bohm, and Gavenda, Phys. Rev. 109, 1394 (1958).

[2]A. B. Pippard, Phil. Mag. 2, 1147 (1957).

[3]D. H. Reneker, preceding Letter [Phys. Rev. Lett. 1, 440 (1958)].

[4]Morse, Bohm, and Gavenda, reference 1.

[5]G. N. Watson, Treatise on the Theory of Bessel Functions (Cambridge University Press, Cambridge, 1944), p. 176.

[6]I am indebted to D. H. Reneker for permission to use this data prior to publication.

RIGOROUS VALIDITY CRITERION FOR TESTING APPROXIMATIONS TO THE ELECTRON GAS CORRELATION ENERGY*

Richard A. Ferrell
University of Maryland,
College Park, Maryland
(Received November 10, 1958)

Various attempts have been made in the past to obtain expressions for the ground-state energy of a degenerate electron gas. Since approximations are inevitably involved in such endeavors, it is clearly desirable to have as many rigorous checks on the results as possible. The

purpose of this note is to point out that there exists a general theorem which provides one such a priori restriction. This restriction must be satisfied by any calculation of the ground-state energy as a function of the electron density. Before stating the theorem we wish to illustrate with the specific case of the calculation of Gell-Mann and Brueckner[1] (GMB). They have derived the formula

$$E(r_s) = 2.21\, r_s^{-2} - 0.916\, r_s^{-1} + 0.0622 \ln r_s - 0.096 \qquad (1)$$

for the ground-state energy per electron, measured in Rydbergs. r_s is the usual radius of the unit sphere measured in Bohr radii, and serves as a dimensionless measure of the electron density. Thus Eq. (1) gives the functional dependence of the ground-state energy on the density, and according to GMB becomes exact in the high-density limit ($r_s \to 0$). Although it is clear that Eq. (1) can only claim approximate validity for finite densities, it is tempting to hope that Eq. (1) may nevertheless be sufficiently accurate to be useful for the density range of practical interest ($2 < r_s < 5.5$). But we shall see that this is definitely not the case. It is not feasible to evaluate directly the error due to the omission of higher powers of r_s in Eq. (1), but it is possible to obtain a rigorous lower bound on the magnitude of the error. On the basis of the theorem stated in the next paragraph we shall establish that as r_s is allowed to become greater than unity a serious error sets in, whose magnitude for $r_s = 3$ amounts already to at least forty percent of the GMB correlation energy itself [the last two terms of Eq. (1)].

The theorem upon which our discussion is based is the following: Theorem 1. The lowest eigenvalue of a Hermitian operator which contains a parameter linearly has a nonpositive second derivative with respect to the parameter. This theorem is readily recognized as being a statement of a familiar property of second-order stationary-state perturbation theory in quantum mechanics. Suppose that the complete set of exact eigenfunctions and eigenvalues is known when the parameter, or "coupling constant," has the value λ. They can then be used to compute the ground-state energy for the neighboring value $\lambda + \Delta\lambda$. By means of perturbation theory one can obtain a power series expansion in $\Delta\lambda$. Recalling that the ground state is always lowered in second order, we see that the coefficient of $(\Delta\lambda)^2$ must be negative, from which follows the theorem as stated. An explicit proof, constructed from the variational principle, will appear along with related items in a more detailed paper on the correlation energy.[2]

Theorem 1 is readily applied to the fictitious, nonphysical alternative problem posed by keeping the electron gas density fixed at the value corresponding to $r_s = 1$, but allowing the strength of the Coulomb interactions to change by the factor λ. In other words, the square of the electron charge is changed from e^2 to λe^2. Let the energy in Rydbergs per electron as a function of λ be $g(\lambda)$. Simple dimensional scaling considerations show that the two problems are related by the equation

$$g(\lambda) = \lambda^2 E(\lambda). \qquad (2)$$

Since the requirement of Theorem 1 is expressed by the equation

$$g''(\lambda) \leq 0, \qquad (3)$$

where we use a prime to denote differentiation, it follows by substitution from Eq. (2) that the same restriction expressed in terms of density variations is

$$E''(r_s) + 4\, r_s^{-1} E'(r_s) + 2\, r_s^{-2} E(r_s) \leq 0. \qquad (4)$$

Comparison of Eqs. (3) and (4) makes it clear that for the present purposes the correlation energy is more easily studied in terms of the picture which involves "turning on the interaction" rather than the picture of "allowing the gas to expand" from its high-density limit.

Substitution of Eq. (1) into (2) gives

$$g(\lambda) = 2.21 - 0.916\,\lambda + 0.0622\,\lambda^2 \ln\lambda - 0.096\,\lambda^2. \qquad (5)$$

Differentiating twice and substituting into Eq. (3) yields

$$\lambda \leq 1.05. \qquad (6)$$

In order that Theorem 1 not be violated for values of λ in excess of 1.05, the remaining higher-order terms neglected in Eqs. (1) and (5) must be included. On the basis of Eq. (3) it is easy to see that they must be negative and amount to at least

$$\Delta g(\lambda) = -0.0622\,\lambda^2 \ln\lambda + 0.096\,\lambda^2 - 0.130\,\lambda + 0.034. \qquad (7)$$

For $\lambda = 3$, Eq. (7) yields $\Delta g = -0.10$, while the last two terms in Eq. (5) (the correlation energy)

amount to -0.25. Thus we see that the GMB calculation greatly underestimates the magnitude of the correlation energy for the larger values of coupling constant, or in terms of density, for the larger values of r_s. The error grows as the density is decreased and amounts to at least 40% for $r_s = 3$. Although this is a rigorous lower limit on the error in Eq. (1) and has been established here without employing any special model or theory, it should be noted that Nozières and Pines[3] reach qualitatively this same conclusion concerning the GMB formula on the basis of a detailed calculation using the Bohm-Pines formalism.

In conclusion, we wish to emphasize that the limitation found here on the range of validity of Eq. (1) is in no way inconsistent with the claims of GMB and in no way detracts from the fundamental theoretical interest of their work as a weak-coupling calculation. We also wish to acknowledge a stimulating discussion with Dr. Michael Cohen which led to this investigation.

---

*Investigation carried out by the author as consultant to the Rand Corporation, while on summer leave from the University of Maryland.

[1]M. Gell-Mann and K. A. Brueckner, Phys. Rev. 106, 364 (1957). This paper should be consulted for references to the earlier work.

[2]R. A. Ferrell (to be published).

[3]P. Nozières and D. Pines, Phys. Rev. 111, 442 (1958). This paper contains references to most of the work which has appeared since the GMB paper. In particular, see also J. Hubbard, Proc. Roy. Soc. (London) A243, 336 (1957).

MEASUREMENT OF THE RANGE OF RECOIL ATOMS

Roman A. Schmitt and Rodman A. Sharp
John Jay Hopkins Laboratory
for Pure and Applied Science,
General Atomic, San Diego, California
(Received November 3, 1958)

An important problem[1] in the interpretation of radiation-damage and sputtering phenomena is the evaluation of the range of an atom which moves through a lattice after having received an initial energy of 10 to 100 kev. A novel experimental technique has been applied to the problem of determining the ranges of atoms in the kev region. Atoms with initial energies in this region are produced by irradiating suitable targets with high-energy bremsstrahlung, and the products of photonuclear reactions, such as photoneutron (γ, n) transmutations, are observed. The bremsstrahlung used in this work were generated by a 24-Mev Allis-Chalmers betatron. The photon spectrum is continuous from 0 to 24 Mev; the energy spectra of evaporated neutrons from copper[2] and lead[3] are centered at about 1.5 Mev, with a full width at half maximum of about 2 Mev. Since (1) the energy thresholds for the photoneutron reactions of the majority of the elements reported in Table I are well below 24 Mev and near the copper and lead photoneutron thresholds and (2) all the photonuclear absorption cross sections of elements in Table I closely resemble the giant-resonance cross-section curve of copper and lead, it is anticipated that the spectra of evaporated neutrons for all the targets studied here are centered at about 1.5 Mev, with corresponding half-widths of 2 Mev.

The nucleus receives a negligible amount of momentum from the incoming gamma ray. However, the nucleus (atom) recoils from neutron emission with an energy E_R, given by the formula $E_R = E_N(M_N/M_A)$, where E_N is the neutron energy and M_N and M_A are the masses of the neutron and atom, respectively. As a result of photoneutron emission, the nuclei of the recoiling atoms are usually unstable to beta (positron) decay and, therefore, are amenable to detection by standard scintillation and beta-counting methods.

The ranges were determined for carbon (C^{11} in polystyrene, CH), fluorine (F^{18} in Teflon, CF_2), chlorine (Cl^{34} in Saran, CHCl), and the metals titanium, iron, zinc, copper, molybdenum, silver, and gold in their respective metallic lattices. The method used was somewhat similar to the stacked-foil technique commonly used in charged-particle excitation-function studies. Thin elemental or plastic target foils about 0.001 in. thick were interleaved between 0.0008-in. thick aluminum catchers (Alcoa 1199-0, 99.986% pure). Before use, the metallic foils were cleaned with organic solvents and etched with appropriate acids; plastic foils were detergent-cleaned. In order to evaluate the background activities present in the aluminum catchers, an equal number of aluminum foils without targets were simultaneously irradiated. About 2000 roentgens per minute of 23-Mev bremsstrahlung were incident on the sandwiched targets.

Immediately after irradiation, the sandwich was disassembled and the radioactivities of the

target foils, aluminum catcher foils, and aluminum background-monitoring foils were measured by scintillation-counting the annihilation radiation (0.51 Mev) of the positrons with the single exception of gold (Au^{196}), which was detected via its 354-kev gamma ray. The recoiling atoms which are close to the target-foil surface are caught in the aluminum foils. If the range of the recoil atoms is small compared with the foil thickness, then the range, R, is related to the fraction N_C/N_f of atoms which recoil out of the target foil and to the foil thickness, x, by $R = 2(N_C/N_f)x$, where N_C and N_f are the numbers of atoms that recoil into the catcher and that are retained in the target foil, respectively.

The ranges, obtained by the formula $2(N_C/N_f)x$, are the vector sums of the tortuous paths traveled by the recoiling atoms. Theoretical ranges, calculated by assuming billiard-ball collisions, were made according to Seitz and Koehler,[1] and, in general, the theoretical ranges were many times higher than those observed. Nielsen,[4] following the lines of Bohr,[5] obtains the following theoretical expression for the range:

$$R = 0.6 \frac{(Z_1^{2/3} + Z_2^{2/3})^{1/2}}{Z_1 Z_2} \frac{A_1 + A_2}{A_1} \times A_2 E_1 (\mu g/cm^2) ,$$

where Z_1, A_1 and Z_2, A_2 are the atomic numbers and masses for the incoming particles and the target atoms, respectively, and E_1 is the energy of the incoming particle in kev. In calculating the theoretical ranges for the nonmetals (C^{11}, F^{18}, and Cl^{34}) in their respective plastic matrices, Z_2 and A_2 have been averaged stoichiometrically over the target-foil atoms, excluding the hydrogen atoms. Agreement between observed and theoretical range values is rather good (within a factor of two for most ranges).

The fraction of metal atoms that recoil out of 0.001-in. foils varies exponentially with $1/A$ (which is proportional to the recoil energy); fluorine, chlorine, and carbon in the plastic

Table I. Fraction (N_C/N_f) of activated atoms recoiling out of 0.001-in. foils and calculated ranges of the recoil atoms. (23-Mev bremsstrahlung incident on foils.)

Recoiling atom	Most probable recoil energy [a] (kev)	$(N_C/N_f) \times 10^4$ [b]	Observed range in A (10^{-8}cm)	Observed range in $\mu g/cm^2$ [c]	Theoretical range in $\mu g/cm^2$ [d]
C^{11}	130	216 ± 20	11 000 [e, f]	117	214 [g]
F^{18}	85	182 ± 18	9200 [e, h]	200	105
Cl^{34}	45	104 ± 10	5300 [e, h]	90	31 [g]
Ti^{45}	33	6.1 ± 0.8	310	14	25
Fe^{53}	30	11.0 ± 1.7	560	44	20
Zn^{63}	25	2.7 ± 0.3	137	9.8	15
Cu^{62}	25 ± 16	3.1 ± 0.2	163	14.5	16
Cu^{64}	25 ± 16	3.2 ± 0.2	157	14.0	16
Mo^{91}	16	1.4 ± 0.4	71	7.3	8.1
Ag^{106}	14	1.4 ± 0.3	71	7.5	6.7
Au^{196}	9	0.55 ± 0.06	28	5.4	3.2

[a] Estimated by assuming that the evaporated-neutron spectra were similar in shape to those observed for copper and lead. The average recoil energy is assumed to be 1.6 times the most probable recoil energy.

[b] Errors are two standard deviations of counting statistics only.

[c] Obtained from the previous column by the formula $R\rho$, where R is the range and ρ is the density of the target foil.

[d] Theoretical ranges calculated according to K. O. Nielsen [reference 4, p. 73, Eq. (13)].

[e] Range of C^{11} is in polystyrene (CH); for Cl^{34}, in Saran (CHCl); and for F^{18}, in Teflon (CF_2). Other ranges are in their respective metallic lattices.

[f] Range of C^{11} (for same recoil energy) in polyethylene (CH_2) and in cellulose acetate ($C_{1.0}H_{1.3}O_{0.7}$) are 10 600 ± 1100 A and 11 900 ± 1800 A, respectively.

[g] With the exception of the hydrogen atoms, it was assumed that the target atoms shared equally in stopping the recoiling atoms. Hydrogen atoms were neglected in the calculations.

[h] Preliminary experiments on recoil ranges of F^{20} and Cl^{38} – produced by (n,γ) reactions and having recoil energies of <0.5 kev–in Teflon and Saran, respectively, indicate anomalously large ranges of several thousand angstroms.

matrices increase slowly with $1/A$. By performing recoil experiments with photoproton, photodeuteron, and photoalpha transmutations, it will be possible to see the effect on N_c/N_f by varying the recoil energy only.

It should be noted that the N_c/N_f fractions for Cu^{62} and Cu^{64} agree well within experimental error. Since the photoneutron thresholds for Cu^{62} and Cu^{64} are nearly equal (10.7 and 10.0 Mev, respectively) and the corresponding photoneutron cross sections are roughly superimposable after normalization by a constant factor, the kinetic energies of the evaporated neutrons are expected to be identical. By measuring the average evaporated photoneutron energy, using the simple recoil technique outlined in this paper, it is possible to compare the nuclear temperatures of pairs of excited nuclei. The comparison should be restricted to a narrow range of atomic numbers because of the variation in recoil range with electronic structure.

We wish to acknowledge helpful discussions with Dr. Victor A. J. van Lint of General Atomic and the generous cooperation of Dr. Waldo K. Lyon and Mr. R. B. Doherty of the U. S. Navy Electronics Laboratory, San Diego, California, in the performance of these irradiations.

[1]F. Seitz and J. S. Koehler, in Solid State Physics, edited by F. Seitz and D. Turnbull (Academic Press, Inc., New York, 1956), Vol. 2, p. 305.

[2]P. R. Byerly, Jr., and W. E. Stephens, Phys. Rev. 83, 54 (1951).

[3]M. E. Toms and W. E. Stephens, Phys. Rev. 108, 77 (1957).

[4]K. O. Nielsen, Electromagnetically Enriched Isotopes and Mass Spectrometry (Academic Press, Inc., New York, and Butterworth and Company, London, 1956).

[5]N. Bohr, Kgl. Danske Videnskab. Selskab, Mat.-fys. Medd. 18, No. 8 (1948).

THERMAL EFFECTS OF THE MARTENSITIC TRANSFORMATION IN LITHIUM

Douglas L. Martin
Division of Pure Physics,
National Research Council,
Ottawa, Canada
(Received November 4, 1958)

Some measurements on sodium showing the influence of the martensitic transformation[1,2] on the specific heat have been reported in a previous letter.[3] The similar transformation in lithium metal[4,5] has now been investigated using the same technique and apparatus. On cooling below about 80°K the body centered cubic lattice begins to change to hexagonal close packed with stacking faults. The extent of the transformation depends on the purity and previous thermal history of the specimen and also on the temperature to which it is cooled. Figure 1 shows the specific heat of b.c.c. lithium as a continuous line and the anomalous specific heat found after cooling to 55°K (from room temperature) as a dotted line. (The experimental points have been omitted for clarity.) The anomaly occurs in the temperature range where that part of the sample which had been transformed on cooling reverts from h.c.p. to b.c.c. lattice. The excess energy absorbed on heating through this region is about 7 cal/g atom. The temperature range observed for reversion agrees well with the x-ray observations of Barrett and Trautz.[5]

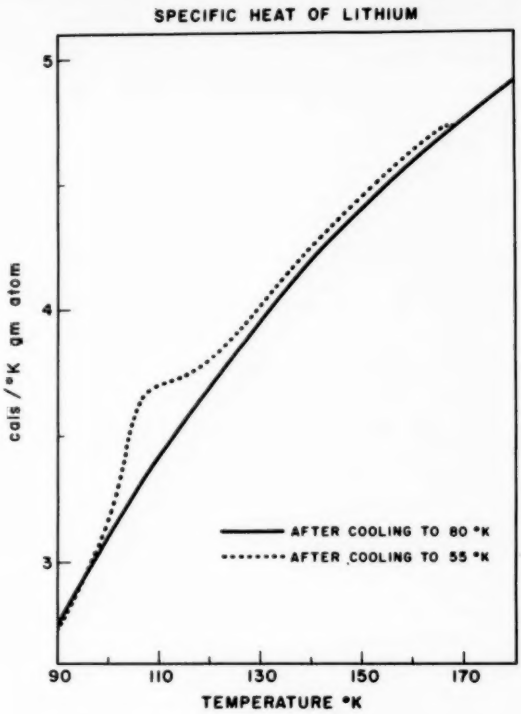

FIG. 1. The specific heat of lithium.

Below the temperature region of the reversion anomaly the specific heat of lithium remains dependent upon the thermal history of the sample. Differences of the order of 1% have been observed and, by observation of the heat content of

the anomaly on warming, are found to correlate directly with the proportion of h.c.p. phase present. As expected thermodynamically the h.c.p. phase has a higher Debye temperature than the b.c.c. phase.

Recent experiments by other workers in this laboratory have shown that the martensitic transformation also affects the electrical[6] and mechanical[7] properties of lithium.

A full account of this work will be published later.

---

[1]C. S. Barrett, J. Inst. Metals 84, 43 (1955).
[2]C. S. Barrett, Acta Cryst. 9, 671 (1956).
[3]D. L. Martin, Phys. Rev. Lett. 1, 4 (1958).
[4]C. S. Barrett, Phys. Rev. 72, 245 (1947).
[5]C. S. Barrett and O. R. Trautz, Trans. Am. Inst. Mining Met. Engrs. 175, 579 (1948).
[6]J. S. Dugdale and D. Gugan (private communication).
[7]L. Verdini (private communication).

MASER ACTION IN THE REGION OF 60°K

C. R. Ditchfield and P. A. Forrester
Physics Department,
Royal Radar Establishment,
Great Malvern, England
(Received November 17, 1958)

A three-level solid-state maser of the type suggested by Bloembergen[1] has been operated successfully by several investigators.[2-6] In these experiments, the cavity containing the active material was cooled to temperatures of a few degrees Kelvin by the use of liquid helium. In the course of our investigations, we have operated such a maser using a cavity cooled by other refrigerants, notably oxygen and nitrogen, to temperatures in the region of 60°K.

The cavity, in the form of a right circular cylinder split midway along its axis, was designed to support the TE_{013} mode at pump frequencies in the neighborhood of 24 kMc/sec and the TE_{111} mode at signal frequencies near 9.3 kMc/sec. It was 1.167 inches long and 0.802 inches in diameter. The pump power was coupled to the cavity from a wave guide through an iris, and the signal-frequency coupling was effected by means of a loop terminating a coaxial line. The paramagnetic material was in the form of a sphere of ruby,[7] 0.625 inches in diameter, which had a nominal concentration of 0.1% chromium. The presence of such a large sample resulted in an increase in the number of cavity resonances which allowed operation at various frequencies in the region of interest.

At the polar angle $\theta = 54° 44'$ the four energy levels of the Cr^{+++} ion are split so that the levels (3) and (4) are the mirror images in energy of the levels (2) and (1). The transitions between the levels (1) and (3) and between (2) and (4) are thus degenerate for all values of the external magnetic field. Hence by using a single pump frequency it is possible to modify the population difference between levels (2) and (3) by a "push-pull" action.[8] It is easy to set up this condition experimentally by observing at room temperature the onset of degeneracy between the above pump transitions, or of the absorption lines arising from the transitions at the signal frequency between levels (2) and (1) and between (3) and (4).

The cavity assembly was enclosed in a conventional double Dewar system. The outer Dewar contained liquid nitrogen at atmospheric pressure and the inner Dewar contained the refrigerant pumped to a low pressure. Below 63.2°K nitrogen at reduced pressures is a solid and some trouble was experienced due to insufficient thermal contact between the refrigerant and the wave guide assembly. Oxygen has been used in preference in later experiments as the triple point is appreciably lower, 54.4°K. The rate of evaporation of the liquid oxygen was about 40 ml per hour so that a run of about 40 hours is possible for one filling of the Dewar.

At 78°K, variation of the pump power level produced a strong interaction on the signal frequency absorption. It was possible, in fact, to remove the center of the absorption line, rendering the sample transparent at this signal frequency, but, to date, no appreciable stimulated emission has been observed at this temperature with the available pump power. However, at temperatures below about 60°K, amplification and oscillation have been observed over the frequency range from 9280 Mc/sec to 9520 Mc/sec, the predicted pump frequencies in the region of 23.5 kMc/sec to 24 kMc/sec being in good agreement with theoretical calculations of D. J. Howarth of this laboratory. At these temperatures "push-pull" pumping should theoretically be about six times more efficient than single pumping in producing a negative spin temperature. Indeed, although single pumping produces a strong interaction with the signal frequency absorption, it has not been found possible to pro-

duce any stimulated emission at 56°K when the crystal was misorientated by more than a degree from the "push-pull" condition.

The results quoted below were obtained by an experiment using liquid oxygen pumped to a pressure of about 2 mm of mercury, which indicated a temperature near to 56°K. The cavity Q was in the region of 20 000. The pump power available was limited, our source being a war surplus 2K33 klystron whose power output was measured to be 50 milliwatts at the frequency of interest. It was apparent that the power entering the cavity was not sufficient to saturate the pump transitions completely. With the cavity undercoupled at the signal frequency, oscillations were observed, the power output being 50 microwatts at a frequency of 9518 Mc/sec. By using increased penetration of the coupling loop, the cavity could be overcoupled at the signal frequency and stable gain was achieved up to 30 db. The product $B\sqrt{G}$ was measured to be 3.8 Mc/sec. This figure was constant for signal levels in the range 10^{-12} to 10^{-7} watts.

The successful operation of a maser at these comparatively high temperatures has both theoretical interest, indicating that the relaxation processes are not so temperature dependent as was at one time envisaged, and also practical importance, as freedom from the use of liquid helium will simplify considerably the operation of maser equipment in the field. In conclusion, we would emphasize that our results are preliminary only, being obtained with restricted pump power, a cavity designed for experiments with another material at helium temperatures, and using an active sample whose size and shape were determined for us by chance. Thus we hope to see better performance data as a result of further development.

[1]N. Bloembergen, Phys. Rev. 104, 324 (1956).
[2]Scovil, Feher, and Seidel, Phys. Rev. 105, 762 (1957).
[3]A. L. McWhorter and J. W. Meyer, Phys. Rev. 109, 312 (1958).
[4]Strandberg, Davis, Faughan, Kyhl, and Wolga, Phys. Rev. 109, 1988 (1958).
[5]Artman, Bloembergen, and Shapiro, Phys. Rev. 109, 1392 (1958).
[6]Makhov, Kikuchi, Lambe, and Terhune, Phys. Rev. 109, 1399 (1958).
[7]This sample was obtained through the courtesy of Dr. A. E. Siegman of Stanford University.

FERROMAGNETIC SUPERCONDUCTORS

B. T. Matthias, H. Suhl, and E. Corenzwit
Bell Telephone Laboratories,
Murray Hill, New Jersey
(Received November 24, 1958)

Studies previously reported,[1] particularly on lanthanum-gadolinium solutions, have raised the possibility that the phenomena of superconductivity and ferromagnetism might overlap, resulting in a ferromagnetic superconductor. An interesting case where this occurs is found in the solid solutions between $CeRu_2$ (superconducting at about 5.1°K) and $PrRu_2$ or $GdRu_2$ (respectively, ferromagnetic at 40° and above 70°K).

The first system, $(Ce,Pr)Ru_2$, is shown in Fig. 1 and the region at which superconductivity and ferromagnetism might overlap is at temperatures below 1°K, not conveniently accessible with our apparatus.

The second system, $(Ce,Gd)Ru_2$, however, gave a temperature region a good deal above 1°K for the simultaneous occurrence of superconductivity and ferromagnetism in the same sample though perhaps not in the same volume element. This is shown in Fig. 2. For a composition of $Ce_{0.94}Gd_{0.06}Ru_2$, Curie point (Cpt) and superconducting transition temperature (T_c) coincide, provided the measuring field is below 10 gauss. With larger fields T_c can be lowered and so be more separated from the corresponding Cpt. For compositions with much higher T_c than Cpt the measurements require the destruction of superconductivity by a magnetic field before ferromagnetism can be detected. The inverse case in which the Cpt is higher than T_c is a much

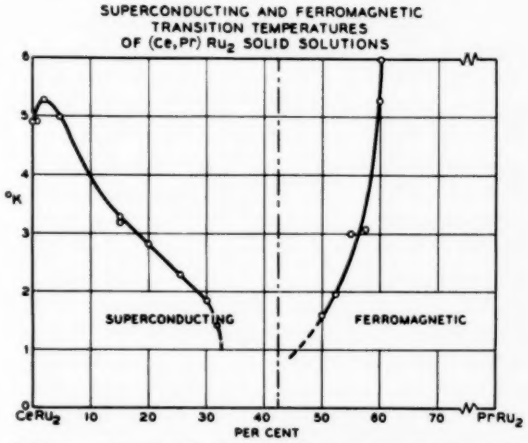

FIG. 1. Superconducting and ferromagnetic transition temperatures of $(Ce, Pr)Ru_2$ solid solutions.

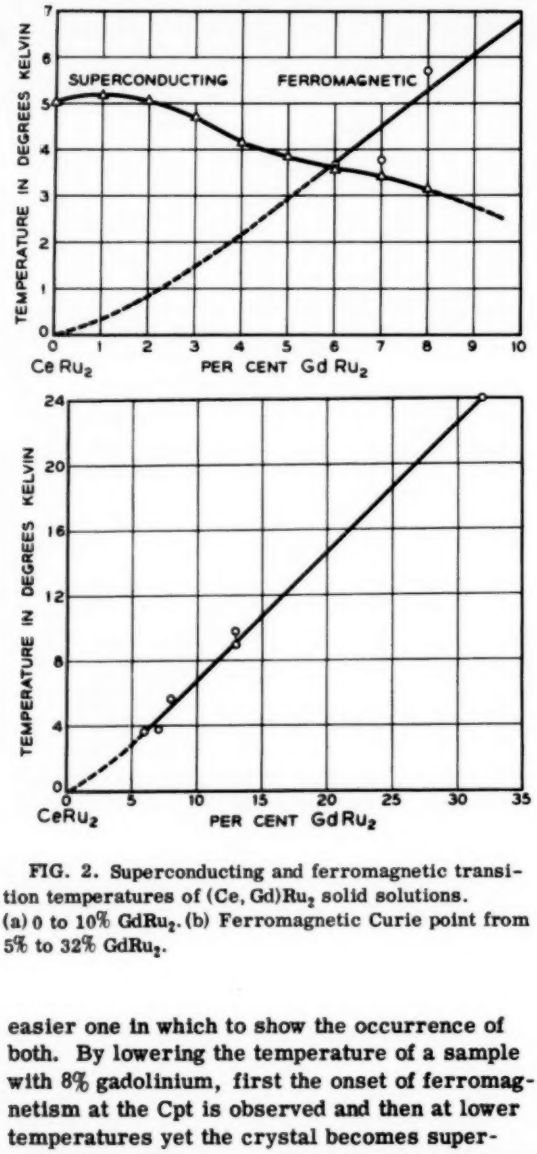

FIG. 2. Superconducting and ferromagnetic transition temperatures of (Ce, Gd)Ru_2 solid solutions. (a) 0 to 10% $GdRu_2$. (b) Ferromagnetic Curie point from 5% to 32% $GdRu_2$.

easier one in which to show the occurrence of both. By lowering the temperature of a sample with 8% gadolinium, first the onset of ferromagnetism at the Cpt is observed and then at lower temperatures yet the crystal becomes superconducting. However, at these low temperatures the spontaneous ferromagnetic polarization is more than an order of magnitude larger than any frozen-in flux would be for a typical nonmagnetic superconductor.

The fact that so much flux escapes the sample even though it is superconducting would suggest that the sample never leaves the intermediate state. If, as seems likely, a typical conduction electron in the sample is acted on by the total flux, the London equation curl $\vec{j} = (1/\lambda c)\vec{B}$ and Maxwell's equations demand that $B \to 0$ in the interior of a massive specimen, and only the flux in a shell of order of the penetration depth can escape, giving a negligible total moment. This is, of course, not the case if there is a pattern of superconducting domains whose sizes adjust themselves to yield the observed flux.

We want to thank Dr. A. M. Clogston for many stimulating discussions, and Mrs. V. B. Compton for all the structural work.

[1]Matthias, Suhl, and Corenzwit, Phys. Rev. Lett. 1, 92 (1958).

MOBILE AND IMMOBILE EFFECTIVE-MASS-PARTICLE COMPLEXES IN NONMETALLIC SOLIDS

Murray A. Lampert
RCA Laboratories,
Princeton, New Jersey
(Received November 14, 1958)

Quite recently the study of excitons has taken a front-rank position among the techniques for the study of nonmetallic solids.[1] It is the purpose of this note to outline a natural extension of the concept of the exciton, namely to consider bound aggregates of two or more charged particles in a nonmetallic solid, at least two of which are effective-mass particles, i.e., electrons in a conduction band or holes in a valence band. We refer to such aggregates as "effective-mass-particle complexes."[2] The exciton itself is, of course, the simplest such complex. The choice of nomenclature reflects the restriction of our discussion to those weakly bound complexes for which the well-known effective-mass approximation gives a good description of the "envelope" motion of the electrons and holes. Therefore our conclusions are particularly relevant to those solids (e.g., Ge, GaAs, CdS) for which the only possible excitons are shallow ones. A complex which has as a constituent member an ion fixed in the lattice is localized about the ion and hence is called an immobile complex. On the other hand, a complex consisting entirely of effective-mass particles is obviously a mobile complex.[3]

We have listed some five types of complexes in Table I, which also contains explanations of the notation. For the sake of simplicity we assume spherical constant-energy surfaces for electrons and holes. In enumerating complexes

in Table I we have omitted those complexes obtained by reversing the sign of all members of a complex, since for simple band models nothing essentially new is obtained by this operation. However, note that for solids with complicated band structures, such as Ge and Si, sign reversal can indeed produce a "new" complex, i.e., one with different energy-level structure.

We are able to describe, without further ado, the electronic structure of the complexes A-E in Table I for limiting values of the ratio of hole to electron effective masses, namely for $m_h/m_e \gg 1$, $=1$, and $\ll 1$. For, in these limits, each complex is analogous, as listed, to either a molecular or polyelectron structure which has already been investigated, at least theoretically, if not experimentally. (An exception is the Type A complex with $m_h/m_e = 1$ for which the author did not find a suitable reference.) The energy level structure of any complex listed in Table I is basically that of its analog. Thus, for those structures analogous to H_2^+, the gross energy level scheme is the electronic level scheme of H_2^+. Each electronic level has a fine structure similar to the vibration-rotation level scheme of H_2^+. A similar description holds for those complexes analogous to H_2. Those complexes analogous to H^- have only a single bound state.[4] The existence or nonexistence of bound, excited states of the polyelectrons which are listed appears not to have been established to date. It is not known whether the complex $\oplus+-$, for $m_h/m_e \ll 1$, is stable. The hole moves in the electrostatic field of a "fixed" dipole determined by $\oplus$ and the instantaneous position of -. If the hole is bound,[5] its orbit moves adiabatically with the electron around the ion. The complex $\oplus+--$, for $m_h/m_e \ll 1$, consists of a hole bound to a Coulomb attractive "center," namely the H^--like complex $\oplus--$. The corresponding hole levels are the hydrogenic levels modified by the spatial extent of the "center."

The discussion in this note should be applicable quantitatively to the semiconductors GaAs, InAs,

Table I. Some complexes and their properties. Notation: $\oplus$ denotes a positive ion[a] fixed in the lattice, + a hole in the valence band, and - and electron in the conduction band. $\oplus+--$ denotes a complex consisting of two electrons and one hole bound to a positive ion, and similarly for other complexes. Units: length, $a_S = \epsilon m a_0/m_e$; energy, $E_S = m_e E_0/m\epsilon^2$. ϵ is the static dielectric constant of the host lattice; m is the mass of the electron in vacuum; m_e is the effective mass of an electron near the minimum of the conduction band; m_h is the effective mass of a hole near the maximum of the valence band; a_0 is the Bohr radius in vacuum, $a_0 = \hbar^2/me^2 \simeq 0.53$ A; $E_0 = e^2/2a_0 \simeq 13.6$ ev; D_0 is the dissociation energy of the complex; $r_{\oplus+}$ is the average separation of $\oplus$ and + in the complex, and similarly for analogous symbols; e^+ is a positron, e^- an electron. $e^+e^+e^-$ and $e^+e^+e^-e^-$ are polyelectrons.[b]

	Complex	m_h/m_e	Analog	D_0	Average separations
A:	$\oplus+-$	$\gg 1$	H_2^+	0.21	$r_{\oplus+} \simeq 2$
		$\ll 1$	See text		
B:	$\oplus--$		H^-	0.055	
C:	$++-$	$\gg 1$	H_2^+	0.21	$r_{\oplus+} \simeq 2$
		1	$e^+e^+e^-$	0.0015[c]	
		$\ll 1$	H^-	$0.055 m_h/m_e$	
D:	$++--$	$\gg 1$	H_2	0.35	$r_{++} \simeq 1.4$
		1	$e^+e^+e^-e^-$	0.010[d]	$r_{++} = r_{--} \simeq 8.5$[d]
					$r_{+-} \simeq 5.7$
		$\ll 1$	H_2	$0.35 m_h/m_e$	$r_{--} \simeq 1.4 m_e/m_h$
E:	$\oplus+--$	$\gg 1$	H_2	0.35	$r_{\oplus+} \simeq 1.4$
		1	H^-e^+	0.0050[e]	
		$\ll 1$	See text		

[a] To avoid complications we assume that the positive ion is such that the lowest state of the $\oplus$-atom is a shallow, hydrogen-like state. Thus, in Ge $\oplus$ might be a Group V substitutional donor ion.

[b] See reference 3.

[c] E. A. Hylleraas, Phys. Rev. 71, 491 (1947).

[d] A. Ore, Phys. Rev. 71, 914 (1947).

[e] A. Ore, Phys. Rev. 83, 665 (1951).

InP, InSb, and GaSb. In these materials the electron effective mass is isotropic and about an order of magnitude, at least, smaller than the average hole mass. Thus we do not expect the complications in the structure of the valence band to alter drastically the estimated dissociation energies of the various complexes, as given for the limiting case $m_h/m_e \gg 1$, although the detailed structure of the envelope wave functions may be complicated. It may be of practical significance that for these materials the dissociation energies of the "excitonic ion" ++- and the "excitonic molecule"++-- are an appreciable fraction of the binding energy of the exciton itself. The situation in Ge and Si calls for a more refined analysis. Although the "average" electron and hole effective masses are approximately equal, the complications both in conduction and valence band structure are such that the polyelectron model for the complexes is probably too simplified to apply in these materials. In any case, the effective-mass formalism for the study of the complexes is a straightforward extension of Dresselhaus' formalism for the description of the exciton.[6]

Observable effects due to the complexes must be sought in the 1-4°K temperature range where at least some of the complexes will have a dissociation energy many times kT. An experiment of particular interest might be the cyclotron resonance of the excitonic ions ++- or --+ which are both charged and mobile. Probably the most efficient means of generating the complexes are through the excitation of free electron-hole pairs, say by light, and subsequent reactions (exciton formation and interaction of excitons among themselves and with free carriers and with ions). The steady-state density of excitons n_x in equilibrium with electrons and holes of densities n and p, respectively, produced by excitation, is given by $n_x = np\bar{v}\sigma_x\tau_x$, where $\bar{v}$ is the rms relative velocity of electrons and holes, σ_x their cross section for exciton formation, and τ_x the exciton life-time. At helium temperatures, taking $\bar{v} \approx 10^6$ cm/sec and $\sigma_x \cong 10^{-12}$ cm^2 then $n_x \approx 10^{-6} np\,\tau_x$. Producing $np \gtrsim 10^{24}$ by light, and assuming[7] $\tau_x \gtrsim 10^{-2}$ sec, $n_x \gtrsim 10^{16}$ cm^{-3} appears readily obtainable.

In similar fashion, rough estimates can be made for attainable densities of the various complexes listed in Table I.

It has been the purpose of this letter to bring to the attention of solid-state physicists a hitherto unexplored area. Work is continuing on more accurate, variational calculations of the dissociation energy of some of the complexes.

The author would like to express his indebtedness to Dr. D. O. North, Dr. F. Herman, and Dr. R. H. Parmenter, and to his other colleagues at the RCA Laboratories who have made incisive suggestions both as to technical content and style.

---

[1]See the review article by H. Haken in Halbleiterprobleme, edited by W. Schottky (F. Vieweg und Sohn, Braunschweig, 1958), Vol. 4, for a survey of the exciton problem and a bibliography. For the most recent developments also see the Proceedings of the International Conference on Semiconductors, Rochester, 1958, J. Phys. Chem. Solids (to be published).

[2]I am indebted to Dr. John Kessler of the RCA Laboratories for assistance in the choice of nomenclature. Dr. Kessler had independently speculated about some of the problems discussed here.

[3]Mobile complexes are analogous to J. A. Wheeler's "polyelectrons"; see Ann. N.Y. Acad. Sci. 48, 219 (1946). Indeed for the case of simple, spherical bands and equal effective masses for the hole and electron, we are able to utilize already-existing calculations on polyelectrons, as evidenced in Table I.

[4]H. A. Bethe and E. E. Salpeter, Handbuch der Physik (Springer-Verlag, Berlin, 1957), Vol. 35, p. 240. With regard to the complex ++-, the fact that in the H^--like limit, $m_h/m_e \ll 1$, there is only one bound state leads to the speculation that for any finite value of m_h/m_e, no matter how large, there are only a finite number of bound states of the corresponding complex. If the speculation is false, it would be of interest to determine the precise value of m_h/m_e at which an infinite number of bound states first appear.

[5]Wallis, Herman, and Milnes have studied the "Energy Levels of an Electron in the Field of a Finite Dipole" [Bull. Am. Phys. Soc. Ser. II, 3, 53, (1958) and to be published]. The authors did not settle the problem of the existence of a bound state in the limiting region where $R/a_0 \ll 1$ (R being the dipole length), which corresponds to the case discussed above. I am indebted to Dr. Wallis for sending me a preprint of the full article.

[6]G. Dresselhaus, J. Phys. Chem. Solids 1, 15 (1956).

[7]Thus the lifetime of the exciton against self-annihilation is assumed to exceed 10^{-8} sec. Its lifetime $\tau_{x,c}$ against any process catalyzed by an "impurity" of density N_C is given by $\tau_{x,c} = (N_C\bar{v}\sigma_C)^{-1} \gtrsim 10^6/N_C$ since $\sigma_C \lesssim 10^{-12}$cm^2, the cross section for a Coulomb-attractive reaction at helium temperatures. Chemical purification achieving $N_C \lesssim 10^{14}$ cm^{-3} guarantees that $\tau_{x,c} \gtrsim 10^{-8}$ sec. A likely catalytic process for breakup of the exciton is a charge-exchange reaction in which, for example, the electron member of the exciton is captured by a positive ion, the hole being freed into the valence band. The cross section for this reaction in Ge is estimated to be about 10^{-12} cm^2. The maximum possible density of excitons $n_{x,\max}$ is obtained if the

excitons are in quasi-thermal equilibrium with the free carriers, i.e., if the most likely mode of breakup of the exciton is thermal dissociation. For a given n and p, $n_{X,\max} \simeq (N_X np/N_V N_C)\exp(E_X/kT) \simeq 4\times 10^{-16}\{m \times (m_e + m_h)/m_e m_h\}^{3/2} T^{-3/2}\, np\exp(E_X/kT)$, where E_X is the binding energy of the exciton, N_X, N_V, N_C are the effective densities of states of the exciton, valence, and conduction bands, respectively, near their respective extrema. Taking $T=4°K$ and assuming that $\{\ \}^{3/2} \approx 1$ and that $E_X \approx 10kT \approx 4\times 10^{-3}$ ev, we obtain $n_{X,\max} \approx 10^{-15} np$ under these conditions.

Li^7 AND F^{19} NUCLEAR MAGNETIC RESONANCES IN NEUTRON-IRRADIATED LiF†

P. J. Ring, J. G. O'Keefe, and P. J. Bray
Physics Department,
Brown University,
Providence, Rhode Island
(Received November 19, 1958)

Nuclear magnetic resonance examinations of LiF samples subjected to neutron dosages of the order of 10^{18} nvt have revealed the presence of constituent nuclei in environments other than those of the normal lattice sites. These nuclei produce narrow lines which are superimposed on the normal broad lines.

The fluorine line, Fig. 1, was observed in a single crystal[1] of LiF which had received a neutron dose of 1×10^{19} nvt. The resonance was observed at a frequency of 28.5 Mc/sec and the separation of the centers of the two derivative traces was 18.5 kc/sec. This is a shift of about 0.07% to a higher frequency for the more narrow

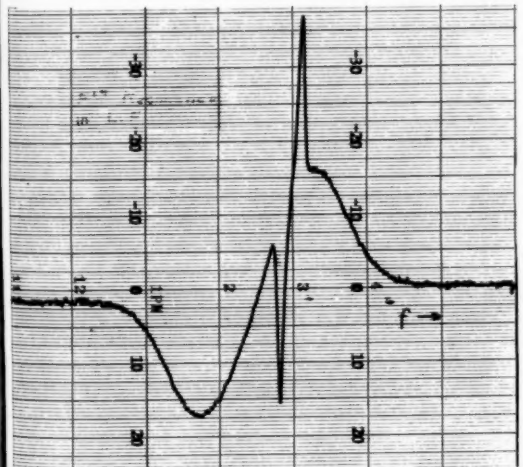

FIG. 1. F^{19} resonances in a neutron-irradiated single crystal of LiF.

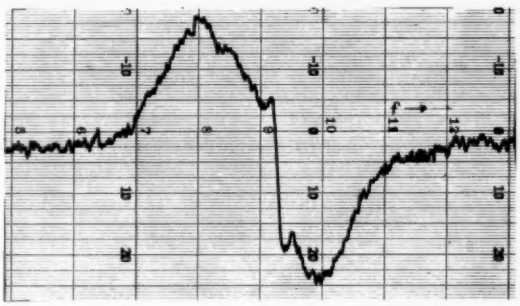

FIG. 2. Li^7 resonances in a polycrystalline sample of neutron-irradiated LiF.

line. This same combination of narrow and broad lines has been observed in another single-crystal sample of LiF that had received a dose of about 10^{18} nvt.

Comparison of the areas under the two F^{19} derivative curves, each of which was obtained with a modulation amplitude appropriate to the particular line, gives a value of 0.07 for the ratio of the area of the more narrow line to the total area. Thus about 7% of the fluorine nuclei are contributing to the narrow line. The frequency shift of the narrow line with respect to the wide line is comparable with the value 0.063% between HF and F_2 given by Gutowsky and Hoffman.[2] Thus the narrow line may be due to molecular fluorine. The frequency shift expected if the nuclei were ionic fluorine is much smaller than that measured.

The line width, that is the separation of maximum derivatives, of the broad line is approximately 47.4 kc/sec which is, within experimental error, in agreement with the value of 46.6 kc/sec calculated from the equation of Van Vleck.[3] The narrow line has a width of about 4 kc/sec.

The lithium line, Fig. 2, has been observed in a polycrystalline LiF sample which received a neutron dose of 1.6×10^{18} nvt. The sample was originally a single crystal[1] but after irradiation was found to be completely fractured.

The intensity of the narrow Li^7 line in the polycrystalline sample is not sufficient to allow a determination of the percentage of Li^7 nuclei contributing to it. Measurement of the frequency of this line and comparison of this value with that of Li^7 in a LiCl solution gives a value of $\Delta f/f = 0.028$ for the shift of the narrow line. This value compares favorably with the value[4] $\Delta H/H = 0.0249$ for the Knight shift in metallic lithium. The fluorine resonance in this polycrystalline sample exhibits a narrow line similar to that of

the single-crystal sample.

The broad lithium line in the single crystal has a separation of maximum slopes of 24 kc/sec for an orientation with the constant magnetic field along a [100] direction. This is larger than the value 20.6 kc/sec calculated from Van Vleck's equations.[3] Interactions of the Li^7 nuclear electrical quadrupole moments with field gradients arising from defects in the irradiated crystal may be responsible for this broadening.

These findings are in agreement with x-ray studies of neutron-irradiated LiF. Smallman and Willis[5] have concluded from their analysis that aggregates of fluorine atoms are trapped within the crystal. Lambert and Guinier[6] have concluded from small-angle scattering analysis that lithium atoms are present in the form of platelets parallel to the (100) planes. Thus the narrow Li^7 and F^{19} lines may be due to colloidal lithium metal and molecular fluorine gas.

Further studies of the lithium and halogen resonances, as functions of radiation dosage and post-irradiation annealing, are in progress on both single crystals and powders of LiF and other lithium halides. Quantitative determinations of the amount of damage and the behavior of the displaced metal and halide ions are now possible.

†Research supported by the U. S. Atomic Energy Commission.

[1]A cylindrical sample 1/2 in. long and 7/16 in. in diameter purchased from the Harshaw Chemical Company.

[2]H. S. Gutowsky and C. J. Hoffman, J. Chem. Phys. 19, 1259 (1951).

[3]J. H. Van Vleck, Phys. Rev. 74, 1168 (1948).

[4]W. D. Knight, Solid State Physics (Academic Press Inc., New York, 1956), Vol. 2, p. 93.

[5]R. E. Smallman and B. T. M. Willis, Phil. Mag. 2, 1018 (1957).

[6]M. Lambert and A. Guinier, Compt. rend. 245, 526 (1957).

OBSERVATION OF VERTICAL-INCIDENCE SCATTER FROM THE IONOSPHERE AT 41 Mc/sec

K. L. Bowles
Central Radio Propagation Laboratory,
National Bureau of Standards,
Boulder, Colorado
(Received November 12, 1958)

The possibility that incoherent scattering from free electrons in the ionosphere, vibrating independently, might be observed by radar techniques has apparently been considered by many workers although seldom seriously, because of the enormous sensitivity required. Recently Gordon recalled this possibility to the writer while remarking that he hoped soon to have a radar sensitive enough to observe incoherent electron scatter in addition to various astronomical objects.[1] Subsequent calculations indicated that a new 41-Mc/sec pulse transmitter, due to be received by the National Bureau of Standards, should permit observation of the incoherent electron scatter if a relatively simple antenna of large cross section were constructed.

The phenomenon of incoherent scattering of electromagnetic radiation by gas molecules has been recognized for many years at optical wavelengths.[2] The suggestion of observing electron scatter at radio wavelengths is a consequence of the relatively large radar cross section of electrons, compared with atoms or molecules. The optical observations have confirmed that the average distance between the scattering particles determines whether the particles may be considered to scatter independently. When they do scatter independently, the scattered power is proportional to the number of particles present. When observing a volume deep in wavelengths containing many particles having a mutual spacing shallow in wavelengths, the particles can no longer be considered to scatter independently. However, statistical fluctuations of the density of particles on a scale comparable to a wavelength gives rise to a different form of scattering, which turns out to be only slightly weaker than the completely independent scatter.[3] Optical experiments have apparently been somewhat inconclusive as to the exact criterion for close versus loose packing and the manner in which the scatter behaves in the transition region. One significant difference between the two kinds of scatter is apparent – that of frequency broadening of the scattering wave. The completely incoherent scatter should be heavily broadened due to Doppler shifting of the component scattered waves by thermal motions of the scatterers. The semi-incoherent scatter, mentioned above, will be broadened only slightly due to thermal fluctuations.[3] In both cases, radar observation of the scatter should provide a means of determining directly the electron density versus height profile of the ionosphere.

The brief observations reported herein were undertaken in an attempt to verify the existence

Table I. Parameters of radar equipment used.

Operating frequency	40.92 Mc/sec
Peak pulse power	(4 to 6) × 10^6 watts
Pulse duration	(50 to 150) × 10^{-6} sec
Average power	4 × 10^4 watts maximum
Receiver bandwidth	10, 15, or 30 kc/sec
Antenna cross section	116 × 140 meters (1024 half-wave elements in phase above ground)
Antenna polarization	north-south
Calculated antenna gain	~35 decibels/isotropic

of the incoherent or semi-incoherent scatter by the free electrons of the ionosphere. The parameters of the equipment used are given in Table I. Operation of the antenna has been checked by total power recordings of the emissions from the radio point source in Cygnus (Cygnus *A*) which happens to pass through the center of the beam. The beam width is within one-half degree of the calculated 3.75° and the intensity of the Cygnus signal is approximately 10 times that of the average galactic background in the same regio of the sky.

Examples of "*A* 'scope" photographs taken on October 21 and 22, 1958, during daylight hours are presented in Fig. 1. The rise in noise level peaking broadly at about 350 km range is inter-

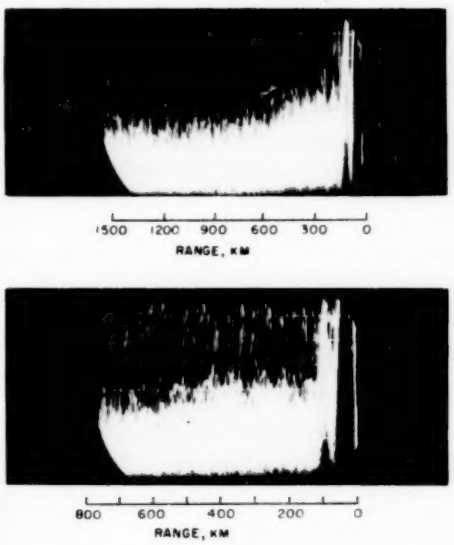

FIG. 1. (a) Pulse width 140 μsec (21 km); bandwidth 10 kc. (b) Pulse width 120 μsec (18 km); bandwidth 15 kc

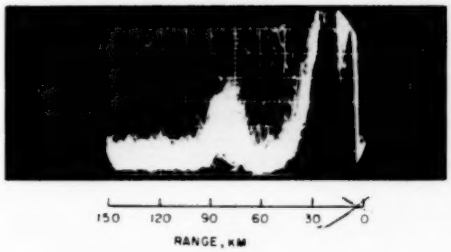

FIG. 2. Pulse width 50 μsec (~8 km); bandwidth 30 kc.

preted by the writer as the scatter type of echo mentioned above. Inverse distance variation makes the echo intensity below this height nearly constant down to *E*-region heights, although the ionization density may be expected to decrease by about a factor of 10. Reception at frequencies slightly separated from the transmitted frequency indicated little thermal broadening (*F*-region line broadening of the order of 100 kc/sec is expected for incoherent electron scatter). Conditions of the experiment did not permit observation of polarization effects.

The strong echo at about 85 km range is illustrated in Fig. 2 on an expanded range scale. This echo, observed continuously at 75 to 90 km height, is interpreted as due to ionospheric scattering of the turbulent variety as discussed in many recent papers.[4]

Care was taken in the observation to eliminate the possibility that other known types of reflections might in fact account for the echoes shown. Owing to shortage of time and difficulties with frequent malfunctions of equipment, the present records are contaminated with impulse noise and were taken only during daylight hours. Efforts are under way to make more extensive higher quality observations.

---

[1]W. E. Gordon, Union Radio-Scientifique Internationale-Institute of Radio Engineers Fall Meeting, Pennsylvania State University, October 22, 1958 (unpublished).

[2]See, for example, discussion and references given by S. Bhagavantam, in Scattering of Light and the Raman Effect (Chemical Publishing Company, Brooklyn, 1942), Chap. 3.

[3]F. Wolfers, J. phys. radium 9, 1-5 (1948).

[4]See, for example, K. L. Bowles, in Annals of the International Geophysical Year (Pergamon Press, London, 1957), Vol. 3, Part 4, pp. 346-360.

RELATIVISTIC CORRECTIONS TO THE FERMI MATRIX ELEMENT*

A. Altman and W. M. MacDonald
Physics Department,
University of Maryland,
College Park, Maryland
(Received November 20, 1958)

The *ft* values for $J = 0^+ \rightarrow J = 0^+$ positron decays of O^{14}, Al^{26}, and Cl^{34} have been used to determine the magnitude of the Fierz interference term.[1] The analysis is subject, however, to an uncertainty in the variations of the *ft* values which could be produced by the Coulomb interaction or by the energy-dependent relativistic correction terms. The Coulomb correction for Cl^{34} has been calculated to be ~1.5%.[2] We now consider the effect of relativistic terms.

There are no relativistic correction terms to the vector nuclear matrix element for a transition between two states of zero angular momentum. The scalar nuclear matrix element would have a relativistic correction term, however. The question one must answer is whether the energy dependence of the correction term would be sufficient to mask the presence of a Fierz interference term. It is important to realize that only a change in the ratio of the *ft* values will affect the limit on the magnitude of the Fierz term.

The scalar matrix element is

$$\int \beta \equiv \int \Psi_f^* \sum_k (t_1^{(k)} + i t_2^{(k)}) \beta^{(k)} \Psi_i , \qquad (1)$$

where Ψ_i, Ψ_f are the initial and final nuclear states and β is a Dirac matrix. The matrix element of $\beta^{(k)}$ is equal to the matrix element of $(1 - v_k^2/2c^2)$ to this order in v/c. The calculation of this matrix element will be made first in the shell model with harmonic oscillator wave functions. The kinetic energy of the proton in an (nl) orbital is

$$T = \tfrac{1}{2}\hbar\omega(2n + l - \tfrac{1}{2}), \quad n = 1, 2, \ldots, \quad l = 0, 1, \ldots . \qquad (2)$$

Only the kinetic energy of the last particle appears in the correction term. Using oscillator parameters determined from Coulomb energy differences we find

for O^{14}: $T = 19.1$ Mev, $1p$ proton;

for Cl^{34}: $T = 21.4$ Mev, $1d$ proton. (3)

The relativistic correction terms decrease the scalar nuclear matrix elements for the Cl^{34}–S^{34} and O^{14}–N^{14*} (2.31 Mev) positron decay by the amounts 2.3% and 2.0% respectively. The ratio of the *ft* values for the O^{14} and Cl^{34} decays would deviate from unity:

$$ft(Cl^{34})/ft(O^{14}) = 1.003. \qquad (4)$$

This ratio is calculated assuming equal amounts of the scalar and vector interaction.

The interesting aspect of this result is that the relativistic corrections are individually large, yet the effect on the ratio of the *ft* values is very small.

To check whether the result is sensitive to the shape of the potential, the calculation was done by using the Dirac wave function for a particle in a finite square well. The radial functions are simply spherical Bessel and Hankel functions. The complete solution can be determined by inserting the nuclear binding energy of the last proton and the radius into a characteristic equation obtained from the requirement of continuity of the current across the circumference of the well.

The nuclear binding energy used must not include the Coulomb energy. The Coulomb energy to be subtracted was found from the differences in binding of mirror nuclei by making a correction for the changes in radius produced by the addition or subtraction of a neutron. The binding by the nuclear potential of the $1p$ proton in O^{14} was found to be 8.15 Mev; and of the $1d$ proton of Cl^{34}, 11.48 Mev. The radii used were the equivalent uniform-model radii deduced from high-energy electron scattering experiments. These radii are 3.24×10^{-13} cm for O^{14} and 4.19×10^{-13} for Cl^{34}.

Using these radii and nuclear binding energies of the last proton, we find the relativistic corrections to produce a decrease in the scalar nuclear matrix elements of 2.3% for Cl^{34}–S^{34} and 1.8% for O^{14}–N^{14*} (2.31 Mev). The ratio of the *ft* values is then calculated to be

$$ft(Cl^{34})/ft(O^{14}) = 1.005. \qquad (5)$$

The comparison of Eqs. (4), (5) shows that while the effect of the relativistic corrections to the ratio of the *ft* values is uncertain in the exact value, the magnitude is a fraction of one percent. These correction terms are insufficient, therefore, to mask the presence of a Fierz

term larger than the limit set by Gerhart.

*Research supported by the U. S. Atomic Energy Commission.

[1]J. B. Gerhart and R. Sherr, Bull. Am. Phys. Soc. Ser. II, 1, 195 (1956); J. B. Gerhart, Phys. Rev. 109, 897 (1958).

[2]W. M. MacDonald, Phys. Rev. 110, 1420 (1958).

ELECTROMAGNETIC MASS CORRECTION FOR SPIN 0 PARTICLES

S. Gasiorowicz* and A. Petermann
Theoretical Study Division, CERN,
Geneve, Switzerland
(Received November 20, 1958)

Because of the requirement of gauge invariance, the electromagnetic coupling of a charged spin-zero field consists of two terms,

$$-ie\left(\varphi^*(x)\cdot\partial_\mu\varphi(x) - \partial_\mu\varphi^*(x)\cdot\varphi(x)\right)A_\mu(x) \qquad (1a)$$

$$-e^2\,\varphi^*(x)\varphi(x)A_\mu(x)A_\mu(x). \qquad (1b)$$

In lowest-order perturbation theory (ignoring for the moment all strong interactions) the two self-energy terms are represented by the diagrams in Fig. 1.

To separate the contributions of the two terms (each of which is gauge dependent), it is useful to choose the gauge in which the photon Green's function in momentum space takes the form

$$D_{F\mu\nu}(K) = \frac{1}{K^2}\left(\delta_{\mu\nu} - \frac{K_\mu K_\nu}{K^2}\right). \qquad (2)$$

With this choice, the contribution of the terms (1a) to the self-energy are seen to be logarithmically divergent, since

$$\int d^4K\,(q-\tfrac{1}{2}K)_\mu\,\frac{1}{(q-K)^2+\mu^2}\,(q-\tfrac{1}{2}K)_\nu\,\frac{1}{K^2}\left(\delta_{\mu\nu}-\frac{K_\mu K_\nu}{K^2}\right)$$

$$= \int d^4K\,\frac{1}{K^2}\,\frac{1}{(q-K)^2+\mu^2}\left(q^2 - \frac{(q\cdot K)^2}{K^2}\right). \qquad (3)$$

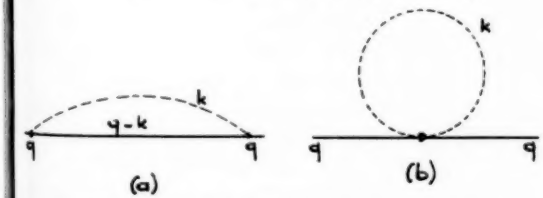

FIG. 1. Lowest order electromagnetic effect.

The contribution of the term (1b) is quadratically divergent. It is proportional to

$$3\,e^2\int\frac{d^4K}{K^2}\,, \qquad (4)$$

which behaves as Λ^2, if Λ is a cutoff momentum for the photon. With this choice of gauge, the familiar result that the spin-zero boson electromagnetic self-energy is quadratically divergent[1] is made very transparent. As would be expected on dimensional grounds, it is also clear that the dominant term [(1b) in this gauge], which is the quadratically divergent one, is independent of the mass of the boson. On these grounds, if it is assumed that the mass difference between charged and neutral members of the same multiplet is purely electromagnetic, one might expect the result

$$\frac{m_{K^+} - m_{K^0}}{m_{\pi^+} - m_{\pi^0}} = \frac{m_\pi}{m_K}. \qquad (5)$$

to hold to good accuracy.

It is of course necessary to enquire how this result is affected by the inclusion of strong interactions. The terms of the type shown in Fig. 2 (a) correspond to taking into account, for example, the fact that in the strong interaction "box," which changes the boson mass from the bare to the physical mass, the masses of intermediate charged and neutral members of a multiplet are their physical (slightly unequal) masses. We expect the contribution of these terms to the electromagnetic mass difference to be rather small. There are also terms of a type exhibited in Fig. 2 (b). We do not, of course, know how to calculate these terms but, if we assume that the vertex operator behaves in a way similar to that indicated by perturbation

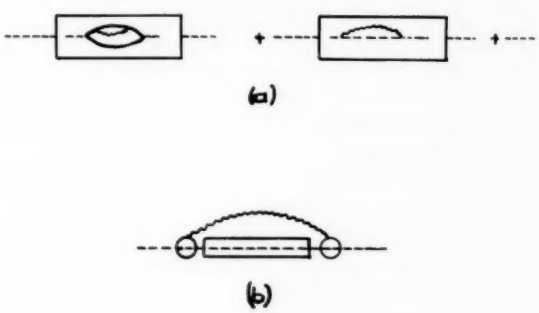

FIG. 2. Strong interactions corrections.

theory (for strong interactions), then these terms are again no more than logarithmically divergent. Thus again Fig. 1 (b) represents the leading contribution to the electromagnetic mass difference and again Eq. (5) may be expected to hold for very large Λ^2.

For a photon cutoff momentum of the order of 1 Bev/c, deviation from (5) will occur that we cannot estimate, whereas for point interactions (5) is exact up to finite α corrections to m_π/m_K.[2]

It is a pleasure for one of us (S.G.) to thank Professor Ferretti and CERN for their hospitality

*National Science Foundation Fellow. On leave from the Radiation Laboratory, Berkeley, California.

[1]R. Feynman and G. Speisman, Phys. Rev. 94, 500 (1954); A. Petermann, Helv. Phys. Acta 27, 441 (1954).

[2]One can actually show that terms $\sim(\Lambda^2/m)\log(\Lambda^2/m^2)$ do never occur.

PHOTOPRODUCTION OF SINGLE POSITIVE PIONS FROM HYDROGEN IN THE 600- TO 1000-Mev REGION*

F. P. Dixon and R. L. Walker
California Institute of Technology,
Pasadena, California
(Received November 17, 1958)

The earlier magnetic spectrometer measurements[1] of pions from the reaction $\gamma+p\rightarrow\pi^++n$, initiated by the bremsstrahlung beam of the Cal-Tech Synchrotron in a liquid hydrogen target, have been extended to cover a range of 20° to about 163° in the center-of-momentum system for laboratory photon energies of 600, 700, 800, 900, and 1000 Mev. The experimental technique was improved by the placement of veto counters along the pole faces of the magnet to eliminate counts from scattered particles and from showers produced in the iron. Also, a Lucite Čerenkov counter was used to discriminate against protons, which could not be clearly separated from pions at momenta above 800 Mev/c by a pulse-height analysis. New data at angles greater than 135° were taken with the same medium-momentum spectrometer used for the previous measurement. However, for pion momenta greater than 600 Mev/c (forward angles) the high-momentum spectrometer described by Vette[2] was employed with the addition of the pole face veto counters and a front "aperture" counter located near the magnet entrance.

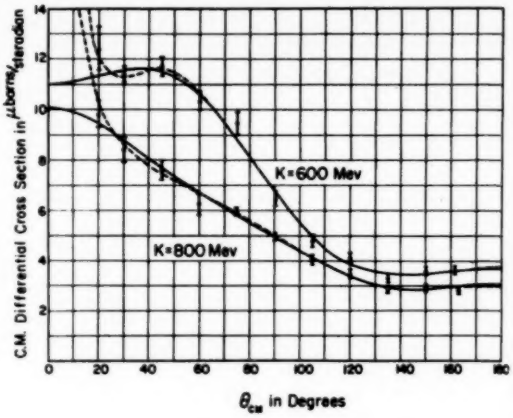

FIG. 1. Angular distributions of pions from $\gamma+p\rightarrow\pi^++n$ for 600- and 800-Mev photons. The solid curves in Figs. 1-3 are least-squares fits to the data, of the form $d\sigma/d\Omega=\Sigma_{n=0}{}^{4}A_n\cos^n\theta$. The dashed curves are fits of the form $(1-\beta\cos\theta)^2(d\sigma/d\Omega)=\Sigma_{n=0}{}^{6}B_n\cos^n\theta$ following Moravcsik.[4]

The data presented in this report have been corrected for empty-target backgrounds, pion decay in flight, absorption of pions in the system, and muon contamination. The background was found to be about 10% of the total counting rate. The worst case was 13% at 11.3° in the laboratory system. Negative-field runs at this position showed no contribution from the hydrogen, since empty- and full-target runs gave equal counting rates amounting to 4% of the total positive-field run with hydrogen in the target. The absorption correction was 14%, where the geometrical value was used for the counters and the attenuation in the half-inch Pb absorber was measured. A preliminary estimate of muon contamination was used and gave 4 ± 2 to 8 ± 4% correction for this effect. With the pion decay loss this resulted in a net correction of 8 to 19% for effects associated with pion decay.

Angular distributions in the center-of-momentum system for each of the five photon energies investigated are shown in Figs. 1-3. In these figures the previous cross sections of reference 1 have been increased about 4% as a result of a recent beam monitor calibration.[3] None of the data should be considered as final, since we plan to make an improved calculation of the corrections for muon contamination, and a future detailed measurement of the breamsstrahlung spectrum could result in some changes in the cross sections. We have used essentially a thin-

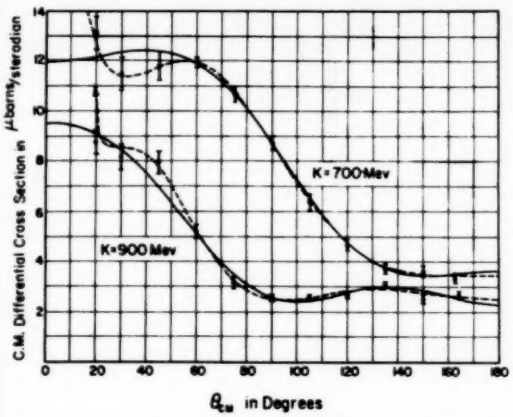

FIG. 2. Angular distributions of pions from $\gamma + p \rightarrow \pi^+ + n$ for 700- and 900-Mev photons.

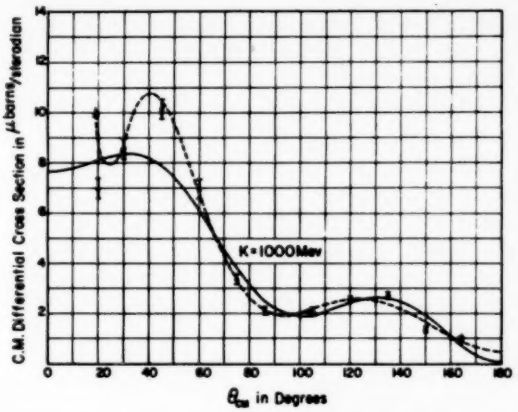

FIG. 3. Angular distributions of pions from $\gamma + p \rightarrow \pi^+ + n$ for 1000-Mev photons.

target spectrum based on an earlier pair-spectrometer measurement. Furthermore, for the 1000-Mev data at angles greater than 60°, the bremsstrahlung upper limit was lower than the maximum limit of acceptance for the spectrometer, and this necessitated corrections in resolution ranging from 3% at 75° to about 40% at the most backward angle. More detailed calculations will also be made of this effect.

Least-squares fits to the data are shown by the curves in Figs. 1-3. The solid curves are for expressions of the form

$$\frac{d\sigma}{d\Omega}(k,\theta) = A_0 + A_1\cos\theta + A_2\cos^2\theta + A_3\cos^3\theta + A_4\cos^4\theta.$$

Total cross sections obtained from the expression $\sigma_T = 4\pi(A_0 + A_2/3 + A_4/5)$ are shown in Table I, as are the coefficients A_0 to A_4. The 1000-Mev data are not fitted well by the $\cos^4\theta$ expression, so that the total cross section shown in Table I is probably a little low. The dashed lines represent least-squares fits of the form

$$(1-\beta\cos\theta)^2\,\frac{d\sigma}{d\Omega}(k,\theta) = B_0 + B_1\cos\theta + B_2\cos^2\theta + \ldots + B_6\cos^6\theta,$$

according to the prescription of Moravcsik.[4] The extra freedom of the seven-coefficient expansion of Moravcsik gives a better fit than the five-coefficient expansion in $\cos\theta$, as might be expected. The 1000-Mev data seem to require a higher power than the $\cos^4\theta$ expression contains in order to obtain a reasonable fit.

The peak in the π^+ photoproduction cross section at 700 Mev has been reported before by both Cornell[5] and CalTech[1] and has been interpreted as a resonance in a state of isotopic spin 1/2. Our cross sections are in agreement with those reported from Cornell[5] at most of the points where they may be compared. The most interesting new feature of the present data is the remarkable change in the angular distribution between

Table I. Total cross sections and coefficients for $(d\sigma/d\Omega)(k,\theta) = \Sigma_{n=0}^{4} A_n \cos^n\theta$.

Photon energy (Mev)	Total cross section[a] (microbarns)	Coefficients for fit in cos θ (microbarns steradian) A_0	A_1	A_2	A_3	A_4
600	89.9±1.2	+6.7±0.2	+7.7±0.5	+2.5±1.1	-4.1±0.7	-1.8±1.2
700	104.0±1.2	+8.7±0.2	+8.1±0.4	-1.6±1.1	-4.0±0.6	+0.7±1.1
800	66.0±0.9	+5.0±0.1	+3.2±0.3	-0.4±0.8	+0.3±0.5	+2.0±1.0
900	51.2±0.9	+2.6±0.1	+2.0±0.3	+6.3±0.7	+1.6±0.5	-2.9±0.8
1000	49.4±0.9	+2.2±0.1	+3.6±0.3	+10.5±0.6	+0.1±0.4	-8.8±0.7

[a]See text for explanation.

800 and 1000 Mev. The 1000-Mev distribution is so distinctive and this character appears so suddenly as the energy is increased, that we are tempted to ascribe it to a $T=1/2$, $J=5/2$ resonance first suggested in pion scattering data[6] near an energy corresponding to photoproduction at 1100 Mev. This temptation is supported by two or three arguments. First, a $D_{5/2}$ state from magnetic quadrupole absorption or an $F_{5/2}$ state from electric quadrupole would have an angular distribution of the form $1+6\cos^2\theta-5\cos^4\theta$ and this appears to be a major component in the 1000-Mev distribution, together with a strong $\cos\theta$ interference term. This interpretation is also useful for π^0 photoproduction, since the above angular distribution fits qualitatively the 940-Mev π^0 data of Vette[2] where the angular distribution was found to be different from that at all lower energies. A second, somewhat weak, point is that the total π^+ cross section shown in Table I does not continue to decrease appreciably between 900 and 1000 Mev, and this is consistent with a resonance at a somewhat higher energy, 1050 or 1100 Mev, which is just the energy expected from the pion scattering data.[6]

A possible difficulty is that the 1000-Mev data seem to require higher powers of $\cos\theta$ than the fourth, in order to achieve a reasonable fit. Perhaps the small-angle behavior can be explained by interference effects with the term in the photoproduction amplitude corresponding to interaction of the photon with the meson current. As Moravcsik has emphasized,[4] this term should not be ignored, and an analysis including it is being attempted. No contribution of this term alone as distinct from interference effects is obvious in the data.

A complete report of this experiment, including the final corrections to the data discussed above, will be published later. We wish to thank Mr. Gerry Neugebauer for helping to take some of the final data.

[*]This work was supported in part by the U. S. Atomic Energy Commission.

[1]F. P. Dixon and R. L. Walker, Phys. Rev. Lett. 1, 142 (1958).

[2]J. I. Vette, Phys. Rev. 111, 622 (1958).

[3]R. Gomez (private communication).

[4]M. J. Moravcsik, Phys. Rev. 104, 1451 (1956).

[5]Heinberg, McClelland, Turkot, Woodward, Wilson, and Zipoy, Phys. Rev. 110, 1211 (1958).

[6]Cool, Piccioni, and Clark, Phys. Rev. 103, 1082 (1956).

POLARIZATION OF RaE ELECTRONS

H. Wegener, H. Bienlein, and H. v. Issendorff
Physikalisches Institut der Universität Erlangen, Erlangen, Germany
(Received October 31, 1958)

For β-decay with $\Delta J=1$, yes, the longitudinal polarization P is $-v/c$, if the ξ-approximation is valid. The ξ-approximation gives an allowed spectrum. There is only one exception, RaE. Therefore one expects $P(\text{RaE})\neq -v/c$. Theoretical investigations by Curtis and Lewis[1] and by Kotani and Ross[2] point out that P(RaE) should give information about time reversal at small energies and about matrix elements at larger energies. First measurements from Geiger et al.[3] with Møller scattering and from Heintze et al.[4] with Mott scattering after deflection by multiple scattering indicate that $|P(\text{RaE})|<v/c$, indeed. Unfortunately the energy discrimination in both measurements is too poor for a detailed conclusion.

We have measured P(RaE) for $E_{\text{kin}}=120$, 155, 209, and 290 kev by Mott scattering after deflection through an electric field. Figure 1 shows our experimental arrangements.[5] The source Q is imaged to the receiving diaphragm of the spherical electric field by a thin magnetic lens. The end of the field (120° deflection) can be imaged to the scattering foil to avoid frame scattering. The depolarization by this lens has been measured earlier. Electrons which are once scattered in the scattering foil and then back-scattered by the walls are suppressed by

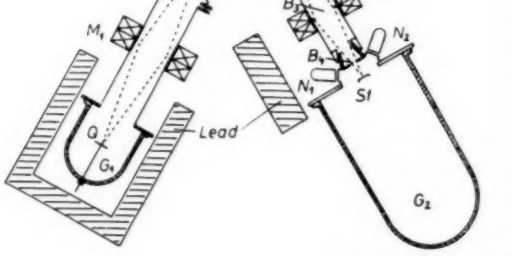

FIG. 1. Experimental arrangement. Q = source, M_1, M_2 = thin magnetic lenses, B_1 - B_4 = diaphragms, N_1, N_2 = counters, St - scattering foil, G_1, G_2 = glass cylinders; the other parts are of metal. The scattering part can be rotated. Lead = lead shielding.

the large glass tube G_2. We use two GM counters N_1 and N_2 and measure with Au and Al foils (scattering angle 120°). The scattering part can be rotated (together with the counters). The RaE source was obtained from a RaD+E solution by precipitating the RaE with Fe carrier. The RaE +Fe was then electroplated to 0.2 mg/cm² Al which was evaporated onto 1 mg/cm² Melinex. We corrected for the following influences: depolarization in the source, plural scattering in the scattering foil,[6] apparatus asymmetry, solid angle corrections, spin deflection, and back scattering from the walls.

The influence of screening to the asymmetry function S (without screening tabulated by Sherman[7]) was measured, assuming full polarization for Co^{60} electrons (allowed GT transition). We find $S_{exp}/S_{theor} = 0.86 \pm 0.02$, 0.96 ± 0.02, and 1.00 ± 0.02 for $v/c = 0.58$ (120 kev), 0.64 (155 kev), and 0.70 (209 kev), respectively.

The results for the degree of longitudinal polarization of RaE electrons are $P/(-v/c) = 0.69 \pm 0.04$, 0.75 ± 0.04, 0.75 ± 0.04, and 0.66 ± 0.06 for $E_{kin} = 120$, 155, 209, and 290 kev, respectively. These values are nearly energy independent and are somewhat higher than the upper limit of the possible values as calculated by Bincer et al.[8] according to the "best fit" of the RaE spectrum. But it is possible to fit the spectrum with parameters which involve a higher degree of polarization. In Fig. 2, $P/(-v/c)$ is shown as a function of E_{kin}. The thoretical limits are taken from reference 8. All experimental data known to us are included.

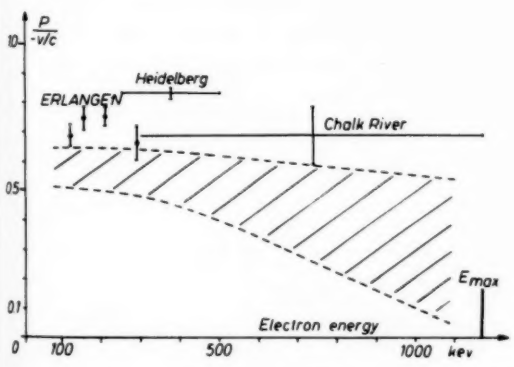

FIG. 2. Electron polarization of RaE versus energy. The range of theoretical values after the "best fit" of the spectrum is shown. The experimental values of Erlangen (present work) have been obtained with Mott scattering after electrostatic deflection, Heidelberg (Heintze et al.) with Mott scattering after deflection by multiple scattering, Chalk River (Geiger et al.) with Møller scattering.

We thank Professor Fleischmann for his interest and advice. Dr. Spang and Mr. Martin (Forschungsinstitut der Siemens-Schuckert-Werke, Erlangen) did the radiochemical work. We had supports from the Deutsches Bundesministerium für Atomkernenergie, Deutsche Forschungsgemeinschaft, and Deutsches Wissenschaftliches Komitee der Research Corporation, New York.

[1]R. B. Curtis and R. R. Lewis, Phys. Rev. 107, 543 (1957).
[2]T. Kotani and M. Ross (to be published).
[3]Geiger, Ewan, Graham, and Mackenzie, Chalk River Report PD 298, 1958 (unpublished).
[4]J. Heintze and W. Bühring, Phys. Rev. Lett. 1, 176 (1958).
[5]Bienlein, Güthner, Issendorff, and Wegener, Nuclear Instr. (to be published).
[6]H. Wegener, Z. Physik 151, 252 (1958).
[7]N. Sherman, Phys. Rev. 103, 1609 (1956).
[8]Bincer, Church, and Weneser, Phys. Rev. Lett. 1, 95 (1958).

STRENGTH FUNCTIONS FOR DEFORMED NUCLEI*

D. J. Hughes, R. L. Zimmerman, and R. E. Chrien
Brookhaven National Laboratory, Upton, New York
(Received November 24, 1958)

Optical models have recently been successful in accounting for the interaction of various particles with nuclei over wide ranges of energy. One fundamental property of the models is the low-energy neutron "strength function," or $\overline{\Gamma}_n^0/D$ ratio, with $\overline{\Gamma}_n^0$ the mean reduced neutron width of s resonances, and D their spacing. This ratio is proportional to the cross section for compound nucleus formation and is thus closely related to the penetrability of the potential barrier at the surface of the nucleus. The compound nucleus formation can be well measured at low energy, where, averaged over resonances, it is inversely proportional to neutron velocity. The experimental strength function has been useful as a test of the applicability of optical models and as a means for establishing their parameters.

Although the "cloudy crystal ball" model of Feshbach, Porter, and Weisskopf,[1] with a spherical sharp-surfaced well, gave better agreement with measured strength functions than a "black" nucleus, it was obvious that more accurate models were needed. Inclusion of a diffuse boundary in the model was made by Feshbach, Porter, and Campbell,[2] using the experimental strength functions and high-energy cross sections of various types to fix the model parameters. The strength functions calculated from this model compared well with measurements except for A near 160; here the theory predicted a single broad peak but experiments[3] indicated a more complicated shape. It was possible, however, that inclusion of nuclear deformations, which are large near $A = 160$, would result in better agreement with experiments. Several calculations[4-7] for aspherical nuclei have been undertaken recently, and the program of strength function measurements with the Brookhaven fast chopper has been devoted to the deformed nuclei in the past few months.

The significance of the strength function in nuclear reaction theory is closely related to the methods for its measurement. Although it can be determined from the neutron widths and spacings of individual resonances, it is actually not a property of the resonances but rather of the penetrability of the nuclear surface. The mean neutron width is an emission probability, but division by the spacing removes the specific level characteristics; the resulting $\overline{\Gamma}_n{}^0/D$ ratio is proportional to compound nucleus formation, averaged over levels. Thus the average cross section for compound nucleus formation, σ_C, gives the strength function directly, in fact, for 1-kev neutron energy:

$$\overline{\Gamma}_n{}^0/D = 13.0\times10^{-4}\,\overline{\sigma}_C\ (\text{barns}).$$

The statistical accuracy of the strength function determined from $\overline{\sigma}_C$ is typically high because of the contribution of many levels.

In the average cross section method, as developed with the Brookhaven fast chopper, the transmission of a thin sample is measured in the region of a few kilovolts. The transmission plotted against time of flight is then a straight line whose slope is directly proportional to the strength function. Experiments at Brookhaven have shown that results at several kilovolts agree with those obtained from individual resonances at low energy, indicating that effects of p waves are unimportant and that the neutron widths are proportional to neutron velocity.

The present Brookhaven results,[8] for elements and separated isotopes, are listed in Table I and plotted in Fig. 1. The experimental method used in each case is designated by the symbol in Fig. 1. For the lower A values in Fig. 1, the averaging method gives higher accuracy, primarily because the number of individual levels available at low energy is small. The theoretical curves shown in Fig. 1 correspond to (1) the black nucleus, (2) the spherical nucleus with diffuse boundary,[2] and (3) the inclusion of nuclear deformations. The last curve is the one computed by Chase, Wilets, and Edmonds,[6] for which the deformations are those corresponding to the experimental values of the nuclear quadrupole moments. It is seen that the experimental points exhibit clearly the double peak predicted by the recent theory, although they are definitely below the theoretical curve for A near 100. The agreement at the double peak is particularly striking in view of the fact that no additional adjustable parameters were present in the calculation of curve (3) relative to curve (2). It is interesting that the strength function varies with atomic weight much less violently than the level spacing, which can change by factors of 100 in a few units of A. In such cases the mean neutron width changes correspondingly and the resulting $\overline{\Gamma}_n{}^0/D$ ratio varies only slowly.

Even though the optical model corresponding to curve (3) is of a relatively simple type, a deformed diffuse well, it shows rather good agreement with the details of the measured

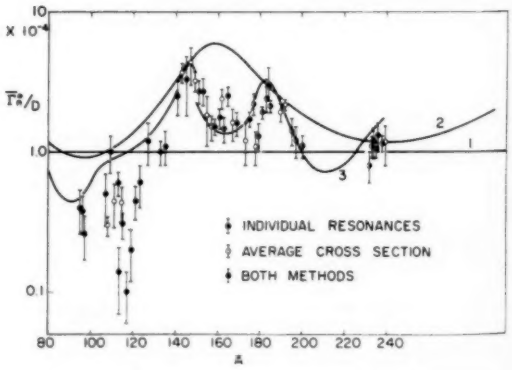

FIG. 1. Experimental strength functions compared with various nuclear models; (1) is the black nucleus, (2) the spherical nucleus with diffuse boundary, (3) the inclusion of nuclear deformations.

Table I. Neutron strength functions. Where no mass number is indicated, the value is for the normal element; "even" signifies an average value for isotopes of even mass number.

Isotope or element	Γ_n^0/D (10^{-4})	Isotope or element	Γ_n^0/D (10^{-4})	Isotope or element	Γ_n^0/D (10^{-4})	Isotope or element	Γ_n^0/D (10^{-4})
Mo even	0.38±0.11	Sb^{123}	0.6 ±0.2	Dy	2.4 ±0.4	Re^{185}	2.1 ±0.2
Mo^{95}	0.40±0.14	I	1.2 ±0.4	Dy^{161}	1.75±0.3	Os	1.9 ±0.3
Mo^{97}	0.26±0.09	Cs	1.0 ±0.2	Dy^{163}	1.45±0.3	Ir	2.2 ±0.2
Ag	0.30±0.05	Ba^{135}	1.1 ±0.3	Ho	2.5 ±0.4	Pt	1.4 ±0.3
Ag^{107}	0.5 ±0.2	Pr	2.5 ±0.7	Er^{167}	1.6 ±0.4	Au	1.2 ±0.3
Ag^{109}	1.0 ±0.3	Nd^{143}	3.7 ±0.6	Tm	1.6 ±0.3	Hg	1.1 ±0.2
Cd^{111}	0.44±0.15	Nd^{145}	3.3 ±1.5	Yb^{173}	1.2 ±0.4	Th	0.8 ±0.2
Cd^{113}	0.14±0.07	Sm^{147}	4.3 ±1.3	Lu^{175}	1.7 ±0.2	U^{233}	1.1 ±0.2
In	0.44±0.12	Sm^{149}	3.2 ±0.5	Hf	1.1 ±0.3	U^{234}	1.2 ±0.3
In^{113}	0.60±0.11	Eu^{151}	2.7 ±0.5	Hf^{177}	2.2 ±0.4	U^{235}	1.05±0.15
In^{115}	0.31±0.06	Eu^{153}	2.7 ±0.6	Hf^{179}	1.3 ±0.3	U^{236}	1.3 ±0.3
Sn even	0.20±0.08	Gd^{155}	1.8 ±0.7	Ta^{181}	1.9 ±0.2	U^{238}	1.15±0.15
Sn^{117}	0.10±0.04	Gd^{157}	1.5 ±0.3	W	3.0 ±1.0	Pu^{239}	1.2 ±0.4
Sb^{121}	0.45±0.12	Tb	1.5 ±0.2	W^{183}	2.4 ±0.5		

strength functions. A similar correspondence between predictions[6] based on the deformed well and experiment has already been found[9] for the potential scattering, related to the radius of the potential well. Strength function measurements are continuing, in order to investigate fine structure in the strength functions, which might be correlated with properties of individual nuclei.

*Work performed under the auspices of the U. S. Atomic Energy Commission.

[1]Feshbach, Porter, and Weisskopf, Phys. Rev. 96, 448 (1954).
[2]Reported by V. F. Weisskopf, Physica 18, 952 (1956).
[3]D. J. Hughes, Physica 22, 994 (1956).
[4]B. Margolis and E. S. Troubetzkoy, Phys. Rev. 106, 105 (1957).
[5]V. V. Vladimirsky and I. L. Ilyina, Nuclear Phys. 5, 295 (1958).
[6]Chase, Wilets, and Edmonds, Phys. Rev. 110, 1080 (1958).
[7]K. W. McVoy, Bull. Am. Phys. Soc. Ser. II, 3, 324 (1958).
[8]Including some values already published; Harvey, Hughes, Carter, and Pilcher, Phys. Rev. 99, 10 (1955).
[9]Seth, Hughes, Zimmerman, and Garth, Phys. Rev. 110, 692 (1958).

SYMMETRIES IN BARYON-K MESON INTERACTIONS*

Y. Shimamoto
Brookhaven National Laboratory, Upton, New York
(Received October 8, 1958)

It was shown by Pais[1] that, under weaker assumptions than those of Gell-Mann[2] and Schwinger,[3] certain symmetries are incompatible with experiment independent of the dynamical cause for the Σ-Λ mass splitting. These symmetries can be expressed in terms of the following two rules: (A) the separate conservation in strong interactions of two quantum numbers S_1 and S_2, which emerge from the assumed baryon-K meson $[B\text{-}K]$ interaction, and (B) the invariance of the latter under a certain interchange. Thus, (A), e.g., forbids processes like $\pi^+ + p \rightarrow \Sigma^+ + K^+$, $K^0 + p \rightarrow K^+ + n$, and $K^- + p \rightarrow \pi^- + \Sigma^+$, while the application of (B) leads to incorrect hyperon production amplitudes in π-p collisions. It has further been shown by Pais[4] that (B) can be eliminated by assuming the relative parity of K^+ and K^0 to be odd, while those processes forbidden by (A) can be reinstated by the introduction of an interaction of the form $[\bar{K}K\pi] = f(2m_K)\,(\bar{K}^+K^0\pi^+ + \bar{K}^0K^+\pi^-)$. Interactions quadrilinear in the fields are also being considered.[5]

It is the purpose of this note to indicate that,

provided one is willing to relinquish $\vec{I}^2$, $\vec{K}^2$, I_3, and K_3 as good quantum numbers in $[B\text{-}K]$, an alternative trilinear interaction exists within the framework of the baryon doublet approximation. The net effect is the violation of rules (A) and (B), and a medium strong interaction requiring no more than charge independence and the strangeness rule.

As in the work of Pais,[1] the following assumptions are essential to our considerations: (a) the baryon and meson spectrum as known today is complete, (b) the normal assignment of spin and isotopic spin for baryons and mesons is correct, (c) the (Σ, Λ) parity is even, (d) the $(\Sigma\text{-}\Lambda)$ constitute a mass degenerate system in the very strong $[\pi\text{-}B]$ interaction, and (e) the baryon-π interaction has the following well-known form:

$$[\pi] = i[G_1\bar{N}_1\gamma_5 N_1 + G(\bar{N}_2\gamma_5 N_2 + \bar{N}_3\gamma_5 N_3) + G_4\bar{N}_4\gamma_5 N_4]\pi, \quad (1)$$

where

$$N_1 = \begin{pmatrix} p \\ n \end{pmatrix}, \quad N_2 = \begin{pmatrix} \Sigma^+ \\ Y^0 \end{pmatrix}, \quad N_3 = \begin{pmatrix} Z^0 \\ \Sigma^- \end{pmatrix}, \quad N_4 = \begin{pmatrix} \Xi^0 \\ \Xi^- \end{pmatrix}$$
$$Y^0 = 2^{-1/2}(\Lambda^0 - \Sigma^0), \quad Z^0 = 2^{-1/2}(\Lambda^0 + \Sigma^0). \quad (2)$$

Global symmetry is not essential to our discussion. In (1) and (2) the baryons and mesons are regarded as direct product representations (i, k) induced by unimodular transformations in a four-dimensional charge space, where i and k individually are representations of the 3-dimensional rotation group. Thus, π = (i-vector, k-scalar), N_1 and N_4 = (i-spinor, k-scalar), and (Σ, Λ) = (i-spinor, k-spinor). As is well known, reflections in the 4-space result in $I \longleftrightarrow K$, and hence are excluded. To complete the known meson spectrum, we add K and K^C = (i-scalar, k-spinor) with

$$K = \begin{pmatrix} K^+ \\ K^0 \end{pmatrix}, \quad K^C = \begin{pmatrix} -\bar{K}^0 \\ \bar{K}^+ \end{pmatrix} \quad (3)$$

where K^C is defined in such a way that K and K^C transform similarly.

In order to write down the $[B\text{-}K]$ interaction it is convenient to introduce the following notation which exhibits the transformation properties of the baryons and mesons in the i and k spaces:

$$I_1 \equiv p, \quad I_2 \equiv n, \quad K_1 \equiv K^+, \quad K_2 \equiv K^0, \quad (4a)$$

or

$$i_1 \equiv \Xi^0, \quad i_2 \equiv \Xi^-, \quad k_1 \equiv -\bar{K}^0, \quad k_2 \equiv \bar{K}^+, \quad (4b)$$

$$M_1^{\,1} \equiv Z^0 \sim I_1\bar{K}_1 \equiv I_1K^1, \quad M_1^{\,2} \equiv \Sigma^+ \sim I_1\bar{K}_2 \equiv I_1K^2,$$
$$M_2^{\,1} \equiv \Sigma^- \sim I_2\bar{K}_1 \equiv I_2K^1, \quad M_2^{\,2} \equiv Y^0 \sim I_2\bar{K}_2 \equiv I_2K^2, \quad (4c)$$

where $\sim$ denotes "transforms similarly to."

Now a scalar in i and k consistent with baryon conservation can be written as

$$\sum_{\alpha,\beta=1,2} I^\alpha M_\alpha^{\ \beta} K_\beta \quad (5a)$$

or

$$\sum_{\alpha,\beta=1,2} i^\alpha M_\alpha^{\ \beta} k_\beta \quad (5b)$$

On placing an η = (1 or $i\gamma_5$) to the left of the M's and adding (5a) and (5b), each multiplied by an appropriate coupling constant, one obtains precisely the expression given by Pais for the baryon-K meson interaction:

$$\{K\} = F_{\mathrm{I}}[\bar{N}_1\eta N_2 K^0 + \bar{N}_1\eta N_3 K^+] + \text{H.c.} + F_{\mathrm{II}}[\bar{N}_4\eta' N_2\bar{K}^+ - \bar{N}_4\eta' N_3\bar{K}^0] + \text{H.c.} \quad (6)$$

We note that the observation of Pais that (6) is invariant under gauge transformations (rule A) leading to quantum numbers S_1 and S_2 stems primarily from the fact that (6) imposes a selection rule $\Delta K_3 = 0$, in spite of the gauge change in N_4, while the fact that (6) is invariant under the combined interchange (rule B) $N_2 \rightarrow N_3$, $K^+ \rightarrow K^0$, $-\bar{K}^0 \rightarrow \bar{K}^+$ is intimately related to the fact that it is a scalar in the i space. Stated in another way, it is the absence in (6) of two terms of the form

$$2I^2M_1^{\,1}K_2 = 2\bar{n}Z^0K^0, \quad (7)$$

and

$$2I^1M_2^{\,2}K_1 = 2\bar{p}Y^0K^+, \quad (8)$$

which forbids the processes mentioned above.

On recognizing that (7) and (8) are precisely the I_+K_- and I_-K_+ terms in the scalar product $\vec{I}\cdot\vec{K} = I_0K_0 + I_+K_- + I_-K_+$ between an i-vector, $\vec{I}$, and k-vector, $\vec{K}$, the manner in which the symmetry in $[B\text{-}K]$ can be broken becomes evident. To construct such a scalar, consistent with baryon conservation, is a simple matter, and we have

$$\{B\text{-}K\} = f_1[\sqrt{2}\,\bar{N}_1\tau_-\eta N_3K^0 + \sqrt{2}\,\bar{N}_1\tau_+\eta N_2K^+ + \bar{N}_1\tau_3\eta N_3K^+ - \bar{N}_1\tau_3\eta N_3K^0] + \text{H.c.} + f_2[\sqrt{2}\,\bar{N}_4\tau_-\eta' N_3\bar{K}^+ - \sqrt{2}\,\bar{N}_4\tau_+\eta' N_2\bar{K}^0 - \bar{N}_4\tau_3\eta' N_3\bar{K}^0 - \bar{N}_4\tau_3\eta' N_3\bar{K}^+] + \text{H.c.}, \quad (9)$$

where the τ's are spin operators in the i space.

It is seen that the structure of (9) does not

provide for any substitutional invariance if $f_1 \neq f_2$, nor does it allow gauge transformations of any kind resulting in assignments of different quantum numbers to the different members of a given charge multiplet other than those already ascribed to them by their transformation properties in the charge space. This last point, of course, is a necessary requirement which must be imposed on any charge multiplet if the introduction of additional symmetries is to be avoided. $\{B\text{-}K\}$, however, is invariant under the hypercharge gauge transformation. Since $\vec{T}^2$ and T_3, where $\vec{T} = \vec{I} + \vec{K}$, are now the only quantities conserved, the charge operator may be defined as $Q = T_3 + \frac{1}{2} U$, in the manner of d'Espagnat and Prentki,[6] where U, the hypercharge quantum number, has the values 0 for π, N_2, and N_3, +1 for N_1 and K, and -1 for N_4 and K^C, with $U = S + N$. In addition to the conservation of $\vec{T}^2$, T_3, and U (or S), $\{B\text{-}K\}$ also imposes the selection rules $\Delta\vec{K} = 0, \pm 1$; $\Delta I = 0, \pm 1$, which, however, will be satisfied with the former.

In virtue of the fact that our $\{B\text{-}K\}$ imposes no more than charge independence (in the conventional sense) and the strangeness rule, simple amplitude relations of the type derived by Pais can no longer be easily obtained. However, certain processes are now favored with more channels than are others, and the implications of this fact are presently being investigated.

Finally we remark that our $\{B\text{-}K\}$ corresponds to taking $F_1 = -3\,F_2$ in the notation of Pais.[7]

It is a pleasure to acknowledge helpful discussions with Professor G. C. Wick and Dr. G. Feinberg.

---

*This work was performed under the auspices of the U. S. Atomic Energy Commission.

[1]A. Pais, Phys. Rev. 110, 574 (1958).
[2]M. Gell-Mann, Phys. Rev. 106, 1296 (1957).
[3]J. Schwinger, Phys. Rev. 104, 1164 (1956); Ann. Phys. 2, 407 (1957).
[4]A. Pais, Phys. Rev. 112, 624 (1958).
[5]G. Feinberg and F. Gürsey (private communication).
[6]B. d'Espagnat and J. Prentki, Nuclear Phys. 1, 33 (1956).
[7]It has been suggested by A. Pais (private communication) that in this connection the comparison of $\gamma + p \to \Lambda^0 + K^+$, $\gamma + p \to \Sigma^0 + K^+$ would be the most important point for a comparison with experiment. It would seem on a simple picture that Λ^0 production should be larger than Σ^0 production, at comparable phase space, by an order of magnitude. Recent results by McDaniel, Silverman, Wilson, and Cortellessa, Phys. Rev. Lett. 1, 109 (1958) indicate comparable efficiency for Λ^0 and Σ^0 production. We are indebted to Professor Pais for his comments.

ELASTIC SCATTERING OF PHOTONS BY TANTALUM*

E. G. Fuller and Evans Hayward
National Bureau of Standards,
Washington, D. C.
(Received November 19, 1958)

The neutron yield cross section for the deformed nucleus Ta^{181} has recently been measured[1,2] and found to consist of two maxima at 12.45 and 15.45.[1] This cross section has been fitted by the superposition of two Lorentz lines. These have been associated with oscillations of the nuclear charge along the one long and two short axes of the ellipsoid according to the suggestions of Okamoto[3] and Danos.[4] The present note describes the results of a measurement of the differential cross section at 120° for the elastic scattering of photons by the tantalum nucleus. The experimental methods employed were described in a previous paper.[5] The results are given in Fig. 1.

For comparison with these results the differential elastic scattering cross section, $d\sigma_S(\theta)/d\Omega$, associated with electric dipole absorption, has been calculated assuming (a) that the nuclear dipole polarizability is a tensor, i.e., that the polarizability has a different value associated with the major and minor axes of the nucleus; and (b) that the nuclear dipole polarizability is

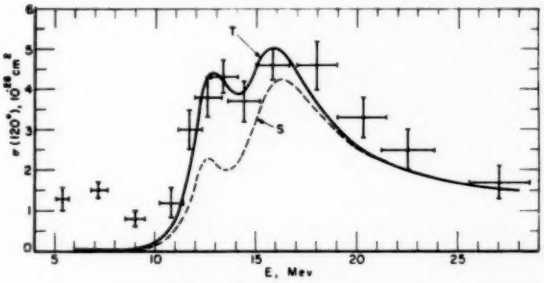

FIG. 1. The differential elastic scattering cross section for tantalum at 120° as a function of photon energy. The smooth curves are calculated using the dispersion relation and the resonance parameters given in reference 1 with the peak cross sections reduced by 10%. The solid curve is the result obtained assuming a tensor electric dipole polarizablity [Eq. (5)]; whereas the dashed curve results from assuming a scalar polarizability [Eq. (6)].

a scalar, i.e., that it is independent of the orientation of the nucleus with respect to the photon's polarization.

In terms of the forward scattering amplitude, f, the relationships between the photon absorption and elastic scattering cross section, σ and σ_S, are

$$\sigma = 4\pi\lambda \operatorname{Im} f,$$
$$d\sigma_S(0^\circ)/d\Omega = |f|^2. \quad (1)$$

Whenever σ can be represented by a Lorentz line, and the nuclear polarizability associated with σ is along the direction of polarization of the incident photon, the forward scattering amplitude is given by

$$f = \frac{\sigma_0 \Gamma}{4\pi\hbar c} \frac{E^2(E_0^2 - E^2) + iE^3\Gamma}{(E_0^2 - E^2)^2 + E^2\Gamma^2}, \quad (2)$$

where σ_0 is the peak absorption cross section, E_0 the resonance energy, and Γ the full width at half maximum of the resonance.

Assuming a tensor electric dipole polarizability, the scattering amplitude for a given nuclear axis, z, arbitrarily oriented with respect to the polarization of the incident photon, is

$$f(\theta) = f_z \cos\eta \sin\rho, \quad (3)$$

where θ is the scattering angle, η is the angle between the photon's polarization and z, ρ is the angle between z and the direction of observation, and f_z is given by Eq. (2) where the resonance parameters associated with the absorption of photons polarized along z are used. Danos has shown that, for an ellipsoidal nucleus, the relationship between the cross sections σ_a and σ_b associated with the absorption of photons polarized along the major and minor axes and the total absorption cross section for an unpolarized photon beam by an unoriented sample is

$$\sigma = \sigma_a/3 + 2\sigma_b/3. \quad (4)$$

For such an ellipsoidal nucleus the scattering cross section at an angle θ will be given by the absolute square of the sum of the scattering amplitudes associated with the three orthogonal nuclear axes, averaged over all orientations of the nucleus with respect to the incident photon's polarization and finally averaged over all polarizations of the photon. If A and α, B and β, are the real and imaginary parts of the scattering amplitudes associated with σ_a and σ_b, and D is the nuclear Thomson scattering amplitude, $-Z^2e^2/AMc^2$, the resulting expression for the differential scattering cross section is

$$\frac{d\sigma_s(\theta)}{d\Omega} = \frac{3}{15}(A^2+\alpha^2) + \frac{11}{30}(B^2+\beta^2) - \frac{1}{15}(AB+\alpha\beta) + \frac{1}{3}AD + \frac{2}{3}BD + \frac{1}{2}D^2 + \left[\frac{1}{15}(A^2+\alpha^2) + \frac{7}{30}(B^2+\beta^2) + \frac{1}{5}(AB+\alpha\beta) + \frac{1}{3}AD + \frac{2}{3}BD + \frac{1}{2}D^2\right]\cos^2\theta. \quad (5)$$

If, on the other hand, the two resonances found for the neutron yield cross sections for tantalum are not associated with different axes, i.e., if the nuclear polarizability is assumed to be a scalar, the dipole moment induced in the nucleus is always along the polarization of the incident photon. The scattering amplitude for the two resonances is then the sum of the amplitudes for the two resonances with an angular dependence determined by the sine of the angle between the polarization of the incident photon and the direction of observation. The differential scattering cross section is then given by the average of the absolute square of this scattering amplitude over all orientations of the photon's polarization:

$$\frac{d\sigma_s(\theta)}{d\Omega} = \frac{1+\cos^2\theta}{2}\left[\left(\frac{A+2B}{3}+D\right)^2 + \left(\frac{\alpha+2\beta}{3}\right)^2\right], \quad (6)$$

where $A/3$ and $2B/3$, $\alpha/3$ and $2\beta/3$ are the real and imaginary parts of the forward scattering amplitudes associated with the two resonances found in the absorption cross section.

Equations (5) and (6), evaluated at 120° and using the parameters of reference 1, are plotted in Fig. 1. The cross section obtained from the scalar expression [Eq. (6)] shows the effects of strong destructive interference between the two resonances. This interference is essentially missing in the tensor polarizability case since the absorption is now associated with the orthogonal axes of the nucleus. The experimental cross section as a function of energy is in better agreement with the result calculated from the tensor expression than that obtained assuming a scalar polarizability. This result tends to confirm the spatial correlation of the dipole polarizability for a deformed nucleus as proposed by Danos and Okamoto.

In order to achieve the agreement in magnitude displayed in Fig. 1, the peak cross sections of

the resonances of reference 1 were reduced by 10%. Since the absolute cross sections of reference 1 are known to only about ±15% and since there are possible systematic errors (as large as ±7%) in the absolute magnitude of the scattering cross section, this adjustment is well within the errors in the absolute sizes of the two cross sections being compared. The difference between the experimental points and the smooth curve at the higher energies is probably significant. It represents more absorption than is given by the two Lorentz lines used to predict the scattering cross section. The neutron yield cross section of reference 1 is also higher than the Lorentz lines in this energy region.

The authors want to thank M. Danos for his help in understanding these results.

---

*This research was supported by the U. S. Air Force, through the Office of Scientific Research of the Air Research and Development Command.

[1]E. G. Fuller and M. Weiss, Phys. Rev. 112, 560 (1958).

[2]B. M. Spicer et al., (private communication).

[3]K. Okamoto, Phys. Rev. 110, 143 (1958).

[4]M. Danos, Nuclear Phys. 5, 23 (1958).

[5]E. G. Fuller and E. Hayward, Phys. Rev. 101, 692 (1956).

DOUBLING OF FERMIONS?

M. Goldhaber

Brookhaven National Laboratory,*
Upton, New York

(Received November 25, 1958)

The recent discovery that the long sought π-e mode of decay does indeed exist,[1,2] and that its intensity[3] relative to the π-μ mode is compatible with the assumption of equal interactions for electrons and μ mesons,[4,5] removes a stumbling block to further thinking about the remarkable similarity between these two particles. Except for their mass difference, the electron and μ meson of a given electric charge behave, as far as their known interactions are concerned—i.e., electromagnetic, as well as weak interactions—like two states of one particle. Tentatively we shall assume that they differ by a hitherto unknown internal parameter. This parameter is presumably connected with their mass difference, but does not affect their known interactions which may be held to be invariant with respect to the internal parameter. Many examples of invariance of interactions with respect to an internal parameter are well established, e.g., the charge independence of nucleon interactions. On this view, one might refer to the μ meson as a "heavy electron"—a name by which it was once known—and use the symbols e_1 and e_2 for e and μ, respectively.

One might go further and ask, again assuming the view outlined to be correct, whether the heavier fermions, the baryons, might not also appear as doublets of which only the lighter members have so far been observed. Although the baryons possess strong interactions, in addition to the electromagnetic and weak ones, it is conceivable that whatever the cause of the doubling of electrons into light and heavy ones might be, it might also be responsible for a doubling of baryons. In the absence of definite knowledge on this point, it would seem worthwhile to start out by inquiring why the "heavy baryons," if they actually do exist, might have so far escaped detection.

Take the case of the proton, where besides the ordinary proton p_1, a "heavy proton," p_2, might exist. Simple considerations show that it would have been difficult to recognize such a particle without a deliberate search. What would be some possible modes of production of p_2? For guidance, let us remind ourselves of the processes which give rise to μ mesons. Two essentially different processes are known: μ mesons may appear as decay products of π or K mesons, or they may be produced by photons in pairs: $\mu^+ + \mu^-$. The pair production is difficult to observe, and it was only discovered as a result of a deliberate and careful search.[6] In analogy with these phenomena, we might look for heavy nucleons both in decay processes and in pair production. Depending on the mass of the heavy nucleons, it might or might not be energetically possible for a heavy nucleon to appear as a decay product of one of the known hyperons. However, a process of this type would only have been found with a reasonable probability if the mass difference $\Delta = m(p_2) - m(p_1)$ were considerably smaller than the Q value of hyperons. There remains, as a more systematic approach, the deliberate search for the pair-production process $p_2 + \bar{p}_2$. Here we have the advantage, compared with the case of μ-pair production, that we can make use of the strong interactions, besides the electromagnetic ones.

What would be the characteristics of a p_2, or its antiparticle $\bar{p}_2$ (apart from their mass), by

which they might be distinguished from the known particles? Since the mass difference Δ cannot be estimated at present, we can only speculate about possible decay modes of p_2. It might, e.g., decay by a β interaction: $p_2 \to n_1 + e_{1,2}^+ + \nu$. Other weak decay modes might exist; in particular, one or more π mesons or K mesons might be emitted if Δ were sufficiently high. Since p_2 must be assumed to have also strong interactions, though not in decay, it may occur bound to other, ordinary, nucleons, and its decay in such a state may resemble a hyperfragment disintegration.[7] The same holds for $\bar{p}_2$, which could either annihilate "slowly" inside a nucleus through its weak interaction, e.g., $\bar{p}_2 + n_1 \to e_{1,2}^- + \bar{\nu}$, or first decay into $\bar{p}_1$ or $\bar{n}_1$ with consequent rapid annihilation.

I wish to thank G. Feinberg, F. Gürsey, and M. Gell-Mann for interesting discussions.

*Under the auspices of the U. S. Atomic Energy Commission.

[1]Fazzini, Fidecaro, Merrison, Paul, and Tollestrup, Phys. Rev. Lett. 1, 247 (1958).

[2]Impeduglia, Plano, Prodell, Samios, Schwartz, and Steinberger, Phys. Rev. Lett. 1, 249 (1958).

[3]Roundtable discussion on π-e decay (Tollestrup, Steinberger, Miller, Anderson, and Pollak) at Gatlinburg Conference on Weak Interactions, October 1958, Revs. Modern Phys. (to be published).

[4]E. C. G. Sudarshan and R. Marshak, Phys. Rev. 109, 1860 (1958).

[5]R. P. Feynman and M. Gell-Mann, Phys. Rev. 109, 193 (1958).

[6]G. E. Masek and W. K. H. Panofsky, Phys. Rev. 101, 1094 (1956); 103, 374 (1956).

[7]From time to time there have been reports of cosmic-ray events observed in photographic emulsions which appear to show a Q value larger than expected from hyperon decay. In the light of the question raised above, some of these events might be worth re-analyzing. See, e.g., Y. Eisenberg, Phys. Rev. 96, 541 (1954); Fry, Schneps, and Swami, Phys. Rev. 97, 1189 (1955), and Nuovo cimento 2, 346 (1955); Castagnoli, Cortini, and Franzinetti, Nuovo cimento 2, 550 (1955).

RADIATIVE CORRECTIONS TO PION BETA DECAY*

S. M. Berman
Norman Bridge Laboratory of Physics,
California Institute of Technology,
Pasadena, California
(Received November 6, 1958)

Recent experiments[1] have shown that the ratio R_0 of the rates Γ_e, Γ_μ for $\pi \to e + \nu$ and $\pi \to \mu + \nu$ modes of decay is in the neighborhood of the value predicted by the universal beta-decay theory,[2,3] i.e., $R_0 = (12.78 \times 10^{-5})$. However, to compare the results of a precise experiment with the predicted number the radiative corrections should be included in the theoretical estimate of the ratio. The corrections do not cancel in the ratio since they depend on the electron and muon masses and, furthermore, produce a surprisingly large correction to the ratio.

Using the universal (V,A) theory[3] we express the general matrix element for the process $\pi \to (e \text{ or } \mu) + \nu + \gamma$ to order e as

$$M_\nu = [f_1 \delta_{\mu\nu} + f_2 k_\mu p_\nu + f_3 p_\mu p_\nu] \times \bar{\Psi}_{l_2} \gamma_\mu (1 + i\gamma_5) \Psi_{l_1} \cdots , \qquad (1)$$

where p and k are the momentum of the pion and photon, respectively, and where each of the covariants f_1, f_2, f_3 depend on the scalars m_π^2, $p \cdot k$, k^2. In addition to M_ν we also consider the matrix elements which arise from bremsstrahlung photons. In writing Eq. (1) we have used the Lorentz condition to eliminate terms such as $k_\nu p_\mu$, $k_\nu k_\mu$. We note that gauge invariance implies that f_1 at $k=0$ is determined by the amplitude for $\pi \to (e \text{ or } \mu) + \mu$

In the phenomenological theory with direct π-$(e \text{ or } \mu)$ coupling only f_1 would be present in Eq. (1). In a realistic theory involving virtual nucleon loops, the other covariants f_2, f_3 would be expected to enter. If we consider the decay of the pion to occur through one virtual nucleon pair then we find that $f_{2,3} \sim (1/M^2) f_1$ where M is the nucleon mass and that in the limit of very large nucleon mass f_1 does not depend on $p \cdot k$ and k^2. If we consider $(k^2/M^2) \ll 1$ then application of the Ward identity leads to the same conclusions to all orders in the pion-nucleon coupling. We therefore have neglected $f_{2,3}$ in the calculation of the radiative corrections, and have assumed f_1 is independent of k. In this case f_1 will cancel out in the ratio of the rates.

Using the first term of Eq. (1) we have calculated the radiative corrections, in the usual manner, by including all possible real and virtual electromagnetic processes to order e^2. Since the inclusion of the inner bremsstrahlung changes the number of particles in the final states from two to three there is now a spectrum of energies available to the electron or muon. If we ask how the ratio of rates is affected for electrons or muons having an energy near the maximum energy and suffering an energy loss less than

ΔE, then we obtain for the new ratio R, in units of $\hbar = c = 1$ and $e^2 \approx 1/137$,

$$R=(12.78\times10^{-5})\left[1-\frac{2e^2}{\pi}\left\{\tfrac{3}{4}\ln(m_\mu/m_e)+\ln(2\Delta E_e/m_e)-\ln(2\Delta E_\mu/m_e)+\left(\frac{m_\pi^2+m_e^2}{m_\pi^2-m_e^2}\right)\times\ln(m_\pi/m_e)\ln\left(\frac{m_\pi^2-m_e^2}{2\Delta E_e m_\pi}\right)-\left(\frac{m_\pi^2+m_\mu^2}{m_\pi^2-m_\mu^2}\right)\times\ln(m_\pi/m_\mu)\ln\left(\frac{m_\pi^2-m_\mu^2}{2\Delta E_\mu m_\pi}\right)-\frac{m_e^2}{m_\pi^2-m_e^2}\times\ln(m_\pi/m_e)+\frac{m_\mu^2}{m_\pi^2-m_\mu^2}\ln(m_\pi/m_\mu)-\ln\left(\frac{m_\pi^2-m_e^2}{m_\pi^2-m_\mu^2}\right)\right\}\right], \quad (2)$$

or

$$R=[11.00+0.27\ln(2\Delta E_e/m_e)]\times10^{-5}, \quad (3)$$

where ΔE_e and ΔE_μ are the energy intervals below the maximum energy over which electron or muon counts are being accepted[4]. We have omitted from Eq. (3) the term which depends on $\ln(\Delta E_\mu/m_e)$ since it is completely negligible. For $2\Delta E_e = m_e \approx 0.5$ Mev the radiative corrections amount to a surprisingly large decrease in the ratio of amount 14%.

We note that even though the rate for $\pi \to (\mu \text{ or } e) + \nu$ contains logarithms of the ultraviolet cutoff, the ratio of rates will not depend on the cutoff as long as we take it to be the same for each of the decay modes.[5] Furthermore, the contributions to Eq. (3) from virtual processes come almost entirely from very low photon momenta. If this were not true, but instead the contributions to R came from regions of large virtual photon momenta, then the radiative corrections might depend on the terms in f_1 dependent on $p\cdot k$ and k^2 and also on the other covariants.

The results given here do not agree with a recent "theorem" by Gatto and Ruderman.[6] However using a theorem due to Ruderman and Watson[7] a closely related statement can be made: Let Γ_P and Γ_A represent the rates for one of the pion decay channels with the leptons coupled with either P or A interaction. Then the ratio Γ_P/Γ_A including electromagnetic effects, expressed in terms of the bare masses, is equal to the ratio Γ_P/Γ_A without including electromagnetic effects. In particular for the electron decay mode $\Gamma_P/\Gamma_A = (m_\pi^{(b)}/m_e^{(b)})^{-1}$ with and without including radiative corrections. If we are interested in

$$\left(\frac{\Gamma_e}{\Gamma_\mu}\right)_A = \left[\frac{(\Gamma_e/\Gamma_\mu)_A}{(\Gamma_e/\Gamma_\mu)_P}\right]\left(\frac{\Gamma_e}{\Gamma_\mu}\right)_P,$$

then we note that the term in brackets is equal to the ratio of the square of the bare masses of the electron and muon with or without including conventional electrodynamics. However, one should also note that $(\Gamma_e/\Gamma_\mu)_P$ receives a large radiative correction which to first order in e^2 is around 11% decrease.

The author is indebted to Dr. Jon Mathews for many useful and illuminating discussions. He also wishes to thank Professor M. Gell-Mann for several helpful discussions.

*Work supported by the Alfred P. Sloan Foundation, Inc.

[1]T. Fazzini et al., Phys. Rev. Lett. 1, 247 (1958); G. Impeduglia et al., Phys. Rev. Lett. 1, 249 (1958).

[2]M. A. Ruderman and R. J. Finkelstein, Phys. Rev. 76, 1458 (1949).

[3]R. P. Feynman and M. Gell-Mann, Phys. Rev. 109, 193 (1958).

[4]Since the neutrino is not observed we have included in Eq. (2), in the calculations of the inner bremsstrahlung, the contributions from all photons having momenta consistent with the conservation laws. This means that in the integration over real photon momenta the maximum photon energy will be a function of x, the cosine of the angle between electron (muon), and of the energy interval ΔE, i.e.,

$$\omega_{\max} = \left(\frac{2m_\pi^2}{m_\pi^2 - m_e^2}\right)\left(\frac{\Delta E}{1+x}\right).$$

[5]If, for example, we take the cutoffs occurring in the virtual processes to be proportional to the respective masses of electron or muon, then R increases by about 1.5% over that given by Eq. (3).

[6]R. Gatto and M. A. Ruderman, Nuovo cimento 8, 775 (1958).

[7]M. A. Ruderman and W. K. R. Watson, Bull. Am. Phys. Soc. Ser. II, 1, 383 (1956).

MUON K-CAPTURE COMPARED TO β DECAY FOR $C^{12} \to B^{12}$

J. O. Burgman, J. Fischer, B. Leontic, A. Lundby, R. Meunier,* J. P. Stroot, and J. D. Teja
CERN, Geneva, Switzerland
(Received November 24, 1958)

Recent refinements of the theory of the V-A universal Fermi interaction[1] have made it desirable to attempt a more precise experimental

comparison of the coupling strengths of electrons and muons to nuclei. For this purpose we have measured the rate ratio $(C^{12}+\mu^- \rightarrow B^{12}+\nu)/(C^{12}+e^- \rightarrow B^{12}+\nu)$. The experiment was originally suggested by Tiomno, and measurements with cosmic-ray muons have been reported by Godfrey.[2]

We used the mixed π^-, μ^-, and e^- beam of 220 Mev/c momentum from the CERN Synchrocyclotron in the arrangement shown in Fig. 1. The beam was pulsed either 54.2 or 13.5 times per sec. Three experimental arrangements were used in which (1) the beam was stopped in C^{12} and decay electrons from muons and B^{12} were viewed with a scintillation telescope, (2) the beam was stopped in a $10\times10\times10$ cm^3 scintillation crystal and the decay electrons were detected with the same crystal, (3) the same as (2) but with a 6-cm thick crystal. In (1) the uncertainties in estimating the counting efficiencies were large; (2) and (3) gave similar results, but (3) was much more comprehensive and will be reported.

Figure 1 shows the delayed activity recorded in the $6\times10\times10$ cm^3 scintillator as a function of Cu absorber in front of the counter. A $1\times30\times30$ cm^3 scintillation counter above suppressed a large fraction of the cosmic-ray background. The data were obtained by triggering a time-to-pulse-height converter (20 channels) by each beam pulse from the cyclotron, and feeding the pulses from the stopping counter to a time-to-amplitude channel. In Fig. 1 we have collected the counts arriving in the time interval from 3.6 msec (beginning of 5th channel) to 14 msec (end of 17th channel). When both π^- and μ^- stop in the crystal a delayed activity is formed. The decays of these activities are shown in Fig. 2. The yield of the 80-msec activity at the π^- peak indicates that somewhat less than 1% of the π^- captures lead to this activity.[3] The half-life at the μ^- absorption peak is 20.7 ± 0.3 msec, in agreement with the presently accepted value[4] of 20.6 msec for B^{12}. The B^{12} activity, extracted as indicated in Fig. 1, was constant when the voltage on the photomultiplier (RCA *C*7170) was varied from 2400 to 3200 volts. The total B^{12} counting rate amounted to about 100 per min at the μ^- peak, or 860 ± 30 for 10^6 monitor counts 1-2. The error is estimated from uncertainties in the extrapolations.

The number of muons stopping in the scintillator was obtained by counting delayed "self-coincidences." A pulse from the counter started a 10-μsec sweep on the time-to-pulse-height converter, and the pulses from the same counter were displayed in the 20 channels. Absorption and photomultiplier voltage curves were also taken for this activity. For 10^6 monitor counts we obtained in this way $41\,800\pm1000$ muons when corrected for the 10% capture probability in C. The error is also in this case estimated from uncertainties in extrapolations.

Both muon and B^{12} counts were found to vary strictly proportional to the intensity of the beam. When a μ^- slows down and stops in the scintillator the probability that it will form B^{12} is thus found to be (2.06 ± 0.10)%.

A short run was made to look for γ rays from possible captures to excited bound states of B^{12}.

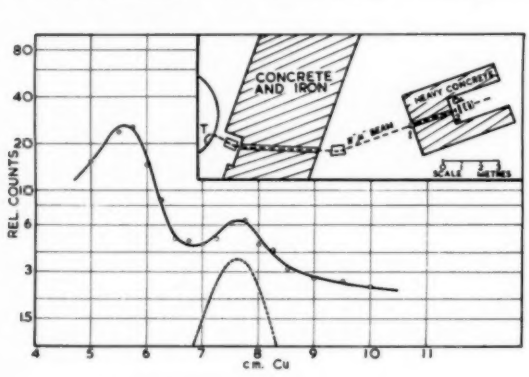

FIG. 1. Experimental arrangement, and absorption curve of activity in the scintillator between the beam pulses of the cyclotron. The dotted curve represents the B^{12} activity after subtraction of background and π-capture activities.

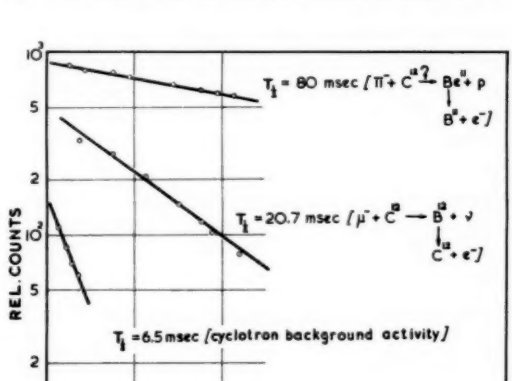

FIG. 2. Decay of the delayed activity at the π^- peak, μ^- peak, and with a large absorber.

The 10-μsec time-to-pulse-height converter was again used with pulses from the plastic (counter 3) commencing the sweeps, and pulses from an 8-cm diameter, 10-cm long NaI(Tl) crystal (No. 4) in anticoincidence with coincidences 3-4 entering the sampling channel. Only accidentals were observed. The limited solid angle of the NaI(Tl) and the shortness of the run did not make it possible to conclude other than that less than 25% of the captures led to excited states.

With the mean life of μ^- in vacuum and in C as 2.21 and 2.02 μsec, respectively,[5] and the mean life of B^{12} as 29.8 msec with a 3% correction[6] for decays to excited states of C^{12}, we get 312 $\pm$18 for the ratio of the μ^- capture rate giving B^{12} to the decay rate of B^{12} to the ground state of C^{12}. The theoretical value given by Godfrey[2] is 228, assuming equal coupling constants for μ^- capture and β^- decay. Our experiment therefore yields a ratio $R=[C_{GT}(\mu^-\text{ capture})/C_{GT}(\beta^-\text{ decay})]^2=1.37\pm0.08$. The gap between experiment and the primitive theory may possibly be bridged by effects as discussed in reference 1. Judging from theoretical estimates,[2] contributions from μ^- captures to excited bound states of B^{12} are not capable of explaining the difference.

Except for possible influences of effects already mentioned,[1] Tolhoek[7] has tentatively interpreted some data on the absolute values of the capture rates and their ratios for a number of nuclei in the neighborhood of Ca^{40} in terms of a universal Fermi interaction with a value for the Gamow-Teller coupling constant which is higher for μ capture than for β decay, but with the same coupling constant for the Fermi part in both cases (use is made of shell model calculations[8]). This interpretation provides roughly a range of 1.4 to 2.2 for the value of R.

We enjoyed the support of Professor C. J. Bakker, Professor G. Bernardini, and Professor W. Gentner, the technical assistance of P. Duteil and R. Thill, the aid of H. Faissner and D. Oldroyd in carrying out the experiment, and the cooperation of the cyclotron staff in providing the beam.

*On leave from C.E.N., Saclay.

[1]M. Gell-Mann, Phys. Rev. 111, 362 (1958); L. Wolfenstein, Nuovo cimento 8, 882 (1958); M. L. Goldberger and S. B. Treiman, Phys. Rev. 111, 354 (1958).

[2]T. N. Godfrey, Phys. Rev. 92, 512 (1953); 94, 756 (1954); thesis, Princeton, 1954 (unpublished).

[3]The activity has very tentatively been ascribed to Be^{11}. We benefitted from discussions with R. Sherr on this point.

[4]J. F. Vedder, University of California Radiation Laboratory Report UCRL-8324, 1958 (unpublished).

[5]J. C. Sens, thesis, Chicago, 1958 (unpublished).

[6]Cook, Fowler, Lauritsen, and Lauritsen, Phys. Rev. 107, 508 (1957).

[7]H. A. Tolhoek (private communication).

[8]H. A. Tolhoek and J. R. Luyten, Nuclear Phys. 3, 679 (1957).

MEASUREMENT OF THE ASYMMETRY PARAMETER IN μ-e DECAY*

Gerald Lynch and J. Orear
Laboratory of Nuclear Studies,
Cornell University, Ithaca, New York
and
S. Rosendorff
Department of Physics,
Columbia University, New York, New York
(Received November 17, 1958)

The angular distribution of the positron from the decay of the positive muon has the form $1-(\xi/3)\cos\theta$, where θ is the angle between the muon spin and the positron direction. The V-A theory predicts that the parameter ξ should be -1.[1] Experimental measurements of the decay asymmetry obtain the quantity $a=P(\xi/3)$ where P is the polarization of the muons at the time of decay. So far all published measurements of $-a$, using muon beams of unknown polarization, have been well below 1/3. For example, the Nevis[2] and Chicago[3] results for μ^+ in graphite are $-a=0.25\pm0.02$ and 0.229 ± 0.008, respectively. This experiment is an attempt to make a measurement of a in a situation in which P is very nearly equal to unity by making use of the fact that a strong magnetic field applied along the muon spin direction can eliminate most of the depolarization on muons before they decay in nuclear emulsion.[4-6]

The muons used in this experiment came from pions which were produced at the Nevis cyclotron. These pions came to rest in 600-micron-thick Ilford $G5$ nuclear emulsion on which was imposed a magnetic field of 25 000 gauss in the plane of the pellicles. Then the decay distribution is of the form $1+a\cos\beta\cos\phi$, where β and ϕ are the angles which the initial directions of the muon and positron make with the magnetic field direction.

The plates were area scanned for muon endings. Only those events were recorded for which

the projected direction of both the muon and the positron were within 45° of the magnetic field direction. Also those events for which the muon ending was within 70 microns from either surface were not recorded. The positron was found in all but 6 of the approximately 11 000 events in which the muon, in addition to satisfying the selection criteria, also was seen to come from a pion. The asymmetry parameter a is obtained from the recorded events using the expression $a = 2[(S-O)/(S+O)]$ where S is the number of recorded events in which the initial muon and positron directions are both in the same quadrant, and O is the number of recorded events in which they are in opposite quadrants. This method of scanning was designed to minimize the scanning time necessary to obtain a result of a given precision, even though it requires more events than an alternative procedure of measuring individual space angles. The expression for a is obtained by integrating over the angles β and ϕ within the limits of ±45° projected direction. It is only fortuitous that this integration gives the same numerical constant as one has in the case of estimating a from simple forward-backward counts.

In the scanning of the emulsions no tracks were followed from one plate to another. When the muon came from a pion which had stopped outside the pellicle in which the muon had stopped, which occurs for one-half of the cases, the initial direction of the muon was approximated by its direction upon entering the pellicle. This approximation introduces an error in the measured asymmetry parameter because the muon angle will have been slightly changed by multiple scattering before entering the pellicle. This effect has been calculated exactly using the multiple scattering distribution of Goudsmit and Saunderson.[7] The result of this calculation is to increase our uncorrected asymmetry parameter by 1.7%. Even smaller corrections taking into account emulsion distortion, muon background, scanning biases, and radiative corrections have also been made.

More than 42 000 μ-e decays have been looked at. Because of our scanning procedure only one half of these μ-e decays have been looked at carefully and only one fourth have been recorded. No case of a muon decaying into three electrons has been observed. The following three processes would have been observed with high efficiency: $\mu^+ \to e^+ + e^+ + e^-$, $\mu^+ \to e^+ +$ pair, and $\mu^+ \to e^+ + \bar{\nu} + \nu +$ pair. Thus on the basis of this experiment alone the sum of the branching ratios for these three modes is probably less than 3×10^{-5}. From 10 791 recorded events, the corrected asymmetry parameter is $a = -0.298 \pm 0.019$. This corresponds to $P\xi = -0.89 \pm 0.06$. This is 1.8 standard deviations below the theoretical prediction of $\xi = -1$.

The minor discrepancy between this result and the successful V-A theory may be due to statistics or to a small amount of residual depolarization or to both. In the simple case of depolarization by muonium formation the depolarization as a function of the magnetic field B is $\frac{1}{2}[1 + B^2/B_0^2]^{-1}$, where the characteristic field $B_0 = 1600$ gauss.[4] This expression predicts a depolarization of 0.2% at 25 000 gauss. However this expression is not the best fit to the emulsion data of Sens et al.[6] If the parameter B_0 is varied to give a better fit to their data, one would predict a depolarization of from 1 to 3% at 25 000 gauss. Sens et al. suggest repeated electron captures as the depolarization mechanism. Using their formula for this, one would predict about 1% depolarization at 25 000 gauss. Since the effect of an unpaired electron in a molecule to which a μ^+ is attached should not be much greater than the effect of the electron in muonium, it seems reasonable to believe that the depolarization in this experiment is less than 3%.

We feel that our experiment helps remove the discrepancy between the prediction of the V-A theory and previous measurements of the μ-e asymmetry. At the Gatlinburg Conference on Weak Interactions, October, 1958, two preliminary results on μ-e asymmetry by Plano and Lecourtois and by Berley and Bardon of Columbia were reported which are consistent with our result.

---

*Supported in part by the joint program of the Office of Naval Research and the U. S. Atomic Energy Commission.

[1]R. P. Feynman and M. Gell-Mann, Phys. Rev. 109, 193 (1958); and E. C. G. Sudarshan and R. E. Marshak, Phys. Rev. 109, 1860 (1958).

[2]M. Weinrich, Nevis Report 56, February, 1958, Physics Department, Columbia University (unpublished).

[3]R. Swanson, Phys. Rev. 112, 580 (1958).

[4]Orear, Harris, and Bierman, Phys. Rev. 107, 322 (1957).

[5]Barkas, Giles, Heckman, Inman, and Smith, Phys. Rev. 107, 911 (1957).

[6]Sens, Swanson, Telegdi, and Yovanovitch, Phys. Rev. 107, 1465 (1957).

[7]H. A. Bethe, Phys. Rev. 89, 1256 (1953).

NUCLEAR GROUND-STATE SPINS OF THALLIUM-198 AND -201†

I. Lindgren, C. M. Johansson, and S. Axensten
Institute of Physics,
University of Uppsala,
Uppsala, Sweden
(Received November 17, 1958)

The atomic beam resonance method[1] has been used to measure the nuclear ground-state spins of Tl^{198} and Tl^{201} with the following values obtained: for the 5.3-hour Tl^{198}, $I=2$, and for the 3.0-day Tl^{201}, $I=\frac{1}{2}$.[2] The ground-state spin of Tl^{198} is particularly important because it confirms the decay schemes of Pb^{198},[3] and of the 1.8-hour isomeric state of Tl^{198}.[4] The isomeric state has been measured with the atomic beam method to have the spin $I = 7$.[5]

For the production of Tl^{198} thallium was bombarded with 85-Mev protons. This gives mainly Pb^{198}, which decays to the ground state of Tl^{198} with a half-life of 2.3 hours. The lead was separated from the thallium by ether extraction and then electroplated together with some milligrams of stable lead and thallium on a copper wire, which was put into the oven. The chemical separation was made a couple of hours after the bombardment in order to let the more short-lived lead isotopes decay away. A few hours after the separation the Tl^{198} activity was strong enough to give good signals. By this procedure an isotopically cleaner sample is obtained than by bombarding mercury and furthermore no isomeric state is produced. The Tl^{201} was produced by bombarding mercury with 25-Mev deuterons and chemically separated in a similar way.

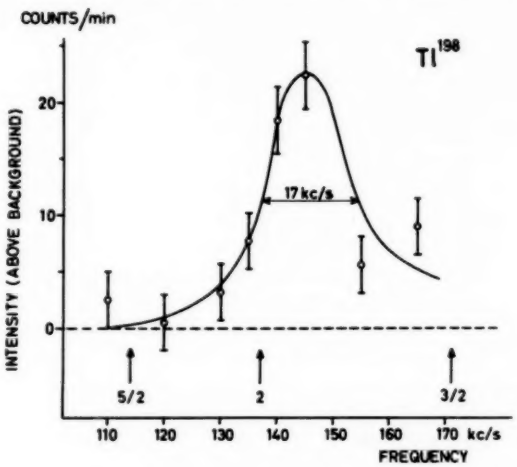

FIG. 1. Resonance curve of Tl^{198} at a field of 0.7 gauss. The arrows indicate the calculated resonance frequencies for different spin values without any quadratic effect.

Figure 1 shows a resonance curve of Tl^{198} at a C field of 0.7 gauss (corresponding to a potassium frequency of 0.5 Mc/sec) and Fig. 2 a curve of Tl^{201} at 2.8 gauss. The spin search of Tl^{198} was made at the lowest possible field to be sure that the quadratic effect should be small. Resonance curves have then been taken at several higher field strengths and they indicate an extremely small magnetic moment. The hfs separation seems to be only about 14 Mc/sec which means that the magnetic moment is smaller than 2×10^{-3} nuclear magnetons. This moment is as far as we know the smallest one for a state with a spin different from zero which has ever been measured. The only known magnetic moment of a radioactive thallium isotope is that of Tl^{204},[5] which is also very small, 0.089 nm.

The spin value of Tl^{198} has also been checked with an isotope-separated source. In the separator the isotope was collected on a copper strip. This was dissolved in acid and the thallium extracted by ether and then electroplated together with some milligrams of stable thallium.

The measurements are now being continued in order to get the hfs separation and magnetic moment of Tl^{198} more accurately and also possibly to find the spin of Tl^{196}.

We want to express our thanks to Professor Kai Siegbahn for his interest and support, to Ing. Å. Svanheden and his cyclotron crew at The Gustav Werner Institute for making the irradia-

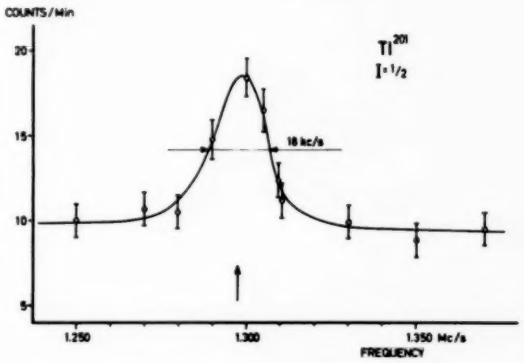

FIG. 2. Resonance curve of Tl^{201} at a field of 2.8 gauss. The arrow indicates the calculated frequency for $I = \frac{1}{2}$.

tions, and to Dr. G. Andersson et al. at the same institute for making the isotope separations.

†This work has been financially supported by the Swedish Atomic Energy Commission.

[1]I. Lindgren, Nuclear Instr. 3, 1 (1958).

[2]The spin value of Tl^{201} has independently been measured by the Berkeley group [L. L. Marino et al., Bull. Am. Phys. Soc. Ser. II, 3, 186 (1958)].

[3]B. Jung, Nuclear Phys. (to be published).

[4]G. Andersson and I. Bergström, Nuclear Phys. 3, 506 (1957).

[5]Brink, Hubbs, Nierenberg, and Worcester, Phys. Rev. 107, 189 (1957).

ANNOUNCEMENT

The period of free subscription to PHYSICAL REVIEW LETTERS for all subscribers to THE PHYSICAL REVIEW ends with this issue. There will be a grace period, but persons who have not sent in their subscriptions will have no just cause for complaint when delivery is halted without further notice.

ABSTRACTS

In this section are printed the abstracts of Articles that have been forwarded to The American Institute of Physics for publication in THE PHYSICAL REVIEW. In quoting information obtained from this section before the appearance of the corresponding Article, reference should be made to "Physical Review (to be published)" rather than to this Journal.

DRIFT VELOCITY OF ELECTRONS IN MERCURY VAPOR AND MERCURY VAPOR-CO_2 MIXTURES. C. W. McCutchen, Cavendish Laboratory, Cambridge, England (Received July 25, 1958).

The drift velocity of electrons in mercury vapor has been measured with an apparatus of the type used in Klema and Allen. The effect of added CO_2 has been investigated. The results are used to calculate the electron mean free path in mercury vapor. It is found that mercury vapor has a mean free path maximum (Ramsauer effect) at low electron energy.

STATISTICAL-MECHANICAL THEORY OF TRANSPORT IN FLUIDS. Hazime Mori, Metcalf Research Laboratory, Brown University, Providence, Rhode Island (Received August 5, 1958).

A statistical-mechanical theory of transport processes in fluids of g components is presented on the assumption that the macroscopic state of the system can be described by one velocity, one temperature, and g mass-density fields. The formulation is based on the explicit recognition of the fact that there are two relaxation processes in fluids: one is the macroscopic process of attaining spatial uniformity and is represented by the hydrodynamical equations, whereas the other is the microscopic process of attaining internal thermal equilibrium in small mass elements of macroscopic size and determines the transport coefficients. For instance, in dilute gases the microscopic process is the relaxation process in momentum space. The coupling of the two processes is investigated to obtain the dissipative terms in the transport equations with the aid of the correlation-function method outlined in a previous paper. The hydrodynamical equations, the equation of entropy balance, and the linear relations between the thermodynamic fluxes and affinities are thus derived with explicit expressions for the coefficients of viscosity, thermal conductivity, and diffusion, which are valid for liquids as well as for gases. The classical limits of these expressions, $\hbar \to 0$, are somewhat different from those obtained by Green for classical mechanical systems.

THEORY OF RADIATIVE DAMPING IN STATIONARY STATES. C. A. Mead,* Chemistry Department, Brookhaven National Laboratory, Upton, New York (Received August 21, 1958).

A formalism is developed for finding the stationary states of systems for which radiative damping effects must be considered. The method includes a criterion for deciding whether or not a given unperturbed state has an exact stationary state corresponding to it. The method is applied to a simple example, the Lee model with unstable V-particle, and it is indicated how more complicated problems may be treated.

* Present address: School of Chemistry, University of Minnesota, Minneapolis, Minnesota.

EFFECT OF SPACE CHARGE IN COLD-CATHODE GAS DISCHARGES. A. L. Ward, Diamond Ordnance Fuze Laboratories, Washington, D. C. (Received August 22, 1958).

Townsend's basic ionization equations for cold-cathode gas discharges between parallel plates are modified by Poisson's equation to account for space charge effects. Numerical calculations have been made for argon on the IBM 704 computer. Calculated voltage-current static characteristics in general show a negative-slope region indicating "breakdown." For low pd products (p being the gas pressure and d the gap distance), a second region of positive slope (abnormal glow) is obtained at higher currents. The electric field distribution across the gap is shown, at high currents, to approach that measured in glow discharges, and the formation of a positive column plasma is indicated by the charge distributions.

ENTROPY OF VACANCIES IN IONIC CRYSTALS. O. Theimer, Department of Physics, University of Oklahoma, Norman, Oklahoma (Received August 25, 1958).

The entropy of vacancies in sodium chloride is calculated from the ionic displacements produced

by the Coulomb field of the vacancies and from the corresponding changes of the lattice frequencies. Using the displacements recently calculated by Tosi and Fumi it is found that, contrary to earlier expectations, the sum of all the frequency changes is positive. Some physical consequences of this result are discussed.

CORRELATION OF ANNIHILATION RADIATION IN ORIENTED SINGLE METAL CRYSTALS. Stephan Berko and John S. Plaskett, University of Virginia, Charlottesville, Virginia (Received July 31, 1958).

Precision measurements of the two-photon annihilation in crystals of Al and Cu are presented. These show relatively small variation with crystal orientation. This is interpreted to mean that the strong high-momentum tail in the Cu distribution is due to annihilation with the $3d$ electrons and that the Fermi surface in Al is very nearly spherical but has slight bulges in the [100] and [111] directions. One-electron calculations of the distributions for Cu and Al agree quite well with the experiments and further confirm the importance of core annihilation in Cu. The calculated positron lifetime in Cu does not disagree with previous experimental observations by more than a factor of two. Electron-positron correlation by any factor much larger than this is therefore precluded.

CRITICAL FIELD MEASUREMENTS ON SUPERCONDUCTING LEAD ISOTOPES. D. L. Decker,* D. E. Mapother, and R. W. Shaw, Physics Department, University of Illinois, Urbana, Illinois (Received August 21, 1958).

The measurement of the isotope effect upon the superconducting critical field of lead has been extended from T_c to 1.28°K, and an accurate critical field curve for lead is reported for this temperature range. The measured critical field curve is expanded as a function of T^2 and used in calculating the thermodynamic properties of lead. The values for the coefficient of the electronic specific heat in the normal state and for the latent heat of the superconducting transition are in good agreement with calorimetric measurements. The electronic specific heat in the superconducting state does not show an exponential $1/T$ dependence but instead a close resemblance to a T^4 dependence below 5°K.

The temperature dependence of the critical field of lead, like that of most superconductors, is not parabolic. However, the observed H_c values lie above a parabola passing through H_0 and T_c which is in the opposite direction from the deviations shown by all other superconductors for which precise data are available. It is shown that an empirical correlation exists for superconductors between the deviation from parabolic behavior and T_c/θ_0, where θ_0 is the Debye temperature at $T=0$°K.

Measurements of the isotope effect upon the critical field below T_c show small differences in the coefficient of the normal electronic specific heat, γ, between specimens but in general give support to the principle of similarity in lead to about the same precision as has been reported for other superconductors.

*Present address: Department of Physics, Brigham Young University, Provo, Utah.

EFFECT OF A MAGNETIC FIELD ON THERMIONIC EMISSION FROM MOLYBDENUM. Joel Greenburg, Department of Physics and Research Laboratory of Electronics, Massachusetts Institute of Technology, Cambridge, Massachusetts (Received August 1, 1958).

An experiment that was performed to explore the possible effect of an external magnetic field on thermionic emission from a clean metal surface demonstrated than an applied field of 6000 gauss or less has no effect on the saturation current density. The purpose of this study was to resolve, if possible, the disagreement between the work of Shelton and that of Nottingham and Hutson on the energy distribution of thermionically emitted electrons.

THERMOELECTRIC POWER AND ELECTRON SCATTERING IN METAL ALLOYS. C. A. Domenicali, Honeywell Research Center, Hopkins, Minnesota (Received August 21, 1958).

A phenomenological theory of thermoelectric power in binary, ternary, and more complex noble-metal base alloys is presented, which is based on the well known thermoelectric power formula of Mott and others. The temperature dependence of certain scattering coefficients leads to information on the variation of scattering cross section with electron kinetic energy; the simple model described appears to be in-

ternally consistent and furnishes considerable insight into the nature of electron scattering from point imperfections in metals. It is found from an experimental study of the series of solutes Cr, Mn, Fe, Co, and Ni in copper, that the cross section depends on electron energy in a manner closely resembling that of the Ramsauer-Townsend effect in slow-electron scattering from atoms in the vapor state. The theory is used to predict the behavior of ternary and more complex alloys from information in binary alloys. Experiments on selected ternary solid solutions are described. The results are in accord with predictions of the theory.

EXCITON AND MAGNETO-ABSORPTION OF THE DIRECT AND INDIRECT TRANSITIONS IN GERMANIUM. Solomon Zwerdling, Benjamin Lax, Laura M. Roth, and Kenneth J. Button, Lincoln Laboratory, Massachusetts Institute of Technology, Lexington, Massachusetts (Received July 14, 1958).

Low-temperature, high-resolution experiments on magneto-absorption effects in germanium have resolved fine structure in the direct interband transition and, in addition, have revealed structure in the indirect transition. In each case, exciton absorption was also observed and the experimental binding energy of the lowest exciton level was measured. The magneto-absorption at photon energies slightly greater than the indirect energy gap has the appearance of a series of absorption edges unlike the series of absorption maxima observed in the direct case. The experimental findings are consistent with the theoretical predictions described in the following article. The detailed spectra were observed by means of a new low-temperature high-resolution spectrometric system providing spectral resolution of the order of 10^{-4} electron volt and steady magnetic fields up to 38.9 kilogauss. An accurate measure of the minimum of the conduction band was obtained by extrapolating a plot of the photon energies of the absorption edges as a function of magnetic field to zero field. The indirect energy gap, 0.744 ± 0.001 electron volt at 1.5°K, was then obtained by subtracting the energy of the emitted longitudinal acoustical phonon which is involved in the indirect transition. The accurate value of the conduction band minimum permits the measurement of the exciton binding energy. The exciton ground state was found to be split into two components 0.0011 electron volt apart with a mean position of 0.0025 ± 0.0004 electron volt. These values are consistent with preliminary theoretical calculations. The Zeeman effect of both the direct and indirect exciton absorptions has also been studied.

THEORY OF OPTICAL MAGNETO-ABSORPTION EFFECTS IN SEMICONDUCTORS. Laura M. Roth, Benjamin Lax, and Solomon Zwerdling, Lincoln Laboratory, Massachusetts Institute of Technology, Lexington, Massachusetts (Received July 14, 1958).

The theory of the effect of a magnetic field on the optical absorption in semiconductors is developed by using the effective mass approximation. For simple parabolic conduction and valence bands and a direct transition which is allowed at $\vec{k} = 0$, absorption peaks occur at energies above the zero-field gap. Since the selection rule for the transition is $\Delta n = 0$ where n is the magnetic quantum number, the spacing between the peaks is the sum of the cyclotron frequencies for the two bands. For degenerate band edges, the spectrum is more complicated. A detailed treatment of the direct transition in germanium is given in which account is taken of the change in curvature of the bands away from $\vec{k} = 0$ and the results are in good agreement with the experimental measurements of Zwerdling, Lax, Roth, and Button. The $\vec{k} = 0$ conduction band mass is found to agree with predictions based on cyclotron resonance in the valence band. In addition, a gyromagnetic ratio for conduction electrons of -2.6 resulted from the calculations. The deviation from $g = 2.0$ is due to spin-orbit interaction. In InSb the effect is much greater, the result being $g = -50$. These are consistent with experimental results. For bands in which the transition probability vanishes at $\vec{k} = 0$, absorption peaks will also occur corresponding to $\Delta n = \pm 1$ but absorption edges occur for $\Delta n = 0$. In the case of indirect transitions, the absorption does not exhibit oscillations but consists of a series of "steps" as has been observed in Ge by Zwerdling et al.

SYMMETRY OF MAGNETIC STRUCTURES: THE MAGNETIC STRUCTURE OF CHALCOPYRITE. G. Donnay, Geophysical Laboratory, Carnegie Institution of Washington, Washington,

D. C., and L. M. Corliss, J. D. H. Donnay,* N. Elliott, and J. M. Hastings, Chemistry Department, Brookhaven National Laboratory, Upton, New York (Received August 19, 1958).

The transformation properties of magnetic moments under symmetry and antisymmetry operations lead to 1421 possible space groups for ferromagnetic and antiferromagnetic crystal structures. A systematic procedure for magnetic structure determination is proposed, which takes into account the restrictions imposed on spin directions by space groups. This method is applied to chalcopyrite, $CuFeS_2$, which is found to be antiferromagnetic at room temperature: the chemical structure is that proposed by Pauling and Brockway, the space group $I\bar{4}2d$ holds for the magnetic structure, in which the two iron (and possibly also the two copper) atoms tetrahedrally bonded to a common sulfur atom have antiparallel spins directed along the c axis. A value of $3.85\mu_B$ is found for the iron moment [$(0\pm0.20)\ \mu_B$ for copper]. The possible existence of a second chalcopyrite modification in nature, suggested by conflicting results on material of Japanese origin, is ruled out, as specimens from both Ugo, Japan, and Joplin, Missouri, are found to have the same structure.

* Permanent address: The Johns Hopkins University, Baltimore, Maryland.

ELECTRICAL CONDUCTIVITY OF NiO NEAR THE CURIE TEMPERATURE. Eiso Yamaka and Kenichi Sawamoto, The Electrical Communication Laboratory, Nippon Telegraph and Telephone Public Corporation, Tokyo, Japan (Received August 19, 1958).

The resistivity of single- and poly-crystalline NiO has been observed experimentally in the temperature range of room temperature to 400°C through the Curie temperature (T_C) in order to study an influence on electrical conduction of the superexchange coupling characteristic to antiferromagnetism. The relation of resistivity vs $1/T$ for single crystals is observed to behave rather linearly in both regions above and below a small and discernible bending (knick) near T_C, from which the corresponding activation energies may be determined. The result seems to support the Heitler-London approach by Heikes in the NiO crystal. The specimens, in which the partial spin alignment was introduced by stress-annealing through T_C along a direction of [111], show the anomalous increase of resistivity along the stress axis near T_C in the heating process, whereas, in the succeeding cooling process, the anomaly in resistivity is not observed. The result seems to show that the spin alignment has been disturbed appreciably during the heating process and then the electrical conduction may be affected by the superexchange coupling, as suggested in the Heitler-London model of NiO.

QUENCHING OF POSITRONIUM LIFETIMES BY MOLECULAR IODINE. C. R. Hatcher* and W. E. Millett, The University of Texas, Austin, Texas (Received August 4, 1958).

Measurements of the mean life of the τ_2 component for decay is solutions of iodine in normal heptane give a value of 10^{-17} cm^2 for the cross section of molecular iodine for annihilating ^3S positronium on collision. This effect is attributed to an enhancement of "pick off" annihilation resulting from either a tendency to form positronium iodide or the high polarizability of molecular iodine. In quenching τ_2 from 2.49×10^{-9} sec to 1.32×10^{-9} sec, the intensity I_2 of the long component was observed to vary over a range from 40% to 27%; however, the errors in I_2 are so large for the shorter lifetimes that it is impossible to tell from the data whether or not I_2 is influenced by the presence of iodine.

* Now at the University of California Radiation Laboratory, Livermore, California.

ENERGY LOSS PER ION PAIR FOR PROTONS IN VARIOUS GASES. H. V. Larson, Hanford Laboratories Operation, General Electric Company, Richland, Washington (Received August 18, 1958).

Values of w for protons in A, N_2, CO_2, dry air, and "tissue-equivalent" gas were measured as 26.66±0.26, 36.68±0.34, 34.37±0.33, 35.18±0.42, and 30.03±0.29 ev/ion pair, respectively. A 2-Mev positive-ion accelerator was used as the source of protons. The energy of the protons was determined with a precision gaussmeter that was calibrated by the Li (p,n) and T(p,n) threshold reactions. These protons were scattered from a gold foil into a parallel plate ionization chamber. The fast electron pulses were collected on one electrode, amplified, and counted. The positive-ion charge was

collected on the other electrode and measured by means of a standard capacitor that was connected between the input and feedback terminals of a vibrating-reed electrometer.

INFRARED AND OPTICAL MASERS. A. L. Schawlow and C. H. Townes,* Bell Telephone Laboratories, Murray Hill, New Jersey (Received August 26, 1958).

The extension of maser techniques to the infrared and optical region is considered. It is shown that by using a resonant cavity of centimeter dimensions, having many resonant modes, maser oscillation at these wavelengths can be achieved by pumping with reasonable amounts of incoherent light. For wavelengths much shorter than those of the ultraviolet region, maser-type amplification appears to be quite impractical. Although use of a multimode cavity is suggested, a single mode may be selected by making only the end walls highly reflecting, and defining a suitably small angular aperture. Then extremely monochromatic and coherent light is produced. The design principles are illustrated by reference to a system using potassium vapor.

*Permanent address: Columbia University, New York, New York.

RADIO-FREQUENCY SPECTRA OF HYDROGEN DEUTERIDE IN STRONG MAGNETIC FIELDS. W. E. Quinn, J. M. Baker, J. T. LaTourrette, and N. F. Ramsey, Harvard University, Cambridge, Massachusetts (Received August 18, 1958).

Molecular beam observations have been made of the radio-frequency spectra corresponding to reorientations of the deuteron, proton, and rotational magnetic moments in the HD molecule. For HD in the zeroth vibrational and first rotational state, these observations were made in magnetic fields of approximately 1700, 3400, and 4800 gauss. The results are found to be consistent with the theory of heteronuclear diatomic molecules. The direct result of these experiments is the determination of the Hamiltonian interaction constants: $(1-\sigma_{J1})\,b/\nu_d$ equals 0.773527 ± 0.000016, c_p is $85\,600 \pm 18$ c/sec, c_d equals $13\,122 \pm 11$ c/sec, d_1 is $17\,761 \pm 12$ c/sec, d_2 equals $22\,454 \pm 6$ c/sec, and f/H^2 is $(-26.90 \pm 0.40)\times10^{-6}$ c/sec gauss^{-2}. From these values of the interaction constants are derived the following physical quantities: the HD rotational magnetic moment ${}^{HD}_{0}\langle u_J/J\rangle_1$ equals 0.663211 ± 0.000014 nuclear magneton, the quadrupole moment Q of the deuteron is $(2.738 \pm 0.014)\times10^{-27}$ cm^2, the rotational magnetic field H_p' at the proton is 19.879 ± 0.006 gauss and H_d' at the deuteron is 20.020 ± 0.028 gauss, the internuclear spacing in the zeroth vibrational and first rotational state is such that ${}^{HD}_{0}\langle R^{-3}\rangle_1^{-\frac{1}{3}}$ equals $(0.74604 \pm 0.00010)\times10^{-8}$ cm, and the dependence of the diamagnetic susceptibility on molecular orientation $(\xi_{\pm1}-\xi_0)$ is $-(3.56 \pm 0.20)\times10^{-31}$ erg gauss^{-2} molecule^{-1}. Combining these values with Ramsey's theory on zero-point vibration and centrifugal stretching in molecules gives: the high-frequency contribution to the molecular susceptibility, ${}^{HD}_{0}\langle \xi^{HF}\rangle_1 = (1.675 \pm 0.005)\times10^{-31}$ erg gauss^{-2} molecule^{-1}, the quadrupole moment of the electron distribution relative to the internuclear axis, ${}^{HD}_{0}\langle Q_e\rangle_1 = (0.324 \pm 0.010)\times10^{-16}$ cm^2, and the high-frequency contribution to the magnetic shielding constant for HD, ${}^{HD}_{0}\langle \sigma^{HF}\rangle_1 = (-0.594 \pm 0.030)\times10^{-5}$.

POSITRON SPECTRA OF Eu^{152} AND Eu^{152m}. D. E. Alburger, S. Ofer, and M. Goldhaber, Brookhaven National Laboratory, Upton, New York (Received August 26, 1958).

An intermediate-image beta-ray spectrometer equipped with spiral baffles has been used to investigate positrons in the decays of Eu^{152} and Eu^{152m}. Thirteen-year Eu^{152} emits a positron group to the 0.122-Mev 2+ first excited state of Sm^{152} with an end-point energy of 0.715 ± 0.010 Mev and an intensity of 1.6×10^{-4} per disintegration ($\log ft$=11.9) and a positron group to the 0.366-Mev 4+ second excited state with an end point of 0.47 ± 0.03 Mev and an intensity of 0.8×10^{-4} per disintegration ($\log ft$=11.5). 9.3-hr Eu^{152m} emits a positron group to the ground state of Sm^{152} with an end-point energy of 0.895 ± 0.005 Mev and an intensity of 7×10^{-5} per disintegration ($\log ft$ =8.65) and a positron group to the 0.122-Mev state with an intensity of 4×10^{-5} per disintegration ($\log ft$=8.6). The shape of the latter group has not been established. However its end point, when the alpha shape factor is applied, gives better agreement with 0.122-Mev energy separation from the ground state beta ray than the end point of the uncorrected spectrum. The result is consistent with but not positive proof of the assumed spin and parity of 0- for Eu^{152m}. The β^-

end-point energies of Eu^{152} and Eu^{152m} are 1.470 ±0.010 Mev and 1.855±0.010 Mev respectively. An energy separation of 0.050 ±0.015 Mev between Eu^{152m} and Eu^{152} is derived from the various β^+ and β^- end-point measurements.

No L-conversion electrons could be found in Eu^{152m} decay corresponding to a 0.05-Mev isomeric transition. An upper limit of 3×10^{-5} per disintegration was obtained for the fractional decay of Eu^{154} by positron emission.

INELASTIC SCATTERING FROM LIGHT NUCLEI— THE ALPHA-PARTICLE MODEL FOR Be^9. J. S. Blair, * Palmer Physical Laboratory, Princeton University, Princeton, New Jersey, and E. M. Henley, Department of Physics, University of Washington, Seattle, Washington (Received June 16, 1958).

The inelastic scattering of nucleons, deuterons, and alpha particles from light nuclei is discussed in terms of direct interactions. The validity of this description, and of the approximations made here and by other authors in calculating cross sections, are analyzed in detail. Physical arguments are given for the use of a collective representation of light nuclei, in order to explain the preferential excitation of certain well defined nuclear states by short-wavelength projectiles. As an example, the alpha-particle model is used to characterize Be^9 and the inelastic cross sections for excitation of rotational, vibrational and single-particle states are calculated with an impulse approximation. The model, and results computed from it, are examined and compared to experimental findings.

*Presently on leave from the University of Washington.

SCATTERING OF 18.7-Mev ALPHA PARTICLES FROM Al, Cu, AND Ag. O. H. Gailar,* E. Bleuler, and D. J. Tendam, Department of Physics, Purdue University, Lafayette, Indiana (Received August 28, 1958).

The scattering of 18.7-Mev alpha particles from Ag, Cu, and Al was studied from 10° to 170° with rms angular resolutions of 0.4° to 0.85°. The scattered alpha particles were separated from singly charged reaction products with the aid of a proportional counter, and their energies were measured with a CsI(Tl) scintillation spectrometer. The elastic scattering for Ag shows the "exponential" drop-off from the Coulomb cross section, without any pronounced structure at large angles. For Cu, definite changes in the slope of the drop-off are observed up to 120°, followed by a shallow minimum near 130° and a very deep, narrow, minimum at 162° (c.m.). The interaction radii deduced from the strong-absorption model agree with those found at higher energies. From the diffraction-like pattern found for Al, an interaction radius of 6.4×10^{-13} cm is derived, appreciably larger than the one obtained at 40 Mev (5.4×10^{-13} cm). There are indications that a direct-process interpretation of the inelastic scattering from Al is possible.

*Now at Combustion Engineering, Incorporated, Windsor, Connecticut.

EFFECTIVE CHARGE OF NEUTRONS IN NUCLEI. A. de Shalit, CERN, Geneva, Switzerland (Received August 25, 1958).

The polarization of closed proton shells by neutrons can be considered as inducing an effective charge on the neutron for some multipoles but not for others. The rough constancy of the effective neutron charge as observed in $E2$ transitions and quadrupole moments in nondeformed odd N-even Z nuclei is discussed, and arguments are presented to explain this phenomenon along the lines of the shell model.

TWO NEW PROMETHIUM ISOTOPES; CROSS SECTIONS OF SOME SAMARIUM ISOTOPES FOR 14.8-Mev NEUTRONS. R. G. Wille and R. W. Fink, Department of Chemistry, University of Arkansas, Fayetteville, Arkansas (Received August 4, 1958).

When highly enriched samples of Sm^{152} and Sm^{154} are irradiated with 14.8-Mev neutrons, activities having half-lives of 6.5±0.5 min and 2.5±0.5 min are observed. On the basis of yields and cross-bombardments, these are assigned to new isotopes Pm^{152} and Pm^{154}, respectively. Cross-section measurements at 14.8 Mev for $(n,2n)$, (n,p), and (n,α) reactions of samarium are reported, the experimental values being as follows: $Sm^{144}(n,2n)$, 706±120 mb; $Sm^{154}(n,2n)$, 1500±300 mb; $Sm^{152}(n,p)$, 3.7±0.2 mb; $Sm^{154}(n,p)$, 3.5±0.2 mb; $Sm^{152}(n,\alpha)$, 10±2 mb; and $Sm^{154}(n,\alpha)$, 9±3 mb. While the $(n,2n)$ cross

sections are within an order of magnitude agreement with statistical evaporation theory, the experimental values for the (n,p) and (n,α) cross sections are several orders of magnitude larger than those calculated from statistical evaporation theory based on the compound-nucleus model.

NEW GERMANIUM ISOTOPE, Ge^{65}. Norbert T. Porile, Chemistry Department, Brookhaven National Laboratory, Upton, New York (Received August 22, 1958).

A new germanium isotope, Ge^{65}, has been produced by the $(\alpha, 3n)$ reaction on Zn^{64}. The mass assignment was established through cross-bombardments, "milking" experiments, and excitation function measurements. The half-life of Ge^{65} is 1.5 ± 0.2 minutes. It decays by positron emission to 15-minute Ga^{65}. The ground-state transition occurs in over 90% of the disintegrations and has a positron end-point energy of 3.7 ± 0.4 Mev and a log (ft) value of 4.8. Gamma rays of 0.67 Mev and 1.72 Mev have been observed with intensities of $0.03/\beta^+$ and $0.02/\beta^+$, respectively.

ANGULAR DISTRIBUTIONS FROM DEUTERON BOMBARDMENT OF BERYLLIUM AND BORON. B. Zeidman* and J. M. Fowler, Washington University, St. Louis, Missouri (Received May 8, 1958).

The angular distributions, from 10° to 160°, of the emergent particles from the reactions $Be^9(d,p)Be^{10,10*}$, $B^{10}(d,p)B^{11,11*}$, and $B^{11}(d,n)C^{12,12*}$ have been investigated. The proton distributions were obtained at incident deuteron energies of 10, 9.2, and 8.1 Mev while the neutron distributions were obtained with 10-Mev deuterons. The proton distributions are analyzed using the Butler theory of deuteron stripping and, with the exception of the distributions from Be^{11*}, are in agreement with $l_n = 1$ at forward angles. The distributions from the first excited state of B^{11} are not in agreement with any curves based upon the Butler theory, indicating that stripping does not play a major part in this reaction. The neutron distributions are analyzed using the treatment of Owen and Madansky, which allows heavy-particle stripping as well as Butler stripping. Reasonable agreement between the data and this theory for the ground state is obtained by using approximately equal amplitudes for Butler and exchange stripping and angular momenta of $l=1$ and $l=0$, respectively, for deuteron and exchange stripping. The analysis of the distribution for the first excited state of C^{12} shows $l=1$ for deuteron stripping, but does not provide a unique choice for the angular momentum in exchange stripping.

* Now at Argonne National Laboratory, Lemont, Illinois.

$N^{14}(d,n)O^{15}$ AND $N^{15}(d,n)O^{16}$ REACTIONS. J. L. Weil and K. W. Jones,* Columbia University, New York, New York (Received August 29, 1958).

Absolute cross sections for the $N^{14}(d,n)O^{15}$ and $N^{15}(d,n)O^{16}$ reactions have been measured at zero degrees to the incident deuteron beam from 0.6 to 5.3 Mev bombarding energy. Both excitation curves show strong resonance structure and have maximum cross sections of about 6 millibarns per steradian. Eight angular distributions were measured for the $N^{15}(d,n)O^{16}$ reaction at points on and off maxima in the excitation curve. A good fit to the angular distributions is obtained by use of the exchange stripping theory of Owen and Madansky.

* Now at The Ohio State University, Columbus, Ohio.

SMALL DEVIATIONS OBSERVED IN BETA SPECTRA: Na^{22}. J. H. Hamilton, L. M. Langer, and W. G. Smith,* Physics Department, Indiana University, Bloomington, Indiana (Received August 7, 1958).

The intense positron spectrum of Na^{22} has been carefully measured in a magnetic spectrometer. This transition proceeds from a 3+ to a 2+ level. The observed Na^{22} spectrum has a nonstatistical shape corresponding to an excess of low-energy electrons. The well-measured spectrum of Pm^{147} was reinvestigated and found to have a statistical shape. The many tests of the experimental procedures all indicate that the observed nonstatistical spectrum of Na^{22} is not the result of instrumental distortions. Theoretical refinements for finite de Broglie wave length, screening, and possible contributions from the twice-forbidden matrix elements were considered and found to be much too small to explain the deviation from the statistical shape observed in Na^{22}. The Fermi-Kurie plot of Na^{22} can be linearized by a $(1 + b/W)$ correction factor. This same factor

has been used to linearize the Fermi-Kurie plots of In^{114}, Y^{90}, and P^{32} (in addition to the once-forbidden, unique shape factor in the case of Y^{90}). In all four cases, the value of the parameter b to yield a linear F-K plot is in the range $0.2 < b < 0.4$. At present, no theoretical explanation is offered for the correction $(1 + b/W)$. It may be regarded as an empirical correction capable of explaining the observed shapes in the case of these four Gamow-Teller transitions. A search was also made for negative electrons accompanying the normal positron decay of Na^{22} A weak, low-energy electron distribution was observed. This distribution may be explained by the theory of "shake-off" electrons.

* Present address: Purdue University, Lafayette, Indiana.

SMALL DEVIATIONS OVSERVED IN BETA SPECTRA: In^{144}, Y^{90}, and P^{32}. O. E. Johnson,* R. G. Johnson,† and L. M. Langer, Physics Department, Indiana University, Bloomington, Indiana (Received August 7, 1958).

The beta spectra of In^{114}, Y^{90}, and P^{32} (all of which decay by pure Gamow-Teller radiations) have been very carefully studied in a magnetic spectrometer. The Fermi-Kurie plots of all three spectra exhibit small deviations from linearity corresponding to an excess of low energy electrons. All of the evidence indicates that the observed nonstatistical shapes represent the true spectra and are not the result of instrumental distortions. The Fermi-Kurie plots of these three isotopes can be linearized by a $(1+b/W)$ correction factor (in addition to the once-forbidden, unique shape factor in case of Y^{90}).

* Present address: Purdue University, Lafayette, Indiana.

† Present address: Lockheed Missile Systems Division, Palo Alto, California.

SCATTERING OF PROTONS FROM HELIUM AND LEVEL PARAMETERS IN Li^5. Philip D. Miller* and G. C. Phillips, The Rice Institute, Houston, Texas (Received August 29, 1958).

The scattering of protons from helium has been investigated experimentally from 2.0 to 5.5 Mev with the Rice Institute Van de Graaff accelerator and a differentially pumped, large volume scattering chamber. Excitation curves reveal no new states in Li^5 up to an excitation energy of 6.5 Mev. A phase-shift analysis has been made of the angular distributions at laboratory bombarding energies of 3.03, 3.51, 4.02, 4.50, and 5.00 Mev. The phase shifts derived from this experiment and from experiments at other laboratories in the energy range 1 to 18 Mev have been interpreted in terms of the dispersion theory, and level parameters have been extracted. The nuclear radius which best fits the P-wave phase shifts is 2.6×10^{-13} cm. For the ground state, $(E_{res})_{lab} = 2.6$ Mev, $J^{\pi} = 3/2^-$, $\gamma_p^2 = 12 \times 10^{-13}$ Mev-cm, and $\theta_p^2 = 0.40$. For the first excited state, $(E_{res})_{lab} = 10.8$ Mev, $J^{\pi} = 1/2^-$, $\gamma_p^2 = 30 \times 10^{-13}$ Mev-cm, and $\theta_p^2 = 1.0$. The S-wave phase shift is moderately well fit by a hard-sphere interaction with a radius of 2.0×10^{-13} cm. At the present time, the D-wave phase shifts are so inaccurately known that very little interpretation is possible.

*Now with the Oak Ridge National Laboratory, Oak Ridge, Tennessee.

SCATTERING OF He^3 FROM He^4 AND STATES IN Be^7. Philip D. Miller* and G. C. Phillips, The Rice Institute, Houston, Texas (Received August 29, 1958).

The range of excitation energies in Be^7 from 3.28 to 4.73 Mev has been investigated by Van de Graaff-accelerated He^{3+} ions scattered from He^4 gas in a differentially pumped, large-volume scattering chamber. The second excited state in Be^7 has been studied, and its laboratory resonant energy and width have been determined to be 5.17 Mev and 0.180 Mev, respectively, corresponding to an excitation energy in Be^7 of 4.53 ±0.02 Mev and a center-of-mass width of 0.102 Mev. The spin and parity are $J^{\pi} = 7/2^-$ and the reduced width is 3.0×10^{-13} Mev-cm. The behavior of the nonresonant phase shifts is shown to be qualitatively consistent with other known states in Be^7, whose resonant energies lie outside the range of the present experiment.

*Now with the Oak Ridge National Laboratory, Oak Ridge, Tennessee.

PHOTOEXCITATION OF Pb^{207m}. U. Farinelli, F. Ferrero, R. Malvano, S. Menardi, and E. Silva,* Istituto di Fisica dell'Universitá di Torino, Torino, Italia, and Istituto Nazionale

di Fisica Nucleare, Sezione di Torino, Italia
(Received June 12, 1958).

The 0.8-sec isomeric activity in lead has been excited by the photoneutron reaction in Pb^{208} and the relative cross section has been calculated from the measured yield. The cross section presents an extremely sharp peak in the giant resonance region with half-width not greater than 2 Mev.

The isomeric level excitation efficienty, $\sigma(\gamma, n\gamma')/\sigma(\gamma,n)$, has been calculated: it reaches a maximum value of 5%, which may be compared with the same quantity relative to inelastic neutron scattering in Pb^{207}, which already at the energy of 11 Mev, in the compound system, assumes a 14% value.

A discussion is given to explain the complete disagreement between the above two values of the excitation efficiency, which is attributed to the difference in angular momentum transferred to the compound system in the above two reactions.

*On leave from the University of São Paulo, São Paulo, Brazil.

INTERNAL CONVERSION ELECTRONS FROM COULOMB EXCITATION OF Ta^{181}. E. M. Bernstein,* Duke University, Durham, North Carolina, and University of Wisconsin, Madison, Wisconsin (Received March 31, 1958).

The conversion electron spectrum following Coulomb excitation of Ta^{181} has been remeasured with greater accuracy. The results are internally consistent with the rotational model of Bohr and Mottelson and are in excellent agreement with the gamma-ray angular distribution and yield data of McGowan and Stelson.

*Now at the University of Wisconsin, Madison, Wisconsin. The data reported here were obtained at Duke University.

ELASTIC SCATTERING OF C^{12} FROM GOLD. E. Goldberg and H. L. Reynolds, Radiation Laboratory, University of California, Livermore, California (Received August 18, 1958).

The angular distribution of C^{12} ions elastically scattered by gold has been measured at the following laboratory energies: 118±2, 101±2, 79.4±3, and 73.6±3 Mev. Heavy ions from the Berkeley heavy-ion linear accelerator were recorded in two Ilford E-1 plates from a scattering angle of 19° to 159°. In all cases the differential cross sections exhibited a Coulomb-like behavior at small angles, a rise above Coulomb of about twenty percent as the scattering angle increased, and then a rapid drop below Coulomb in much the same manner as alpha particles scattered from heavy elements in the 20- to 40-Mev range. The Blair "sharp cutoff" model reproduces closely the character of the data; however, small oscillations predicted from the model are not experimentally observed. Interaction distances of (11.8±0.3), (12.1±0.3), (11.85±0.4), and 11.85 ±0.45) $\times 10^{-13}$cm, respectively, for the above energies are inferred from application of the Blair model.

DECAY OF Ca^{39}. O. C. Kistner and B. M. Rustad, Columbia University, New York, New York, and Brookhaven National Laboratory, Upton, New York (Received August 20, 1958).

The "doubly closed shell ± one nucleon" mirror transition, $Ca^{39}(\beta^+)K^{39}$, has been investigated in order to obtain a more precise ft value. The beta spectrum was measured with a magnetic, thin-lens spectrometer and has a maximum energy of 5.490 ± 0.025 Mev. A search for gamma rays was made with a NaI(Tl) scintillation spectrometer, and an upper limit of 0.12% was placed on transitions to the lowest known excited levels in K^{39} between 2.5 and 3.5 Mev. A half-life of 0.88±0.01 second was determined. The ft value calculated from these results is 4320± 100 seconds.

HYPERFRAGMENTS PRODUCED BY K^0 MESONS FROM K^+ CHARGE EXCHANGE. M. Baldo-Ceolin, H. Huzita,* and S. Natali, Istituto Nazionale di Fisica Nucleare, Sezione di Padova, and Istituto di Fisica dell'Universita, Padova, Italy; and U. Camerini† and W. F. Fry, Department of Physics, University of Wisconsin, Madison, Wisconsin (Received August 18, 1958).

Stacks of C-2 emulsion were exposed to neutral K mesons. These were produced by the charge exchange, in dense material, of K^+ mesons from the Berkeley Bevatron. Hyperfragments were found in these stacks.

It is concluded that the hyperfragments were produced by K_2^0 mesons in the $\bar{K}^0$ mode. These were generated by the decay of the K_1^0 compon-

ent of the K^0 beam as would be expected from the Gell-Mann-Pais scheme. Other possible mechanisms of production of the hyperfragments have been considered and shown to be unimportant.

*On leave of absence from St. Paul's University, Tokyo, Japan.

†On leave of absence from Centro Brasileiro de Pesquisas Fisicas, Rio de Janeiro, Brazil.

HIGH-ENERGY BREMSSTRAHLUNG IN ELECTRON-PROTON COLLISIONS. R. A. Berg and C. N. Lindner, Stanford University, Stanford, California (Received August 29, 1958).

The cross section for the bremsstrahlung resulting from high-energy collisions of electrons with protons is calculated, considering the electrons as extreme relativistic and taking into consideration the proton's recoil, anomalous magnetic moment, bremsstrahlung, and form factors. The final cross section is integrated over the recoil proton and final photon to obtain a formula of interest for the Stanford accelerator experiments. The computation of the integrated cross section made without regard for radiative corrections and mesonic contributions is estimated to be accurate to 2% in the energy ranges of interest. This cross section is corrected for radiative effects, which produce an additional uncertainty of less than 5% and possibly as little as 1%. Resonance effects due to meson interactions in the "virtual Compton effect" diagrams, however, become significant in the range of interest. Their contribution to the cross section is discussed.

ELECTRON NUMBER DISTRIBUTION IN ELECTRON-PHOTON SHOWERS. J. C. Butcher and H. Messel, The F. B. S. Falkiner Nuclear Research and Adolph Basser Computing Laboratories, School of Physics, The University of Sydney, Sydney, New South Wales, Australia (Received August 18, 1958).

Numerical results for the number distribution of electrons above a given energy due to primary electrons and photons are given. The average numbers derived from the distributions are also given. Values are presented both for the case of approximation A and for more accurate cross sections at low energies in air. Collision losses and Compton effect are taken into account but scattering at low energies is neglected. The calculations were carried out using Monte Carlo methods on the electronic digital computer Silliac. The results of the calculations are discussed and compared with previous work on the subject.

MU-MESON DECAY WITH INNER BREMSSTRAHLUNG. C. Fronsdal and H. Überall, CERN, Geneva, Switzerland (Received August 21, 1958).

The differential transition probability for the radiative decay of a polarized mu meson with the most general choice of coupling constants is calculated and integrated over electron energies. The extent to which this process may be useful for determining the coupling constants is discussed.

PRODUCTION OF HELIUM IN IRON METEORITES BY THE ACTION OF COSMIC RAYS. John H. Hoffman and Alfred O. Nier, University of Minnesota, Minneapolis, Minnesota (Received August 18, 1958).

The helium distribution in a slice from the iron meteorite, Grant, has been measured and plotted in the form of contour maps. The contours of constant helium show a minimum helium content and isotopic ratio, He^3/He^4, near the center of the slice, the isotopic ratio varying from 0.26 near the center to 0.30 at the surface. A cosmogenic helium production rate equation was fitted to the data giving a He^3/He^4 production ratio by primary cosmic rays of 0.50 and by secondary particles of 0.14. Primary and secondary particle interaction cross sections were found to be 540 mb and 720 mb respectively. The ratio of the average post-atmospheric radius to the pre-atmospheric radius of Grant was calculated to be 0.65.

TWO-PAIR DECAY AND THE SPIN OF THE NEUTRAL PION. David W. Joseph, The Enrico Fermi Institute for Nuclear Studies and the Department of Physics, The University of Chicago, Chicago, Illinois (Received August 22, 1958).

The rare decay mode π^0→two electron pairs is investigated as a possible means of directly measuring the π^0 spin; chief consideration

is given to the case of spin 2, since the occurrence of the two-photon decay requires the spin to be 0 or ≥ 2. If the angle between the planes of the two pairs is denoted by ϕ, the distribution in ϕ is proportional to $(1 + \lambda\cos 2\phi)$. For spin and parity 2^+, λ is calculated to be +0.001, while for 2^-, only the restriction $-0.19 < \lambda < 0$ is found; this is to be compared with the values for spins $0^\pm$ (previously calcualted by Kroll and Wada) of ± 0.19. The rate of occurrence of events in which the two pairs share the energy quite unequally is also calculated. It is found that a small value of $|\lambda|$ for spin 2^- should be accompanied by a value of this rate and of the ratio $(\pi^0 \to 4e)/(\pi^0 \to 2\gamma)$ both considerably greater than for spins $0^\pm$, while for large $|\lambda|$ or for spin 2^+ these quantities should be close to the spin $0^\pm$ values.

HELICITY OF THE ELECTRON AND POSITRON IN MUON DECAY. Pierre C. Macq, Kenneth M. Crowe, and Roy P. Haddock, Radiation Laboratory, University of California, Berkeley, California (Received August 29, 1958).

The helicity of the electron and positron from muon decay has been measured by determining the sense of circular polarization of their bremsstrahlung by the method of absorption in iron magnetized against or along the direction of motion of the particles. The positron is found to be right-handed and the electron left-handed.

The results are consistent with the two-component neutrino theory, which assumes (V, A) interaction, conservation of leptons, and left-handed neutrinos.

ELECTRON SCATTERING FROM THE DEUTERON AND THE NEUTRON-PROTON POTENTIAL. John A. McIntyre* and George R. Burleson, Department of Physics and High-Energy Physics Laboratory, Stanford University, Stanford, California (Received August 25, 1958).

Electron scattering by the deuteron has been studied experimentally at 400 Mev and 500 Mev. The results of the scattering are compared with the scattering expected by three different static deuteron models. All three models satisfy the usual deuteron requirements such as binding energy, effective range, etc. Two of the models have Yukawa neutron-proton potentials, the third has a repulsive-core potential. The experimental results agree with the repulsive-core model and disagree with the Yukawa models. This result applies only to the triplet-S neutron-proton potential.

*Now at Yale University, New Haven, Connecticut.

ENERGY SPECTRUM OF π MESONS PRODUCED BY INTERACTION OF COSMIC RADIATION WITH EMULSION NUCLEI. Herman Yagoda, Geophysics Research Directorate, Ionospheric Physics Laboratory, Bedford, Massachusetts

(Received June 12, 1958; revised manuscript received September 25, 1958).

An analysis of 958 π mesons ejected from stars which terminate their range in G5 emulsion exposed in the stratosphere shows a predominance of negative mesons. The average ratio from all emulsion interactions over a pion kinetic energy ≤ 45 Mev is $\pi^-/\pi^+ = 5.17 \pm 0.41$. Further study shows that this ratio varies with the charge of the target nuclei and is strongly dependent on the kinetic energy of the emitted mesons. By classifying the stars on the basis of the sum of the charges on the evaporation tracks, a large fraction of the stars can be attributed to the disintegration of heavy (Ag-Br-I) or light (C-N-O) target nuclei. On this basis 537 pions originate from heavy nuclei and 297 from light nuclei. The residual group of 124 mesons arise from peripheral collisions with heavy or light target nuclei, interactions with hydrogen, photomeson production, and fundamental-particle decay processes. The variation of the charge ratio with pion kinetic energy is evaluated for both the light and heavy emulsion nuclei and compared with the yield from targets of similar charge employed in cyclotron studies. The energy spectrum of the mesons produced by cosmic-ray interactions on emulsion nuclei from 1.5 to 33 Mev shows good agreement with early Bristol measurements of shower particles originating from stars and with more recent studies of ejected mesons by the Russian group. The form of the differential energy spectrum appears to be largely independent of geomagnetic latitude and altitude of the exposure when the meson yield is expressed in units of particles per shower star per Mev.

PHOTOPRODUCTION OF NEUTRAL PIONS FROM HYDROGEN IN THE ENERGY RANGE 700-1100 Mev. H. H. Bingham and A. B. Clegg,* California Institute of Technology, Pasadena, California (Received August 19, 1958).

Gamma rays from the decay of neutral pions photoproduced from hydrogen by the bremsstrahlung beam of the Caltech synchrotron have been studied with a thallium chloride crystal total absorption spectrometer. The energy spectrum of the decay gamma rays produced by a range of incident photon energy is obtained by the photon difference method and this spectrum enables a separation of the gamma rays into two groups: (i) those from the decay of neutral pions produced singly from hydrogen and (ii) those from the decay of neutral pions from multiple production reactions. The cross sections for the single production reaction are in agreement with the recoil proton experiments at Caltech and Cornell. For the multiple production reactions we measure the cross section for producing neutral pions within a range of kinetic energies:

Incident photon energy	Center-of-mass angle	π^0 kinetic energy range (c.m.)	$\frac{d\sigma}{d\Omega}$ (c.m.)
990 Mev	91°	175 Mev to 360 Mev	$(5.9\pm1.6)\times10^{-30}$cm^{2}sterad^{-1}
990 Mev	118°	80 Mev to 360 Mev	$(8.1\pm1.9)\times10^{-30}$cm^{2}sterad^{-1}
810 Mev	114°	75 Mev to 290 Mev	$(3.7\pm1.0)\times10^{-30}$cm^{2}sterad^{-1}

It is shown that all available multiple production data can be explained in terms of two compound states, one at about 750 Mev and the other at some higher energy. This is in agreement with an analysis of the single photoproduction data, which is given in an appendix. These two states are respectively ($T=1/2$, $J=1/2+$) and ($T=3/2$, $J=1/2+$).

*Now at Clarendon Laboratory, Oxford, England.

GENERAL RELATIVITY AND PARTICLE DYNAMICS. L. H. Thomas, International Business Machines Watson Scientific Computing Laboratory, Columbia University, New York, New York (Received August 18, 1958).

In order to adapt the Hamiltonian dynamics of a system of classical (nonquantum) particles to general relativity it seems necessary to generalize the transformations used from contact transformations of phase space to extended point transformations of a joint observer and phase space. When this is done the curvature of observer space is seen to arise from the physical interaction of particles without the introduction of new gravitational field variables.

In order to extend this theory to quantized particles and field theory, it seems necessary to extend the unitary transformations of quantum mechanics in a similar manner, to linear transformations of matrices maintaining the trace of the product of two matrices, the Hermitian nature of a matrix, and the unit matrix. Such transformations do not preserve the phases of wave functions or the product of two matrices, but do preserve the characteristic values of matrices and the traces of the products of any number of matrices. That observers should be designated by q-numbers, not c-numbers, makes it difficult to interpret the theory except in the classical limit.

DISPERSION RELATION FOR NONRELATIVISTIC POTENTIAL SCATTERING. Benjamin W. Lee, University of Pittsburgh, Pittsburgh, Pennsylvania (Received August 19, 1958).

A new dispersion relation for nonrelativistic potential scattering, when the potential has a finite range, is derived by completing the contour of integration along a semicircle of infinite radius in the lower half of the complex λ plane ($\mathrm{Re}\lambda=k$). The residue terms then explicitly exhibit the contributions from virtual states and radioactive decaying states. Resemblance between the residue term arising from a radioactive decaying state and the Breit-Wigner resonance formula is noted and the Breit-Wigner formula is shown to follow correctly from the analytic properties of the S matrix.

SPACE-TIME STRUCTURE OF A STATIC SPHERICALLY SYMMETRIC SCALAR FIELD. H. Treder, Forschungsinstitut für Mathematik der Deutschen Akademie der Wissenschaften zu Berlin, Berlin, Germany (Received July 1, 1958).

Bergmann and Leipnik have derived some special solutions of the general-relativistic field equations in which the metric has the Schwarzschild or the Minkowski form, although a scalar field is assumed to be present. It will be shown that in reality this scalar field vanishes.

$K_{\nu 3}$ AND $K_{\mu 3}$ DECAY MODES. M. Sugawara, Purdue University, Lafayette, Indiana (Received August 18, 1958).

A viewpoint is presented in which some Boson pairs are included among members which exert universal weak interactions on each other. The inclusion of K meson-pion pairs leads to direct terms responsible for $K_{\nu 3}$ and $K_{\mu 3}$ decay modes. It is shown that these direct terms may result in too rapid decays of $K_{\nu 3}$ and $K_{\mu 3}$ if one assumes the universality of the weak coupling constant, while the branching ratio of these decay modes is quite consistent with data.

AUTHOR INDEX TO VOLUME 1

References with (E) are to Errata. The notation "et al." designates authors, other than the first, of Letters having more than one author.

ABASHIAN, A. and E. M. HAFNER. Experimental test of time-reversal invariance in strong interactions 255
ABRAGAM, A. and J. M. WINTER. Proposal for a source of polarized protons 374
ACCARDO, CARL A. Beryllium-7 extreme high-temperature experiment 180
AGARWAL, SOM PRAKASH, et al. Further observations on nature of the current reduction in the primary cosmic ray intensity 107; 183(E)
—— et al. Nature of the current reduction in the primary cosmic-ray intensity 65
AGNEW, LEWIS E., JR., TOM ELIOFF, WILLIAM B. FOWLER, LOUIS GILLY, RICHARD LANDER, LARRY OSWALD, WILSON M. POWELL, EMILIO SEGRÈ, HERBERT M. STEINER, HOWARD S. WHITE, CLYDE WIEGAND, and TOM YPSILANTIS. Elastic scattering of antiprotons on carbon at 30 to 200 Mev 27
ALLEN, J. S., et al. Determination of the Gamow-Teller beta-decay interaction from the decay of helium-6 61
ALMQVIST, E., et al. F^{18} levels near 1 Mev 260
—— et al. Gamma-ray branching and some spin and parity assignments in B^{11} 414
—— et al. Neutron threshold measurements using the Chalk River tandem Van de Graaff accelerator 251
ALTMAN, A. and W. M. MacDONALD. Relativistic corrections to the Fermi matrix element 456
ANDERSON, GERALD S. and SAM LEGVOLD. Conduction electron-magnetic ion interaction in rare earths 322
ANDERSON, K. A. Ionizing radiation associated with solar radio noise storm 335
ANDERSON, L. WILMER, FRANCIS M. PIPKIN, and JAMES C. BAIRD, JR. Optical polarization of atomic hydrogen 229
APPLE, E. F., et al. Radiative energy transfer in ZnS 134
ARNOLD, G. P., et al. Energy vs momentum relation for the excitations in liquid helium 9
ATKINS, K. R., et al. Coefficient of thermal expansion of liquid He^3 near 0°K 315
AUER, PETER L. Vlasov instability in longitudinal plasma oscillations 411
AXENSTEN, S., et al. Nuclear ground-state spins of thallium 198 and 201 473
BAIRD, JAMES C. JR., et al. Optical polarization of atomic hydrogen 229
BALDO-CEOLIN, M., et al. Anti-lambda hyperon 179
BARANGER, ELIZABETH and SYDNEY MESHKOV. Configuration mixing in the C^{14} ground state 30; 119(E)
BARDEEN, JOHN. Two-fluid model of superconductivity 399
BARNES, C. A., W. A. FOWLER, H. B. GREENSTEIN, C. C. LAURITSEN, and M. E. Nordberg. Nature of the Li^8 beta-decay interaction 328
—— et al. Angular correlation of alpha particles from decay of Li^8 326
BARNES, R. G. and R. A. HULTSCH. Indirect nuclear spin-spin interactions in pure quadrupole resonance spectra 227
BARSHAY, SAUL. Determination of the parities of strange particles from dispersion relations 177; 263(E)
——. K meson-nucleon interactions and the relative Σ-Λ parity 97
BASTIDE, R. P., et al. Neutron threshold measurements using the Chalk River tandem Van de Graaff accelerator 251
BATTERMAN, BORIS W. Effect of chemical impurities on x-ray integrated intensities in nearly perfect germanium 228
BEATY, E. C., et al. Optical detection of narrow Rb^{87} hyperfine absorption lines 311
BECKER, R. L., et al. Polarization of conversion electrons following β decay 116
BEHRNDT, M. E., et al. Observation of microwave cyclotron resonance by cross modulation 59
BENDER, P. L., E. C. BEATY, and A. R. CHI. Optical detection of narrow Rb^{87} hyperfine absorption lines 311
—— et al. Proton gyromagnetic ratio 413

BENDT, P. J., et al. Energy vs momentum relation for the excitations in liquid helium 9
BERLEY, D., R. L. GARWIN, G. GIDAL, and L. M. LEDERMAN. Electric dipole moment of the muon 144; 263(E)
BERMAN, S. M. Radiative corrections to pion beta decay 468
BIENLEIN, H., et al. Polarization of RaE electrons 460
BINCER, A., E. CHURCH, and J. WENESER. Shape and polarization of the beta spectrum of radium E 95
BISI, A. and L. ZAPPA. Circular polarization of external bremsstrahlung 332
BLAND, G. F., et al. New experimental test of special relativity 342
BLOOM, STEWART D., et al. Circular polarization of A^{37} internal bremsstrahlung 34; 79(E)
BOEHM, F., VOLKER SOERGEL, and BERTHOLD STECH. Higher-order effects in the allowed beta decay of F^{20} 77
BOLDT, ELIHU, HERBERT S. BRIDGE, DAVID O. CALDWELL, and YASH PAL. Helicity of the proton from Λ^0 decay 256
——, DAVID O. CALDWELL, and YASH PAL. Λ^0, θ_1^0, θ_2^0, and $\overline{\theta}^0$ lifetimes 148
——, DAVID O. CALDWELL, and YASH PAL. θ_1^0-θ_2^0 mass difference 150
BOLLINGER, L. M., et al. Gamma-ray spectra from neutron capture in resonances of Mn^{55} 76
BÖMMEL, H. E. and K. DRANSFELD. Excitation of very-high-frequency sound in quartz 234
BONFIGLIOLI, G., P. BROVETTO, and C. CORTESE. *F* and *V* centers thermoluminescent recombination 94; 263(E)
BOWEN, THEODORE, JUDSON HARDY, JR., GEORGE T. REYNOLDS, GUIDO TAGLIAFERRI, ALBERT E. WERBROUCK, and WILLIAM H. MOORE. Observation of unpolarized Λ's produced by 1.5-Bev π^- interactions in Pb, Fe, and C 11
BOWERS, K. D., et al. Microwave spin echoes from donor electrons in silicon 368
BOWERS, V. A., et al. Electron spin resonance spectra of the NH_2 and ND_2 free radicals at 4.2°K 91
BOWLES, K. L. Observation of vertical-incidence scatter from the ionosphere at 41 Mc/sec 454
BOZORTH, R. M. Origin of weak ferromagnetism in rare-earth orthoferrites 362
——, VIVIAN KRAMER, and J. P. REMEIKA. Magnetization in single crystals of some rare-earth orthoferrites 3
BRAID, T. H., et al. Determination of the Gamow-Teller beta-decay interaction from the decay of helium-6 61
BRAY, P. J., et al. Li^7 and F^{19} nuclear magnetic resonances in neutron-irradiated LiF 453
BREIT, G. Effects of atomic electrons on *p-p* and *n-p* scattering 200
BREMER, JOHN W. and V. L. NEWHOUSE. Thermal propagation effect in thin superconducting films 282
BRIDGE, HERBERT S., et al. Helicity of the proton from Λ^0 decay 256
BROMLEY, D. A., et al. F^{18} levels near 1 Mev 260
—— et al. Gamma-ray branching and some spin and parity assignments in B^{11} 414
—— et al. Neutron threshold measurements using the Chalk River tandem Van de Graaff accelerator 251
BROOKS, N., et al. Neutron threshold measurements using the Chalk River tandem Van de Graaff accelerator 251
BROVETTO, P., et al. *F* and *V* centers thermoluminescent recombination 94; 263(E)
BRUECKNER, K. A. and K. R. ATKINS. Coefficient of thermal expansion of liquid He^3 near 0°K 315
BRYAN, R. A., J. J. de SWART, R. E. MARSHAK, and P. S. SIGNELL. Semi-phenomenological theory of Σ^+ hyperon-proton scattering up to 150 Mev 70
BUCK, P., et al. Quadrupole moment of Ne^{21} 214
BÜHRING, WOLFGANG and JOACHIM HEINTZE. Electron polarization in the β decay of RaE 176
BUNEMAN, O. Instability, turbulence, and conductivity in current-carrying plasma 8; 119(E)
BURGMAN, J. O., J. FISCHER, B. LEONTIC, A. LUNDBY, R. MEUNIER, J. P. STROOT, and J. D. TEJA. Muon *K*-capture compared to β decay for C^{12}—B^{12} 469
BURGY, M. T., V. E. KROHN, T. B. NOVEY, G. R. RINGO, and V. L. TELEGDI. Test of time-reversal invariance of the beta interaction in the decay of free polarized neutrons 324

BURMAN, R. L., et al. Determination of the Gamow-Teller beta-decay interaction from the decay of helium-6 61
BUSH, WILLIAM B., et al. Magnetic field effects on bow shock stand-off distance 58

CALDWELL, DAVID O., et al. Λ^0, θ_1^0, θ_2^0, and $\overline{\theta}^0$ lifetimes 148
—— et al. θ_1^0-θ_2^0 mass difference 150
—— et al. Helicity of the proton from Λ^0 decay 256
CALL, R. L., et al. Search for mass-550 particles 203
CARLSON, R. O., et al. Spin of Fe^{57} 295
CARPENTER, R. T., et al. Gamma-ray spectra from neutron capture in resonances of Mn^{55} 76
CEDARHOLM, J. P., G. F. BLAND, B. L. HAVENS, and C. H. TOWNES. New experimental test of special relativity 342
CHAMPNESS, C. H. Interpretation of the transverse magnetoresistance in p-type indium antimonide at liquid nitrogen temperature 439
CHESNE, A., et al. Discovery of a new mendelevium isotope 215
CHI, A. R., et al. Optical detection of narrow Rb^{87} hyperfine absorption lines 311
CHILDS, W. J., L. S. GOODMAN, and L. J. KIEFFER. Spin and magnetic dipole moment of 2.6-hr Mn^{56} 296
CHIU, H.-Y. and J. HAMILTON. π^- scattering and dispersion relations 146
CHRIEN, R. E., et al. Strength functions for deformed nuclei 461
CHURCH, E., et al. Shape and polarization of the beta spectrum of radium E 95
CLARK, M. A., J. M. ROBSON, and R. NATHANS. Investigation of time-reversal invariance in the β decay of the neutron 100
COCHRAN, E. L., et al. Electron spin resonance spectra of the NH_2 and ND_2 free radicals at 4.2°K 91
COHEN, E. RICHARD and JESSE W. M. DuMOND. Changes in the 1955 atomic constants occasioned by revision of μ_e/μ_0 291; 382 (E)
COLE, H. and E. KINEKE. Lattice vibrational spectra of Si and Ge 360
COLEGROVE, F. D., et al. Alignment of metastable helium atoms by unpolarized resonance radiation 316
COMMINS, E. D. and P. KUSCH. Upper limit to the magnetic moment of He^6 208
CONNOR, R. J., et al. Neutron threshold measurements using the Chalk River tandem Van de Graaff accelerator 251
COOK, L. F. JR., and N. WILLIAMS, JR. Polarization effects in cascade showers 262
CORENZWIT, E., et al. Ferromagnetic superconductors 449
——, et al. Spin exchange in superconductors 92; 152(E)
CORRIGAN, J. J., S. F. SINGER, and M. J. SWETNICK. Cosmic-ray increases produced by small solar flares 104
CORTELLESSA, G., et al. Photoproduction of K mesons 109; 263(E)
CORTESE, C., et al. F and V centers thermoluminescent recombination 94; 263(E)
CRAWFORD, FRANK S., JR., MARCELLO CRESTI, MYRON L. GOOD, GEORGE R. KALBFLEISCH, M. LYNN STEVENSON, and HAROLD K. TICHO. Beta decay of the Λ 377
——, MARCELLO CRESTI, MYRON L. GOOD, FRANK T. SOLMITZ, and M. LYNN STEVENSON. Search for parity nonconservation in the associated production process 209
CRESTI, MARCELLO, et al. Beta decay of the Λ 377
—— et al. Search for parity nonconservation in the associated production process 209

DASH, WILLIAM C. Generation of prismatic dislocation loops in silicon crystals 400
DeSORBO, WARREN. Energy released on annealing quenched-in defects in gold 238
DESSLER, A. J. Large-amplitude hydromagnetic waves above the ionosphere 68
de SWART, J. J., et al. Semiphenomenological theory of Σ^+ hyperon-proton scattering up to 150 Mev 70
DITCHFIELD, C. R. and P. A. FORRESTER. Maser action in the region of 60°K 448
DIXON, F. P. and R. L. WALKER. Photoproduction of single positive pions from hydrogen in the 500-1000 Mev region 142
——, and R. L. WALKER. Photoproduction of single positive pions from hydrogen in the 600- to 1000-Mev region 458
DONAHUE, T. M. Determination of upper atmosphere sodium abundance from D_2/D_1 measurements in twilight 287

DORAN, D. G., G. R. FOWLES, and G. A. PETERSON. Shock-wave compression of aluminum 402
DOUSMANIS, GEORGE C. Proposal for detection of negative-mass carriers by cyclotron resonance 55
——, R. C. DUNCAN, JR., J. J. THOMAS, and R. C. WILLIAMS. Experimental evidence for carriers with negative mass 404
DRANSFELD, K., et al. Excitation of very-high-frequency sound in quartz 234
DRISCOLL, R. L. and P. L. BENDER. Proton gyromagnetic ratio 413
DuMOND, JESSE W. M., et al. Changes in the 1955 atomic constants occasioned by revision of μ_e/μ_o 291; 382(E)
DUNCAN, R. C., JR., et al. Experimental evidence for carriers with negative mass 404

EKSPONG, A. G. and S. NILSSON. Protonic Σ-decay with an associated electron pair 36
ELIOFF, TOM , et al. Elastic scattering of antiprotons on carbon at 30 to 200 Mev 27
ELMORE, W. C., E. M. LITTLE, and W. E. QUINN. Neutrons of possible thermonuclear origin 32
ESSEN, L., et al. Frequency of cesium in terms of ephemeris time 105

FAZZINI, T., G. FIDECARO, A. W. MERRISON, H. PAUL, and A. V. TOLLESTRUP. Electron decay of the pion 247
FELD, B. T. and B. C. MAGLIĆ. Asymmetry in scattering of 150-Mev polarized protons in nuclear emulsions 375
FERGUSON, A. J., H. E. GOVE, J. A. KUEHNER, A. E. LITHERLAND, E. ALMQVIST, and D. A. BROMLEY. Gamma-ray branching and some spin and parity assignments in B^{11} 414
—— et al. Neutron threshold measurements using the Chalk River tandem Van de Graaff accelerator 251
FERRELL, RICHARD A. Rigorous validity criterion for testing approximations to the electron gas correlation energy 443
FIDECARO, G., et al. Electron decay of the pion 247
FINK, R. W., et al. New isotope of beryllium 23
FISCHER, J., et al. Muon K-capture compared to β decay for C^{12}—B^{12} 469
FISHER, M. E., et al. Susceptibility of the Ising model of an antiferromagnet 321

FJELSTADT, PAUL, et al. Broken atomic beam resonance experiment 232
FLIPPEN, R. B., et al. Piezoelectric effect in indium antimonide 233
FONER, S. N., E. L. COCHRAN, V. A. BOWERS, and C. K. JEN. Electron spin resonance spectra of the NH_2 and ND_2 free radicals at 4.2°K 91
FORBUSH, S. E., et al. Correlation of cosmic ray intensity and solar activity 173
FORRESTER, P. A., et al. Maser action in the region of 60°K 448
FOWLER, T. K. Optical model of inelastic scattering 371; 420(E)
FOWLER, W. A., et al. Angular correlation of alpha particles from decay of Li^8 326
—— et al. Nature of the Li^8 beta-decay interaction 328
FOWLER, WILLIAM B., et al. Elastic scattering of antiprotons on carbon at 30 to 200 Mev 27
FOWLES, G. R., et al. Shock-wave compression of aluminum 402
FRANKEN, P. A. and R. D. COLEGROVE. Alignment of metastable helium atoms by unpolarized resonance radiation 316
FRANKEN, P., R. SANDS, and J. HOBART. Polarization of free potassium atoms by exchange collisions with sodium atoms and free electrons 52; 118(E)
FRANTZ, LEE M., ROBERT L. MILLS, ROGER G. NEWTON, and ANDREW M. SESSLER. Exclusion principle and phenomenological optical-model potentials 340
FREDEN, S. C., F. C. GILBERT, and R. S. WHITE. Decay of a negative τ' meson 217
FRIEDMAN, LEWIS. Experimental limit of the neutrino rest mass 101
FRYE, GLENN M., JR. Antiproton annihilation into neutral pions 14
FUJII, SHIN'ICHI, et al. Ferroelectricity in $NaNO_2$ 320
FULLER, E. G. and EVANS HAYWARD. Elastic scattering of photons by tantalum 465

GALSTER, S. and H. SCHOPPER. Circular polarization of external bremsstrahlung produced by beta rays 330
GARVIN, HUGH L., THOMAS M. GREEN, and EDGAR LIPWORTH. Nuclear spin of 12.6-hr iodine-130 292

——, T. M. GREEN, E. LIPWORTH, and W. A. NIERENBERG. Level inversion in the hyperfine structure of bromine-76. Nuclear moments of bromine-76 293
——, T. M. GREEN, E. LIPWORTH, and W. A. NIERENBERG. Nuclear spin of astatine-211 74
GARWIN, R. L., et al. Electric dipole moment of the muon 144; 263(E)
GASIOROWICZ, S. and A. PETERMANN. Electromagnetic mass correction for spin 0 particles 457
GATTI, R., et al. Discovery of a new mendelevium isotope 215
GHIORSO, A., T. SIKKELAND, J. R. WALTON, and G. T. SEABORG. Attempts to confirm the existence of the 10-minute isotope of 102 17
——, T. SIKKELAND, J. R. WALTON, and G. T. SEABORG. Element No. 102 18
GIDAL, G., et al. Electric dipole moment of the muon 144; 263(E)
GILBERT, F. C., et al. Decay of a negative τ' meson 217
GILLY, LOUIS., et al. Elastic scattering of antiprotons on carbon at 30 to 200 Mev 27
GOEBEL, C. Determination of the π-π interaction strength from π-N scattering 337
GOLDHABER, M. Doubling of fermions? 377
GOOD, MYRON L., et al. Beta decay of the Λ
—— et al. Search for parity nonconservation in the associated production process 209
GOODMAN, L. S., et al. Spin and magnetic dipole moment of 2.6-hr Mn^{56} 296
GORDON, J. P. and K. D. BOWERS. Microwave spin echoes from donor electrons in silicon 368
GOVE, H. E., J. A. KUEHNER, A. E. LITHERLAND, E. ALMQVIST, D. A. BROMLEY, A. J. FERGUSON, P. H. ROSE, R. P. BASTIDE, N. BROOKS, and R. J. CONNOR. Neutron threshold measurements using the Chalk River tandem Van de Graaff accelerator 251
—— et al. Gamma-ray branching and some spin and parity assignments in B^{11} 414
GREEN, M. S. Bose-Einstein condensation and the λ-transition in liquid helium 409
GREEN, T. M., et al. Level inversion in the hyperfine structure of bromine-76. Nuclear moments of bromine-76 293
—— et al. Nuclear spin of astatine-211 74
—— et al. Nuclear spin of 12.6-hr iodine-130 292
GREENSTEIN, H. B., et al. Nature of the Li^8 beta-decay interaction 328
GROSOF, G. M., P. BUCK, W. LICHTEN, and I. I. RABI. Quadrupole moment of Ne^{21} 214
GÜRSEY, FEZA. Possible connection between strangeness and parity 98
GUTOWSKY, H. S., and D. E. WOESSNER. Spin lattice relaxation resonances in solids 6

HAFNER, E. M., et al. Experimental test of time-reversal invariance in strong interactions 255
HALL, R. GLENN, et al. Frequency of cesium in terms of ephemeris time 105
HALL, THOMAS C., et al. Surface mobility in germanium and silicon 276
HALSTED, R. E., E. F. APPLE, and J. S. PRENER. Radiative energy transfer in ZnS 134
HAMBURGER, A. I., et al. Angular distributions of tritons from the $C^{14}(d,t)C^{13}$ reaction 29; 119(E)
HAMILTON, J., et al. π^- Scattering and dispersion relations 146
HARDY, JUDSON, JR., et al. Observation of unpolarized Λ's produced by 1.5-Bev π^- interactions in Pb, Fe, and C 11
HARRISON, MICHAEL J. Magnetic field dependence of ultrasonic attenuation 442
HASEGAWA, HIROSHI, et al. Theory of galvanomagnetic effect at high magnetic field 279
HASHITSUME, NATSUKI, et al. Theory of galvanomagnetic effect at high magnetic field 279
HAVENS, B. L., et al. New experimental test of special relativity 342
HAWKINS, T. D. H., et al. Low-level absorption in germanium 129
HAYWARD, EVANS, et al. Elastic scattering of photons by tantalum 465
HEINTZE, JOACHIM, et al. Electron polarization in the β decay of RaE 176
HENSHAW, D. G. Energy-momentum relation in liquid helium by inelastic scattering of neutrons 127
HERRMANNSFELDT, W. B., R. L. BURMAN, P. STÄHELIN, J. S. ALLEN, and T. H. BRAID. Determination of the Gamow-Teller beta-decay interaction from the decay of helium-6 61
HIGGS, PETER W. Integration of secondary constraints in quantized general relativity 373
HOBART, J., et al. Polarization of free potassium atoms by exchange collisions with sodium atoms and free electrons 52; 118(E)

HOFMANN, F. W., et al. Cyclotron resonance in flames 408
HOLLANDER, LEWIS E., JR. Piezoresistivity in reduced single-crystal rutile (TiO_2) 370
HOLLOWAY, W. W., JR. and R. NOVICK. Determination of the hyperfine structure of atomic nitrogen by optical orientation 367
HONIG, A. and E. STUPP. Electron spin-lattice relaxation in phosphorus-doped silicon 275
HORNIG, A. W., R. C. REMPEL, and H. E. WEAVER. Interpretation of electron paramagnetic resonance in $BaTiO_3$ 284
HROSTOWSKI, HENRY J. and R. H. KAISER. Infrared spectra of heat treatment centers in silicon 199
HUGHES, D. J., R. L. ZIMMERMAN, and R. E. CHRIEN. Strength functions for deformed nuclei 461
HULDT, LENNART and TORSTEN STAFLIN. Infrared absorption of photogenerated free carriers in germanium 236
——. Valence band structure of silicon 313
HULTSCH, R. A., et al. Indirect nuclear spin-spin interactions in pure quadrupole resonance spectra 227

IGO, GEORGE. Optical model potential at the nuclear surface for the elastic scattering of alpha particles 72
IMPEDUGLIA, G., R. PLANO, A. PRODELL, N. SAMIOS, M. SCHWARTZ, and J. STEINBERGER. β decay of the pion 249
ISSENDORFF, H. v., et al. Polarization of RaE electrons 460

JEN, C. K., et al. Electron spin resonance spectra of the NH_2 and ND_2 free radicals at 4.2°K 91
JOHANSSON, C. M., et al. Nuclear ground-state spins of thallium 198 and 201 473
JOHNSON, W. B. Observations on the plasma produced in a magnetic mirror geometry 333

KAISER, R. H., et al. Infrared spectra of heat treatment centers in silicon 199
KAISER, W., et al. Optical properties of crystalline boron 230; 382(E)
KALBFLEISCH, GEORGE R., et al. Beta decay of the Λ 377
KENNETT, T. J., L. M. BOLLINGER, and R. T. CARPENTER. Gamma-ray spectra from neutron capture in resonances of Mn^{55} 76
KENNEY, ROBERT W., et al. Photoproduction of positive pions from protons 12
KERR, E. C., et al. Energy vs momentum relation for the excitations in liquid helium 9
KEUFFEL, J. W., R. L. CALL, W. H. SANDMANN, and M. O. LARSON. Search for mass-550 particles 203
KIEFFER, L. J., et al. Spin and magnetic dipole moment of 2.6-hr Mn^{56} 296
KINEKE, E., et al. Lattice vibrational spectra of Si and Ge 360
KITTEL, C. Paramagnetic centers as detectors of ultrasonic radiation at microwave frequencies 5
KLEPPNER, DANIEL, NORMAN F. RAMSEY, and PAUL FJELSTADT. Broken atomic beam resonance experiment 232
KNAPP, EDWARD A., et al. Photoproduction of positive pions from protons 12
KOTANI, TSUNEYUKI and MARC ROSS. Simple approximation for the nonunique first forbidden transitions 140
KRAMER, VIVIAN, et al. Magnetization in single crystals of some rare-earth orthoferrites 3
KROHN, V. E., et al. Test of time-reversal invariance of the beta interaction in the decay of free polarized neutrons 324
KUBO, RYOGO, HIROSHI HASEGAWA, and NATSUKI HASHITSUME. Theory of galvanomagnetic effect at high magnetic field 279
KUEHNER, J. A., E. ALMQVIST, and D. A. BROMLEY. F^{18} levels near 1 Mev 260
—— et al. Gamma-ray branching and some spin and parity assignments in B^{11} 414
—— et al. Neutron threshold measurements using the Chalk River tandem Van de Graaff accelerator 251
KUSCH, P., et al. Upper limit to the magnetic moment of He^6 208

LAMPERT, MURRAY A. Mobile and immobile effective-mass-particle complexes in nonmetallic solids 450
LANDER, RICHARD., et al. Elastic scattering of antiprotons on carbon at 30 to 200 Mev 27

LANDOVITZ, L. and B. MARGOLIS. Nucleon spectrum in strong-coupling theory 206
LARSON, M. O., et al. Search for mass-550 particles 203
LAURITSEN, C. C., et al. Angular correlation of alpha particles from decay of Li^8 326
—— et al. Nature of the Li^8 beta-decay interaction 328
LAURITSEN, T., C. A. BARNES, W. A. FOWLER, and C. C. LAURITSEN. Angular correlation of alpha particles from decay of Li^8 326
LAUTERBUR, PAUL C., et al. Anisotropy of the C^{13} chemical shift in calcite 343
LAX, MELVIN. Optical properties of diamond type crystals 131
——. Quadrupole interactions and the vibration spectra of diamond type crystals 133
LeCRAW, R. C., et al. Magnetoacoustic resonance in yttrium iron garnet 241
LEDERMAN, L. M., et al. Electric dipole moment of the muon 144; 263(E)
LEGVOLD, SAM, et al. Conduction electron-magnetic ion interaction in rare earths 322
LEONTIC, B., et al. Muon K-capture compared to β decay for C^{12}—B^{12} 469
LEVINE, ARNOLD D. Multiple meson production in electron-proton collisions 111
LICHTEN, W., et al. Quadrupole moment of Ne^{21} 214
LINDGREN, I., C. M. JOHANSSON, and S. AXENSTEN. Nuclear ground-state spins of thallium 198 and 201 473
LIPWORTH, E., et al. Level inversion in the hyperfine structure of bromine-76. Nuclear moments of bromine-76 293
—— et al. Nuclear spin of 12.6-hr iodine-130 292
—— et al. Nuclear spin of astatine-211 74
LITHERLAND, A. E., et al. Gamma-ray branching and some spin and parity assignments in B^{11} 414
—— et al. Neutron threshold measurements using the Chalk River tandem Van de Graaff accelerator 251
LITTLE, E. M., et al. Neutrons of possible thermonuclear origin 32
LORD, NORMAN W. Electron-nuclear double resonance of F centers in lithium fluoride 170
LOW, W. and D. SHALTIEL. Electron paramagnetic resonance in $BaTiO_3$ 286
——, and D. SHALTIEL. Electron spin resonance in single crystals 51
LUDWIG, G. W., H. H. WOODBURY, and R. O. CARLSON. Spin of Fe^{57} 295
—— et al. Spin of Ni^{61} 16
LUNDBY, A., et al. Muon K-capture compared to β decay for C^{12}—B^{12} 469
LUNDY, R. A., J. C. SENS, R. A. SWANSON, V. L. TELEGDI, and D. D. YOVANOVITCH. Experimental evidence for the influence of atomic binding on the decay rate of negative muons 102; 263(E)
——, J. C. SENS, R. A. SWANSON, V. L. TELEGDI, and D. D. YOVANOVITCH. Precise measurements of muon magnetic moments by "stroboscopic coincidences" 38
LYNCH, GERALD, J. OREAR, and S. ROSENDORFF. Measurement of the asymmetry parameter in μ-e decay 471
MacDONALD, W. M., et al. Relativistic corrections to the Fermi matrix element 456
MAGLIĆ, B. C., et al. Asymmetry in scattering of 150-Mev polarized protons in nuclear emulsions 375
MANN, LLOYD G., JOHN A. MISKEL, and STEWART D. BLOOM. Circular polarization of A^{37} internal bremsstrahlung 34; 79(E)
MANNING, JOHN R. Correlation correction to the activation energy for diffusion in crystalline solids 365
MARGOLIS, B., et al. Nucleon spectrum in strong-coupling theory 206
MARKOWITZ, W., R. GLENN HALL, L. ESSEN, and J. V. L. PARRY. Frequency of cesium in terms of ephemeris time 105
MARSHAK, R. E., et al. Divergenceless currents and K-meson decay 25; 119(E)
—— et al. Range of the spin-orbit force between two protons 416
—— et al. Semiphenomenological theory of Σ^+ hyperon-proton scattering up to 150 Mev 70
MARTIN, DOUGLAS L. Thermal effects of the martensitic transition in sodium 4
——. Thermal effects of the martensitic transition in lithium 447
MATTHIAS, B. T., H. SUHL, and E. CORENZWIT. Ferromagnetic superconductors 449

——, H. SUHL, and E. CORENZWIT. Spin exchange in superconductors 92; 152(E)
—— et al. Diamagnetic nuclear magnetic resonance shifts in alloys 278
McDANIEL, B. D., A. SILVERMAN, R. R. WILSON, and G. CORTELLESSA. Photoproduction of K mesons 109; 263(E)
McGRUER, J. N., et al. Angular distributions of tritons from the $C^{14}(d,t)C^{13}$ reaction 29; 119(E)
MERRISON, A. W., et al. Electron decay of the pion 247
MESHKOV, SYDNEY, et al. Configuration mixing in the C^{14} ground state 30; 119(E)
MEUNIER, R., et al. Muon K-capture compared to β decay for C^{12}—B^{12} 469
MILLEA, MICHAEL F. and THOMAS C. HALL. Surface mobility in germanium and silicon 276
MILLS, ROBERT L., et al. Exclusion principle and phenomenological optical-model potentials 340
MISKEL, JOHN A., et al. Circular polarization of A^{37} internal bremsstrahlung 34; 79(E)
MOON, P. B., G. G. SHUTE, and B. S. SOOD. Electron-capture energy and level lifetime by temperature effect in Sm^{152} gamma-ray resonance 21
MOORE, W. E., J. N. McGRUER, and A. I. HAMBURGER. Angular distributions of tritons from the $C^{14}(d,t)C^{13}$ reaction 29; 119(E)
MOORE, WILLIAM H., et al. Observation of unpolarized Λ's produced by 1.5-Bev π^- interactions in Pb, Fe, and C 11
MOREL, PIERRE. Evaluation of the contribution of the umklapp-processes to the electron-phonon interaction 244
MORITA, M. Beta-neutrino-alpha directional correlation 112
MOSS, T. S. and T. D. H. HAWKINS. Low-level absorption in germanium 129
MOSZKOWSKI, S. A. and B. L. SCOTT. Proposed boundary condition potential for the two-nucleon problem 298
MUGA, L., et al. Discovery of a new mendelevium isotop 215

NATHANS, R., et al. Investigation of time-reversal invariance in the β decay of the neutron 100
NEHER, H. V. and S. E. FORBUSH. Correlation of cosmic ray intensity and solar activity 173
NEWHOUSE, V. L., et al. Thermal propagation effect in thin superconducting films 282
NEWMAN, R., et al. Thermal conductivity of MnO and NiO 359
NEWTON, J. O. and F. S. STEPHENS. Experimental observation of double Coulomb excitation 63
NEWTON, ROGER G., et al. Exclusion principle and phenomenological optical-model potentials 340
NIERENBERG, W. A., et al. Level inversion in the hyperfine structure of bromine-76. Nuclear moments of bromine-76 293
—— et al. Nuclear spin of astatine-211 74
NILSSON, S., et al. Protonic Σ-decay with an associated electron pair 36
NOMURA, SHOICHIRO, et al. Ferroelectricity in $NaNO_2$ 320
NORDBERG, M. E., et al. Nature of the Li^8 beta-decay interaction 328
NORDIN, PAUL, JAY OREAR, LEONARD REED, ARTHUR H. ROSENFELD, FRANK T. SOLMITZ, HORACE D. TAFT, and ROBERT D. TRIPP. Leptonic decays of hyperons 380
NOVEY, T. B., et al. Test of time-reversal invariance of the beta interaction in the decay of free polarized neutrons 324
NOVICK, R. and H. E. PETERS. Orientation of rubidium atoms by spin exchange with optically pumped sodium atoms 54; 152(E)
—— et al. Determination of the hyperfine structure of atomic nitrogen by optical orientation 367
NURMIA, M. J. and R. W. FINK. New isotope of beryllium 23

O'KEEFE, J. G., et al. Li^7 and F^{19} nuclear magnetic resonances in neutron-irradiated LiF 453
OKUBO, S., et al. Divergenceless currents and K-meson decay 25; 119(E)
OREAR, JAY, et al. Leptonic decays of hyperons 380
—— et al. Measurement of the asymmetry parameter in μ-e decay 471
OSWALD, LARRY , et al. Elastic scattering of antiprotons on carbon at 30 to 200 Mev 27

PAIS, A. Parity and other symmetries in strong interactions 418
PAL, YASH, et al. Helicity of the proton from Λ^0 decay 256
—— et al. Λ^0, θ_1^0, θ_2^0, and $\bar{\theta}^0$ lifetimes 148
—— et al. θ_1^0-θ_2^0 mass difference 150
PARRY, J. V. L., et al. Frequency of cesium in terms of ephemeris time 105
PAUL, H., et al. Electron decay of the pion 247
PEIERLS, RONALD F. Photopion cross sections and a second resonance 174
PEREZ-MENDEZ, VICTOR, et al. Photoproduction of positive pions from protons 12
PETERMANN, A., et al. Electromagnetic mass correction for spin 0 particles 457
PETERS, H. E., et al. Orientation of rubidium atoms by spin exchange with optically pumped sodium atoms 54; 152(E)
PETERSON, G. A., et al. Shock-wave compression of aluminum 402
PETERSON, L. and J. R. WINCKLER. Short γ-ray burst from a solar flare 205
PHILLIPS, L., R. GATTI, A. CHESNE, L. MUGA, and S. THOMPSON. Discovery of a new mendelevium isotope 215
PHILLIPS, NORMAN E. Heat capacity of superconducting zinc 363
PINES, D. and J. R. SCHRIEFFER. Theory of the Meissner effect 407
PIPKIN, FRANCIS M., et al. Optical polarization of atomic hydrogen 229
PLANO, R., et al. β decay of the pion 249
POMERANTZ, MARTIN A. and SOM PRAKASH AGARWAL. Further observations on the nature of the current reduction in the primary cosmic-ray intensity 107; 183(E)
——, S. P. AGARWAL, and V. R. POTNIS. Nature of the current reduction in the primary cosmic-ray intensity 65
POTNIS, V. R., et al. Nature of the current reduction in the primary cosmic-ray intensity 65
POWELL, WILSON M., et al. Elastic scattering of antiprotons on carbon at 30 to 200 Mev 27
PRENER, J. S., et al. Radiative energy transfer in ZnS 134
PRICE, O. R., D. H. STORK, and H. K. TICHO. K^+ meson-nucleon scattering phase shift analysis 212
PRODELL, A., et al. β decay of the pion 249
PROWSE, D. J. and M. BALDO-CEOLIN. Anti-lambda hyperon 179
QUINN, W. E., et al. Neutrons of possible thermonuclear origin 32
RABI, I. I., et al. Quadrupole moment of Ne^{21} 214
RAMSEY, NORMAN F., et al. Broken atomic beam resonance experiment 232
RAUCH, C. J., et al. Observation of microwave cyclotron resonance by cross modulation 59
REDMOND, PETER J. and JACK L. URETSKY. Conjecture concerning the properties of nonrenormalizable field theories 147
REED, LEONARD, et al. Leptonic decays of hyperons 380
REMEIKA, J. P., et al. Magnetization in single crystals of some rare-earth orthoferrites 3
REMPEL, R. C., et al. Interpretation of electron paramagnetic resonance in $BaTiO_3$ 284
RENEKER, D. H. New oscillatory absorption of ultrasonic waves in bismuth in a magnetic field 440
REYNOLDS, GEORGE T., et al. Observation of unpolarized Λ's produced by 1.5-Bev π^- interactions in Pb, Fe, and C 11
RICHARDS, P. L. and M. TINKHAM. Far infrared energy gap measurements in bulk superconductors 318
RICHTER, BURTON. Large-angle electron pair production from hydrogen 114
RING, P. J., J. G. O'KEEFE, and P. J. BRAY. Li^7 and F^{19} nuclear magnetic resonances in neutron-irradiated LiF 453
RINGO, G. R., et al. Test of time-reversal invariance of the beta interaction in the decay of free polarized neutrons 324
ROBSON, J. M., et al. Investigation of time-reversal invariance in the β decay of the neutron 100
ROLFE, J. Hydroxide absorption band in alkali halide crystals 56
ROSE, M. E. and R. L. BECKER. Polarization of conversion electrons following β-decay 116
ROSE, P. H., et al. Neutron threshold measurements using the Chalk River tandem Van de Graaff accelerator 251
ROSENDORFF, S., et al. Measurement of the asymmetry parameter in μ-e decay 471

ROSENFELD, ARTHUR H., et al. Leptonic decays of hyperons 380
ROSENZWEIG, NORBERT. Spacings of nuclear energy levels 24
ROSS, MARC, et al. Simple approximation for the nonunique first forbidden transitions 140

SAKURAI, J. J. Rest mass of the neutrino 40
——. Wilson-Peierls ambiguity in high-energy photoproduction 258
SAMIOS, N., et al. β decay of the pion 249
SANDMANN, W. H., et al. Search for mass-550 particles 203
SANDS, R., et al. Polarization of free potassium atoms by exchange collisions with sodium atoms and free electrons 52; 118(E)
SAWADA, SHOZO, SHOICHIRO NOMURA, SHIN'ICHI FUJII, and IKUSHI YOSHIDA. Ferroelectricity in $NaNO_2$ 320
SCHIFF, L. I. Sign of the gravitational mass of a positron 254
SCHMITT, ROMAN A. and RODMAN A. SHARP. Measurement of the range of recoil atoms 445
SCHNEIDER, JÜRGEN and F. W. HOFMANN. Cyclotron resonance in flames 408
SCHOEN, A. H. Correlation and the isotope effect for diffusion in crystalline solids 138; 184(E)
SCHOPPER, H., et al. Circular polarization of external bremsstrahlung produced by beta rays 330
SCHRIEFFER, J. R., et al. Theory of the Meissner effect 407
SCHWARTZ, M., et al. β decay of the pion 249
SCOTT, B. L., et al. Proposed boundary condition potential for the two-nucleon problem 298
SEABORG, G. T., et al. Attempts to confirm the existence of the 10-minute isotope of 102 17
—— et al. Element No. 102 18
SEAVEY, M. H., JR., and P. E. TANNENWALD. Direct observation of spin-wave resonance 168
SEGRÈ, EMILIO, et al. Elastic scattering of antiprotons on carbon at 30 to 200 Mev 27
SENITZKY, I. R. Behavior of a two-level solid-state maser 167
SENS, J. C., et al. Experimental evidence for the influence of atomic binding on the decay rate of negative muons 102; 263(E)
—— et al. Precise measurements of muon magnetic moments by "stroboscopic coincidences" 38
SESSLER, ANDREW M., et al. Exclusion principle and phenomenological optical-model potentials 340
SHALTIEL, D., et al. Electron paramagnetic resonance in $BaTiO_3$ 286
—— et al. Electron spin resonance in single crystals 51
SHARP, RODMAN A., et al. Measurement of the range of recoil atoms 445
SHIMAMOTO, Y. Symmetries in baryon-K meson interactions 463
SHULMAN, R. G., B. J. WYLUDA, and B. T. MATTHIAS. Diamagnetic nuclear magnetic resonance shifts in alloys 278
SHUTE, G. G., et al. Electron-capture energy and level lifetime by temperature effect in Sm^{152} gamma-ray resonance 21
SIGNELL, P. S., R. ZINN, and R. E. MARSHAK. Range of the spin-orbit force between two protons 416
—— et al. Semiphenomenological theory of Σ^+ hyperon-proton scattering up to 150 Mev 70
SIKKELAND, T., et al. Attempts to confirm the existence of the 10-minute isotope of 102 17
—— et al. Element No. 102 18
SILVERMAN, A., et al. Photoproduction of K mesons 109; 263(E)
SIMMS, P. C. and R. M. STEFFEN. β-γ angular correlation experiments and time-reversal invariance of the beta interaction 289
SINGER, S. F. "Radiation belt" and trapped cosmic-ray albedo 171
——. Trapped albedo theory of the radiation belt 181; 300(E)
—— et al. Cosmic-ray increases produced by small solar flares 104
SLACK, G. A. and R. NEWMAN. Thermal conductivity of MnO and NiO 359
SLEPIAN, JOSEPH. Inapplicability of certain hydromagnetic principles to the ionic centrifuge 287
SLIFKIN, L., et al. Diffusion along dislocations 243
SOERGEL, VOLKER, et al. Higher-order effects in the allowed beta decay of F^{20} 77
SOLMITZ, FRANK T., et al. Leptonic decays of hyperons 380

—— et al. Search for parity nonconservation in the associated production process 209
SOOD, B. S., et al. Electron-capture energy and level lifetime by temperature effect in Sm^{152} gamma-ray resonance 21
SPAEPEN, J. Density of neutron-irradiated lithium fluoride crystals 281
SPENCER, E. G. and R. C. LeCRAW. Magnetoacoustic resonance in yttrium iron garnet 241
SPIEWAK, M. Magnetic field dependence of high-frequency penetration into a superconductor 136
SPITZER, W. G. and W. KAISER. Optical properties of crystalline boron 230; 382(E)
STAFLIN, TORSTEN, et al. Infrared absorption of photo-generated free carriers in germanium 236
—— et al. Valence band structure of silicon 313
STAHELIN, P., et al. Determination of the Gamow-Teller beta-decay interaction from the decay of helium-6 61
STAPP, HENRY P. Structure of mesons 296
STECH, BERTHOLD, et al. Higher-order effects in the allowed beta decay of F^{20} 77
STEFFEN, R. M., et al. β-γ angular correlation experiments and time-reversal invariance of the beta interaction 289
STEIN, P. C. Search for a long-lived charged particle 21
STEINBERGER, J., et al. β decay of the pion 249
STEINER, HERBERT M., et al. Elastic scattering of antiprotons on carbon at 30 to 200 Mev 27
STEPHENS, F. S., et al. Experimental observation of double Coulomb excitation 63
STEVENSON, M. LYNN, et al. Beta decay of the Λ 377
—— et al. Search for parity nonconservation in the associated production process 209

STORK, D. H., et al. K^+ meson-nucleon scattering phase shift analysis 212

STROOT, J. P., et al. Muon K-capture compared to β decay for C^{12}—B^{12} 469

STUPP, E., et al. Electron spin-lattice relaxation in phosphorus-doped silicon 275
SUDARSHAN, E. C. G., et al. Divergenceless currents and K-meson decay 25; 119(E)

SUHL, H., et al. Ferromagnetic superconductors. 449
—— et al. Spin exchange in superconductors 92; 152(E)
SWANSON, R. A., et al. Experimental evidence for the influence of atomic binding on the decay rate of negative muons 102; 263(E)
—— et al. Precise measurements of muon magnetic moments by "stroboscopic coincidences" 38
SWETNICK, M. J., et al. Cosmic-ray increases produced by small solar flares 104
SYKES, M. F. and M. E. FISHER. Susceptibility of the Ising model of an antiferromagnet 321

TAFT, HORACE D., et al. Leptonic decays of hyperons 380
TAGLIAFERRI, GUIDO, et al. Observation of unpolarized Λ's produced by 1.5-Bev π^- interactions in Pb, Fe, and C 11
TANNENWALD, P. E., et al. Direct observation of spin-wave resonance 168

TEJA, J. D., et al. Muon K-capture compared to β decay for C^{12}—B^{12} 469

TELEGDI, V. L., et al. Experimental evidence for the influence of atomic binding on the decay rate of negative muons 102; 263(E)
—— et al. Precise measurements of muon magnetic moments by "stroboscopic coincidences" 38
—— et al. Test of time-reversal invariance of the beta interaction in the decay of free polarized neutrons 324
TEUTSCH, W. B., et al. Divergenceless currents and K-meson decay 25; 119(E)
THOMAS, J. J., et al. Experimental evidence for carriers with negative mass 404
THOMPSON, S., et al. Discovery of a new mendelevium isotope 215
TICHO, HAROLD K., et al. Beta decay of the Λ 377
—— et al. K^+ meson-nucleon scattering phase shift analysis 212
TINKHAM, M., et al. Far infrared energy gap measurements in bulk superconductors 318
TOLLESTRUP, A. V., et al. Electron decay of the pion 247
TOWNES, C. H., et al. New experimental test of special relativity 342

TRIPP, ROBERT D., et al. Leptonic decays of hyperons 380

URETSKY, JACK L., ROBERT W. KENNEY, EDWARD A. KNAPP, and VICTOR PEREZ-MENDEZ. Photoproduction of positive pions from protons 12
—— et al. Conjecture concerning the properties of nonrenormalizable field theories 147

WALKER, R. L., et al. Photoproduction of single positive pions from hydrogen in the 500-1000 Mev region 142
—— et al. Photoproduction of single positive pions from hydrogen in the 600- to 1000-Mev region 458
WALTON, J. R., et al. Attempts to confirm the existence of the 10-minute isotope of 102 17
—— et al. Element No. 102 18
WARBURTON, E. K. Gamma transitions in self-conjugate nuclei 68
WARNER, CHARLES, III. Strong interactions and associated production 246
WASILIK, J. H. and R. B. FLIPPEN. Piezoelectric effort in indium antimonide 233
WEAVER, H. E., et al. Interpretation of electron paramagnetic resonance in $BaTiO_3$ 284
WEGENER, H., H. BIENLEIN, and H. v. ISSENDORFF. Polarization of RaE electrons 460
WEINBERG, S., R. E. MARSHAK, S. OKUBO, E. C. G. SUDARSHAN, and W. B. TEUTSCH. Divergenceless currents and K-meson decay 25; 119(E)
WEISS, M. T. Microwave and low-frequency oscillation due to resonance instabilities in ferrites 239
WENESER, J., et al. Shape and polarization of the beta spectrum of radium E 95
WERBROUCK, ALBERT E., et al. Observation of unpolarized Λ's produced by 1.5-Bev π^- interactions in Pb, Fe, and C 11
WHITE, HOWARD S., et al. Elastic scattering of antiprotons on carbon at 30 to 200 Mev 27
WHITE, R. S., et al. Decay of a negative τ' meson 217
WIEGAND, CLYDE, et al. Elastic scattering of antiprotons on carbon at 30 to 200 Mev 27
WILLIAMS, G. P., JR., and L. SLIFKIN. Diffusion along dislocations 243
WILLIAMS, N, JR., et al. Polarization effects in cascade showers 262
WILLIAMS, R. C., et al. Experimental evidence for carriers with negative mass 404
WILSON, R. R., et al. Photoproduction of K mesons 109; 263(E)
WINCKLER, J. R., et al. Short γ-ray burst from a solar flare 205
WINTER, J. M., et al. Proposal for a source of polarized protons 374
WOESSNER, D. E., et al. Spin-lattice relaxation resonances in solids 6
WOODBURY, H. H. and G. W. LUDWIG. Spin of Ni^{61} 16
—— et al. Spin of Fe^{57} 295
WYLUDA, B. J., et al. Diamagnetic nuclear magnetic resonance shifts in alloys 278

YARNELL, J. L., G. P. ARNOLD, P. J. BENDT, and E. C. KERR. Energy vs momentum relation for the excitations in liquid helium 9
YOSHIDA, IKUSHI, et al. Ferroelectricity in $NaNO_2$ 320
YOVANOVITCH, D. D., et al. Experimental evidence for the influence of atomic binding on the decay rate of negative muons 102; 263(E)
—— et al. Precise measurements of muon magnetic moments by "stroboscopic coincidences" 38
YPSILANTIS, TOM, et al. Elastic scattering of antiprotons on carbon at 30 to 200 Mev 27

ZAPPA, L., et al. Circular polarization of external bremsstrahlung 332
ZEIGER, H. J., C. J. RAUCH, and M. E. BEHRNDT. Observation of microwave cyclotron resonance by cross modulation 59
ZIEMER, RICHARD W. and WILLIAM B. BUSH. Magnetic field effects on bow shock stand-off distance 58
ZIMMERMAN, R. L., et al. Strength functions for deformed nuclei
ZINN, R., et al. Range of the spin-orbit force between two protons 416